

ADA 038240

(12) 7  
NRL Memorandum Report 3442

## Semidiurnal Hough Mode Extensions in the Thermosphere and Their Application

RICHARD S. LINDZEN

*Plasma Dynamics Branch  
Plasma Physics Division*

and

SIU-SHUNG HONG

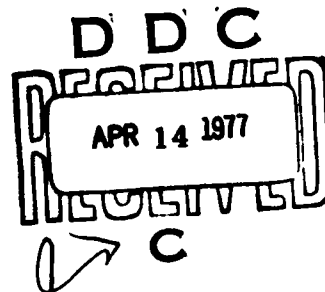
*Cooperative Institute for Research  
in Environmental Sciences  
Boulder, Colorado*

and

JEFFREY FORBES

*Boston College*

February 1977



AD NO. 1233 FILE COPY

This work was supported by the Defense Nuclear Agency under Subtask S99QAXHC065, work unit 08, and work title Late Time Debris Motion.



NAVAL RESEARCH LABORATORY  
Washington, D.C.

Approved for public release; distribution unlimited.

SECURITY CLASSIFICATION OF THIS PAGE (When Data Entered)

REPORT DOCUMENTATION PAGE		READ INSTRUCTIONS BEFORE COMPLETING FORM
1. REPORT NUMBER NRL Memorandum Report 3442	2. GOVT ACCESSION NO. (9)	3. RECIPIENT'S CATALOG NUMBER <i>Interim Rept.</i>
4. TITLE (and Subtitle) (6) SEMIDIURNAL HOUGH MODE EXTENSIONS IN THE THERMOSPHERE AND THEIR APPLICATION		5. TYPE OF REPORT OR OTHER COVERED Interim report on a continuing NRL problem.
6. PERFORMING ORG. REPORT NUMBER		7. CONTRACT OR GRANT NUMBER(s)
8. AUTHOR(s) (10) Richard S. Lindzen, Siu-shung Hong and Jeffrey Forbes		9. PROGRAM ELEMENT, PROJECT, TASK AREA & WORK UNIT NUMBERS NRL Problem H02-27B DNA Subtask S99QAXHC065
10. PERFORMING ORGANIZATION NAME AND ADDRESS Naval Research Laboratory Washington, D.C. 20375		11. REPORT DATE (11) February 1977
11. CONTROLLING OFFICE NAME AND ADDRESS Defense Nuclear Agency Washington, D.C. 20305		12. NUMBER OF PAGES 75
12. MONITORING AGENCY NAME & ADDRESS (if different from Controlling Office) (12) 69p.		13. SECURITY CLASS. (of this report) UNCLASSIFIED
13. DISTRIBUTION STATEMENT (of this Report) Approved for public release; distribution unlimited.		14. DECLASSIFICATION/DOWNGRADING SCHEDULE APR 14 1977 C
14. DISTRIBUTION STATEMENT (of the abstract entered in Block 20, if different from Report) (14) NRL-MK-3442		
15. SUPPLEMENTARY NOTES This work was supported by the Defense Nuclear Agency under Subtask S99QAXHC065, work unit 08, work title Late Time Debris Motion.		
16. KEY WORDS (Continue on reverse side if necessary and identify by block number) Tides Semidiurnal Thermosphere Hough mode extensions		
17. ABSTRACT (Continue on reverse side if necessary and identify by block number) Semidiurnal tidal modes propagate vertically without change of meridional structure in the lower atmosphere. However, in the thermosphere where viscosity, ion drag, and other processes assume importance, individual tidal modes, propagating into the thermosphere from below, begin to change meridional structure as they propagate vertically. In addition, the modes are subject to attenuation. The extent of meridional alteration and vertical attenuation depends on the mean thermal structure of the thermosphere and the degree of ionization, both of which vary during the (Continues)		

next page

DD FORM 1473 1 JAN 73

EDITION OF 1 NOV 68 IS OBSOLETE  
S/N 0102-014-6601

SECURITY CLASSIFICATION OF THIS PAGE (When Data Entered)

251950

AB

## 20. Abstract (Continued)

cont

solar cycle. This note gives the results of numerical calculations of the explicit behavior of the 2,2, 2,3, 2,4, and 2,5 Hough modes within the thermosphere under conditions typical of sunspot maximum and minimum. In addition we present a numerical description of semidiurnal tides excited within the thermosphere. For the convenience of the reader a copy of a paper by Hong and Lindzen giving details of the numerical program is included. The present report can be considered an extensive addendum to this paper.



## CONTENTS

I. INTRODUCTION .....	1
II. BRIEF DESCRIPTION OF RESULTS .....	2
III. REMARKS .....	5
IV. APPLICATIONS .....	5
ACKNOWLEDGEMENTS .....	8
REFERENCES .....	9

APPROVED FOR	
THIS	WILL BE
NO	BE
USING	
DEFINITION	
BY	
DOCUMENT AND	
DATE	
A	

## SEMIDIURNAL HOUGH MODE EXTENSIONS IN THE THERMOSPHERE AND THEIR APPLICATION

### I. Introduction

In Hong and Lindzen (1976) a general computation of the semi-diurnal tide in the thermosphere was presented in detail. It was noted in that paper that the semidiurnal tide in the thermosphere was primarily forced from below, though at sunspot maximum tides from below were severely attenuated in the thermosphere so that in situ thermospheric forcing was of comparable importance for the semidiurnal tide in the upper thermosphere (above 200 km). In all cases, the lower thermosphere was dominated by higher order Hough modes whose origin is primarily the troposphere and mesosphere. The presentation of results in Hong and Lindzen (1976) was made particularly difficult by the fact the amplitudes and phases of the higher order modes (2,3: 2,4: 2,5) were sensitive to detailed variations of the wind and temperature below 100 km - variations which could occur within a single season. To a lesser extent this sensitivity holds for the 2,2 mode itself. Thus, it was obvious that observers might need information on the upward extension of individual Hough modes incident on the thermosphere at, say, 100 km. Such information could permit observers to deduce the global implications of observations at a

Note: Manuscript submitted January 4, 1977.

few stations. Unfortunately, it is difficult to present such information in a compact form since the linearized equations for tides in the thermosphere are no longer separable in their latitude and altitude dependence due to the presence of ion drag and molecular viscosity; i.e., the latitude structure of a given mode forced below 100 km will change with height above 100 km or; equivalently, vertical structure will vary with latitude. Moreover, such 2-dimensional structures will vary with solar cycle insofar as ion drag (proportional to electron density) and neutral temperature vary with the solar cycle. To present the upward extension of a single mode at sunspot minimum and maximum has required 24 fairly detailed diagrams, and extensions of four modes are necessary. In addition we must include 16 additional diagrams which display the atmospheric response to in situ EUV and Schumann-Runge forcing within the thermosphere during sunspot maximum and minimum. One hundred and twelve diagrams exceed the tolerance of most editors, and generally interfere with the convenient reading of a paper. However, for specialists these diagrams are of considerable use. We have, therefore, prepared this report wherein the above mentioned diagrams are presented as a supplement to our paper.

## II. Brief Description of Results

In view of the non-separability of the tidal equations in the thermosphere, the use of the term, Hough mode, is by no means unambiguous. What we shall mean by the term is that configuration of fields in the thermosphere forced by an upcoming wave at 100 km consisting in that Hough mode alone. Note that Hough modes in the

conventional sense (Chapman and Lindzen, 1970) are well defined at 100 km. To distinguish the Hough mode in the thermosphere from the conventionally defined Hough mode, we will use the term, Hough mode extension, (HME). Computational details are given in Hong and Lindzen (1976), which is included as an appendix.

Figures 1a, 2a, 3a, and 4a show the vertical variation of the amplitude of the 2,2 Hough mode extensions, at various latitudes at sunspot minimum, for the temperature, northerly velocity, westerly velocity and vertical velocity fields, respectively; while Figures 1b, 2b, 3b, and 4b show the vertical variation of the phase of the 2,2 Hough mode extension (HME) in each of these fields for the same latitudes and sunspot conditions. Figures 5-8 show the same quantities at sunspot maximum. The assumed conditions at sunspot maximum and minimum are described in Hong and Lindzen (1976). Note that for a given HME, all amplitudes are arbitrary to within a single constant factor (appropriate to all fields to all altitudes and latitudes) while all phases are arbitrary to within a single constant phase displacement. In other words, Figures 1-8 give only relative amplitudes and phases for the 2,2 HME under sunspot minimum and maximum conditions. Figures 1-8 offer results for only a limited number of latitudes ( $0^{\circ}$ ,  $15^{\circ}$ ,  $30^{\circ}$ ,  $45^{\circ}$ , and  $60^{\circ}$ ). In order to aid the reader in interpolating these results to other latitudes we present in Figures 9-12 the variations of amplitudes and phases with latitude at specific altitudes. These altitudes have been chosen as representative of the lower and upper thermosphere and of an intermediate level. Results are shown for both sunspot maximum and minimum conditions. All amplitudes in

Figures 9-12 have been normalized by maximum values at a given altitude. Hence, these values must be calibrated by values from Figures 1-8. Figures 9-12 show clearly the extent to which non-separability affects HME's in the thermosphere. In classical tidal theory (Chapman and Lindzen, 1970) latitudinal structures are independent of altitude and phases are independent of latitude.

The counterparts of Figures 1-12 for the 2,3 HME are shown in Figures 13-24. Note that since the 2,3 mode is antisymmetric about the equator, temperature, westerly velocity and vertical velocity amplitudes are zero at the equator while northerly velocity amplitudes are non-zero there. The counterparts of Figures 1-12 for the 2,4 HME are shown in Figures 25-36, and the counterparts for the 2,5 mode are shown in Figures 37-48.

A caveat is in order concerning accuracy. The calculations used for this report had somewhat better numerical resolution than those in Hong and Lindzen (1976). Nevertheless, we estimate the accuracy of our results for the 2,2 and 2,3 HME's to be only 5% of maximum values at any altitude; for the 2,4 and 2,5 HME's the corresponding accuracy is only about 10%. We believe these accuracy estimates to be conservative. However, small relative amplitudes at any given altitude are naturally suspect, as are the phases corresponding to such small relative amplitudes. In most practical problems, this should be of little consequence.

Finally, in Figures 49-52 we show the amplitudes and phases of the semidiurnal tidal fields, as functions of height at various latitudes, due to in situ thermospheric forcing at sunspot minimum.



Figures 53-56 give the corresponding results for sunspot maximum. The heating functions are described in Hong and Lindzen (1976). For sunspot maximum we used the lower values for the flux in the Schumann-Runge continuum. We approximated the latitude dependence of the in situ heating by a classical 2,2 Hough function. This, in fact, accounts for the bulk of the heating; and since the resulting amplitudes are, in general, relatively small, we do not feel that the corrections to our simple heating structure will prove significant. Similarly, we have not included any detailed latitude distributions of in situ response. In general, this response is very smooth and interpolation directly from Figures 49-56 should prove adequate.

### III. Remarks

As already noted in Hong and Lindzen (1976), as concerns height of maximum amplitude, attenuation of amplitude from maximum to top of thermosphere, and phase variation with height, the 2,2 and 2,3 modes are quite similar and would be hard to distinguish at a single station. The same degree of similarity exists between the 2,4 and 2,5 modes. It is not so surprising that essentially similar modes should occur in pairs differing only in symmetry.

### IV. Applications

The main use of the present report will be to deduce global implications from observations of semidiurnal tides at a few stations. An example of how this may be done may be found in a recent paper (Lindzen, 1976) wherein lower thermospheric data from Millstone Hill ( $46.6^{\circ}\text{N}$ ), St. Santin ( $45^{\circ}\text{N}$ ) and Arecibo ( $18^{\circ}\text{N}$ ) were used to determine the amplitudes and phases of the 2,4 and 2,5 modes which dominate the

semidiurnal tide below 120 km. Lindzen (1976) used classical Hough modes, whereas with the present work it will be possible to repeat this work with the more appropriate Hough mode extensions. It is our intention to use data from the above stations for the upper and lower thermosphere to deduce the amplitudes and phases of all the HME's in this report, using the following procedure:

(1) It is now well established that the semidiurnal tide in the lower thermosphere is dominated by the 2,4 and 2,5 modes. Thus data from these levels may be used to calibrate these HME's in a manner entirely analogous to that used in Lindzen (1976).

(2) Using results in this report for the thermospherically-forced semidiurnal tide (Figures 48-56), the results from item 1 above, and the 2,4 and 2,5 HME's from this report, we can calculate the combined contribution from in situ forcing and the 2,4 and 2,5 modes to the semidiurnal tide in the upper thermosphere where the 2,2 and 2,3 modes assume considerable prominence. Thus, the difference between the above contributions and upper thermospheric observation will permit us to evaluate the contributions from the 2,2 and 2,3 modes forced from below the thermosphere.

(3) The results from item 2, above, can be used to improve the results from item 1, above, and so on.

The above observationally based estimates will permit not only the generation of global models on the basis of limited observations, but will also provide reasonable tests of the predictions provided by models for the generation of tides in the lower atmosphere such as that of Lindzen and Hong (1974).

A complete picture of daily variations in the thermosphere will require a knowledge of the diurnal as well as the semidiurnal tide in the thermosphere. The former will not require any counterpart of the present semidiurnal HME's because it can be shown that the diurnal tide in the thermosphere is almost entirely forced in situ (Lindzen, 1971), primarily by EUV absorption. One of the present authors (J. Forbes) is currently completing a calculation of the thermospherically-forced diurnal tide similar to the calculations of Hong and Lindzen (1976) for the semidiurnal tide. It is hoped that the diurnal calculations will be sufficiently accurate to improve our current knowledge of the EUV flux, and hence, among other things, improve our calculations of the thermospherically-forced semidiurnal tide.

### Acknowledgements

The authors wish to thank Steven Piacsek, Steven Zalesak, Darrell Strobel, Donna Morin and Tazewell Rufty for their aid in the preparation of this report.

## References

1. Chapman, S., and R. S. Lindzen, 1970, Atmospheric Tides, D. Reidel, Dordrecht, Holland, 200 pp.
2. Hong, S., and R. S. Lindzen, 1976, Solar Semidiurnal Tide in the Thermosphere. J. Atmos. Sci., 33, in press.
3. Lindzen, R. S., 1971, Internal Gravity Waves in Atmospheres with Realistic Dissipation and Temperature: Part III. Daily Variations in the Thermosphere. Geophys. Fluid Dyn., 2, 89-121.
4. Lindzen, R. S., 1976, A Modal Decomposition of the Semidiurnal Tide in the Lower Thermosphere. J. Geophys. Res., 81, 2923-2926.
5. Lindzen, R. S. and S. Hong, 1974, Effects of Mean Winds and Horizontal Temperature Gradients on Solar and Lunar Semidiurnal Tides in the Atmosphere. J. Atmos. Sci., 31, 1421-1446.

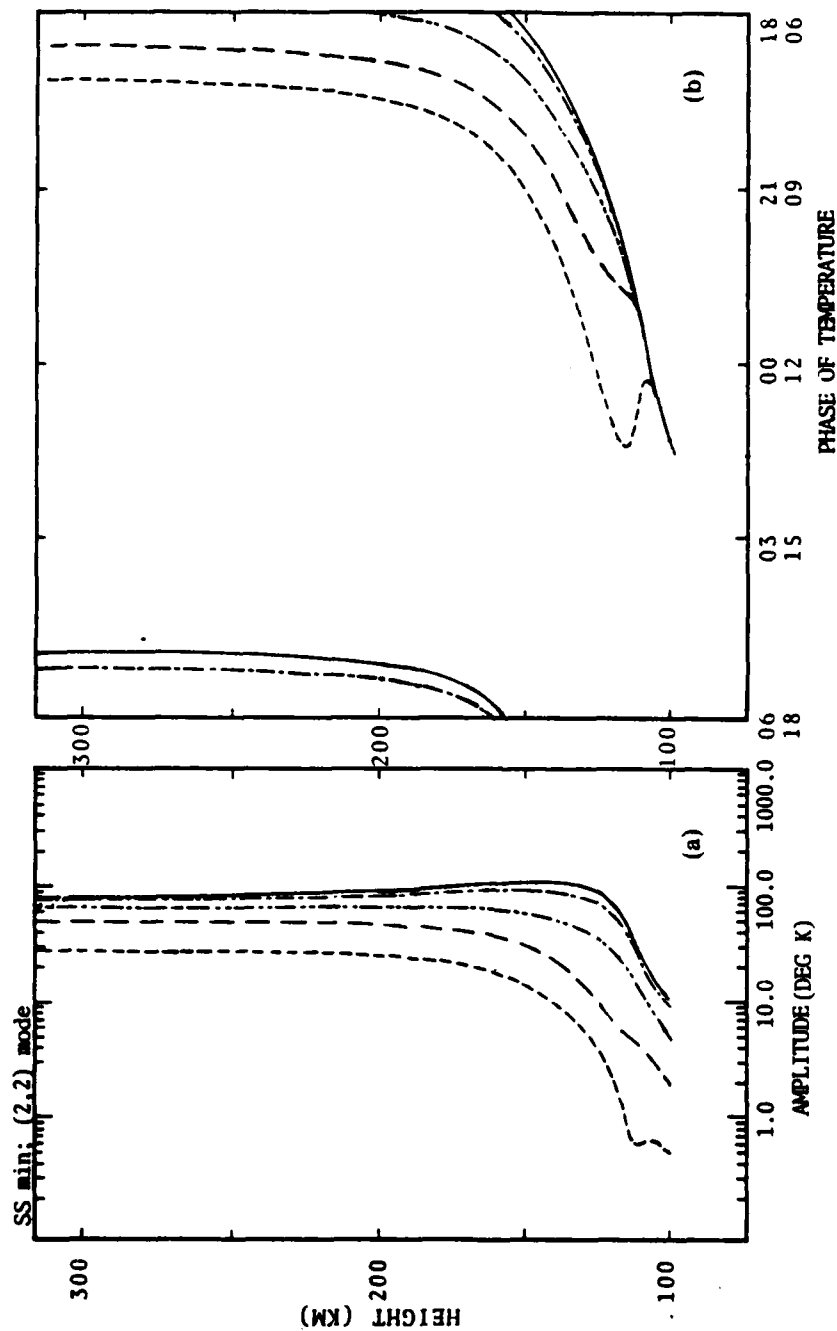


Fig. 1 -- (a) Amplitude of temperature oscillation of the 2,2 Hough mode extension (HME) as a function of altitude for various latitudes under minimum sunspot conditions. Different line conventions apply to different latitudes as follows: —, 0°; ---, 15°; - - - , 30°; - - - - , 45°; - - - - - , 60°. (b) Phase of temperature oscillation (hour of maximum, local time) of the 2,2 Hough mode extension (HME) as a function of altitude for various latitudes under minimum sunspot conditions. Line convention as in (1a).

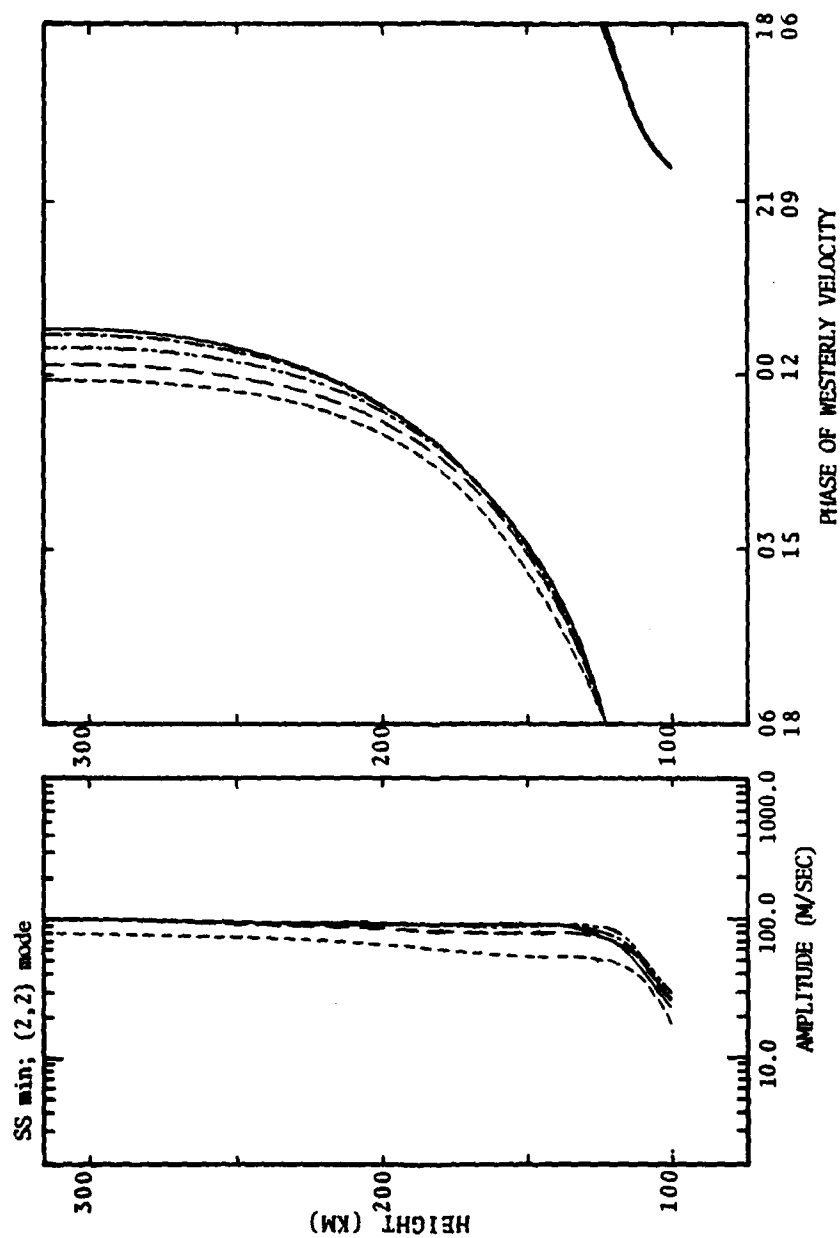


Fig. 2 — Same as Fig. 1, but for the westerly velocity oscillation of the 2,2 HME under minimum sunspot conditions

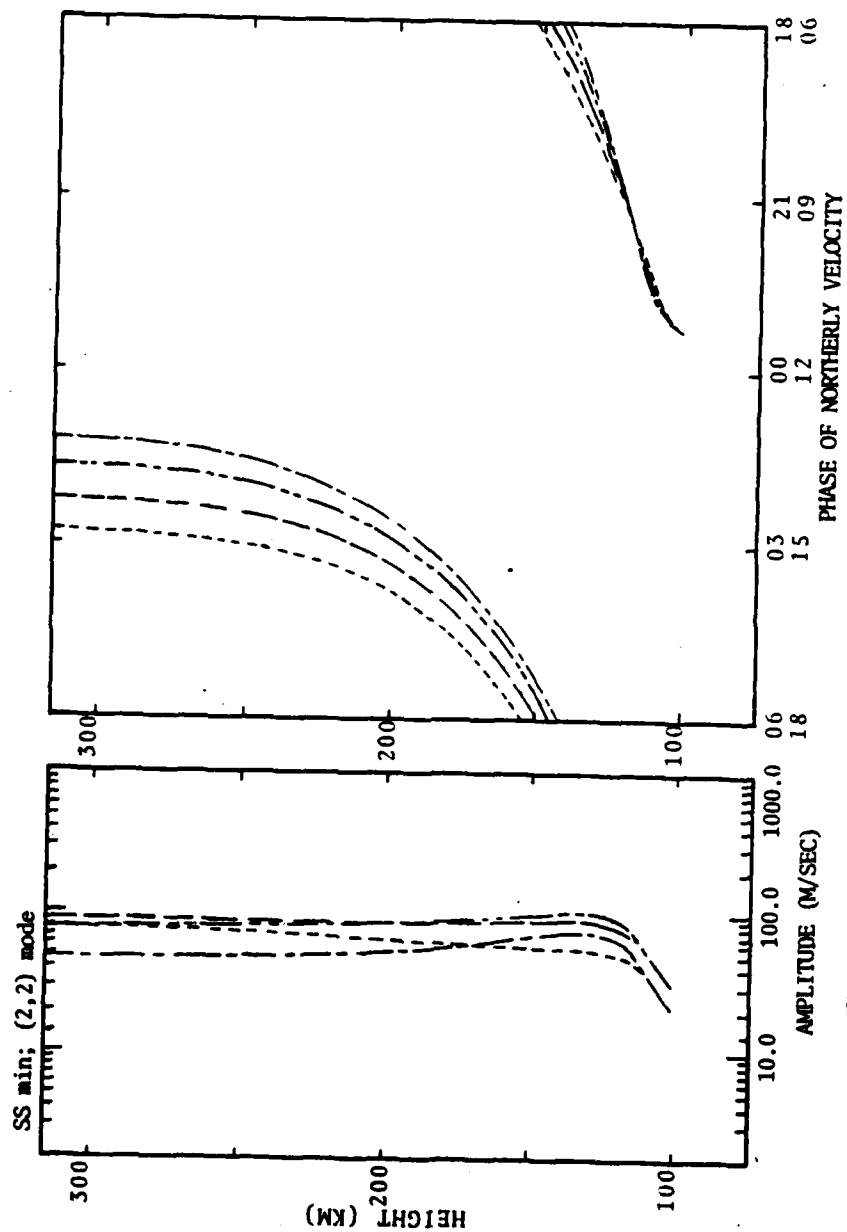


Fig. 3 — Same as Fig. 1, but for the northerly velocity oscillation of the 2,2 HME under minimum sunspot conditions



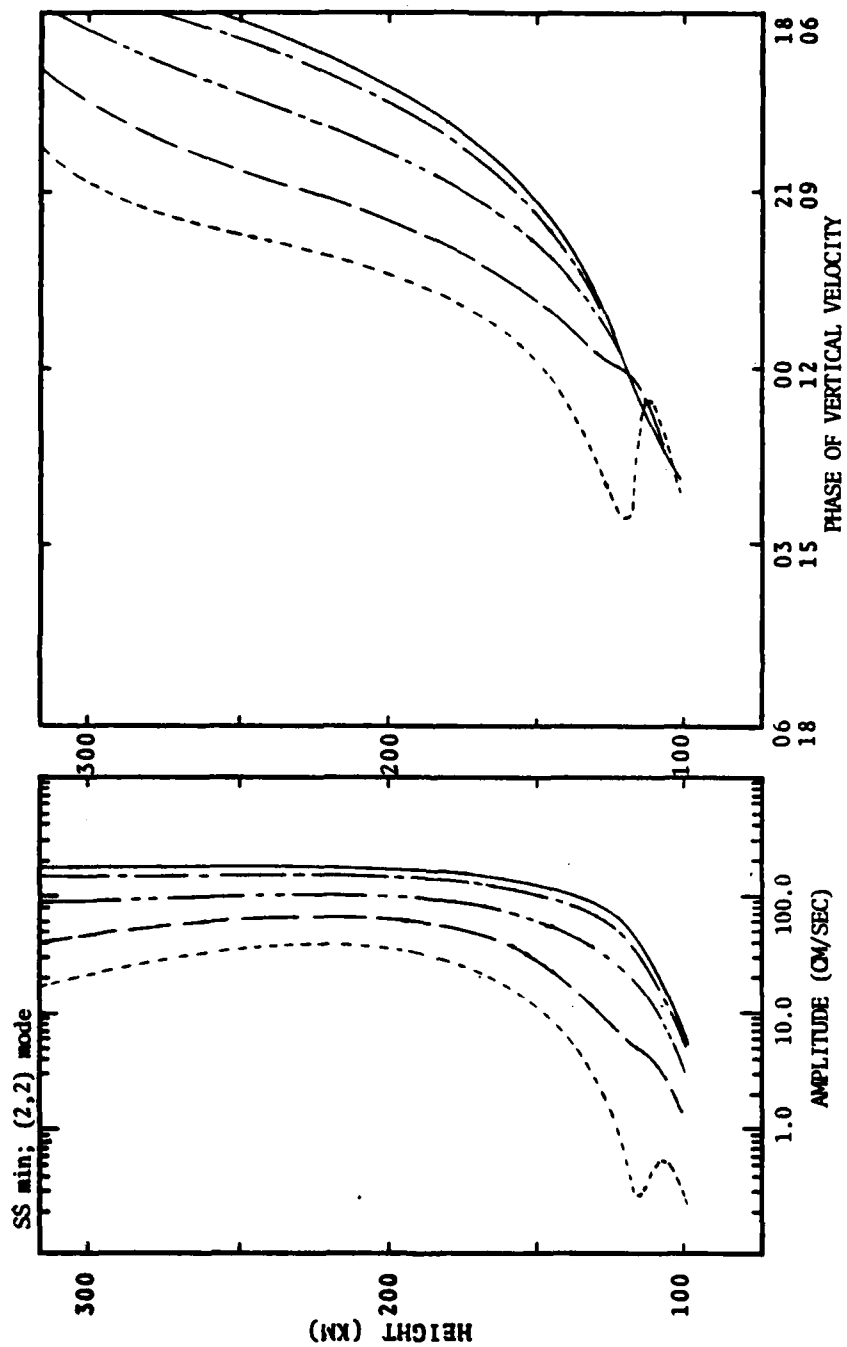


Fig. 4 — Same as Fig. 1, but for the vertical velocity oscillation of the 2,2 HME under minimum sunspot conditions

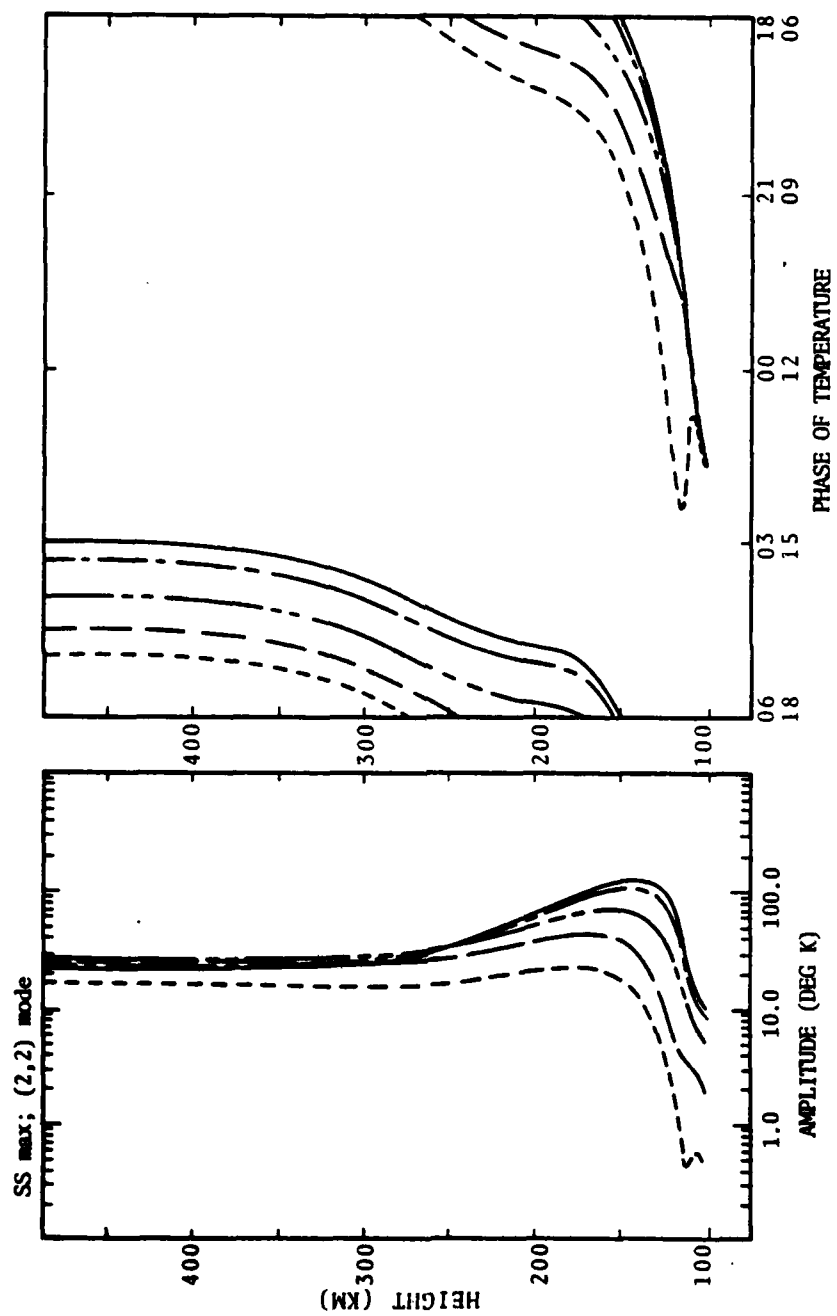


Fig. 5 -- Same as Fig. 1 but for maximum sunspot conditions

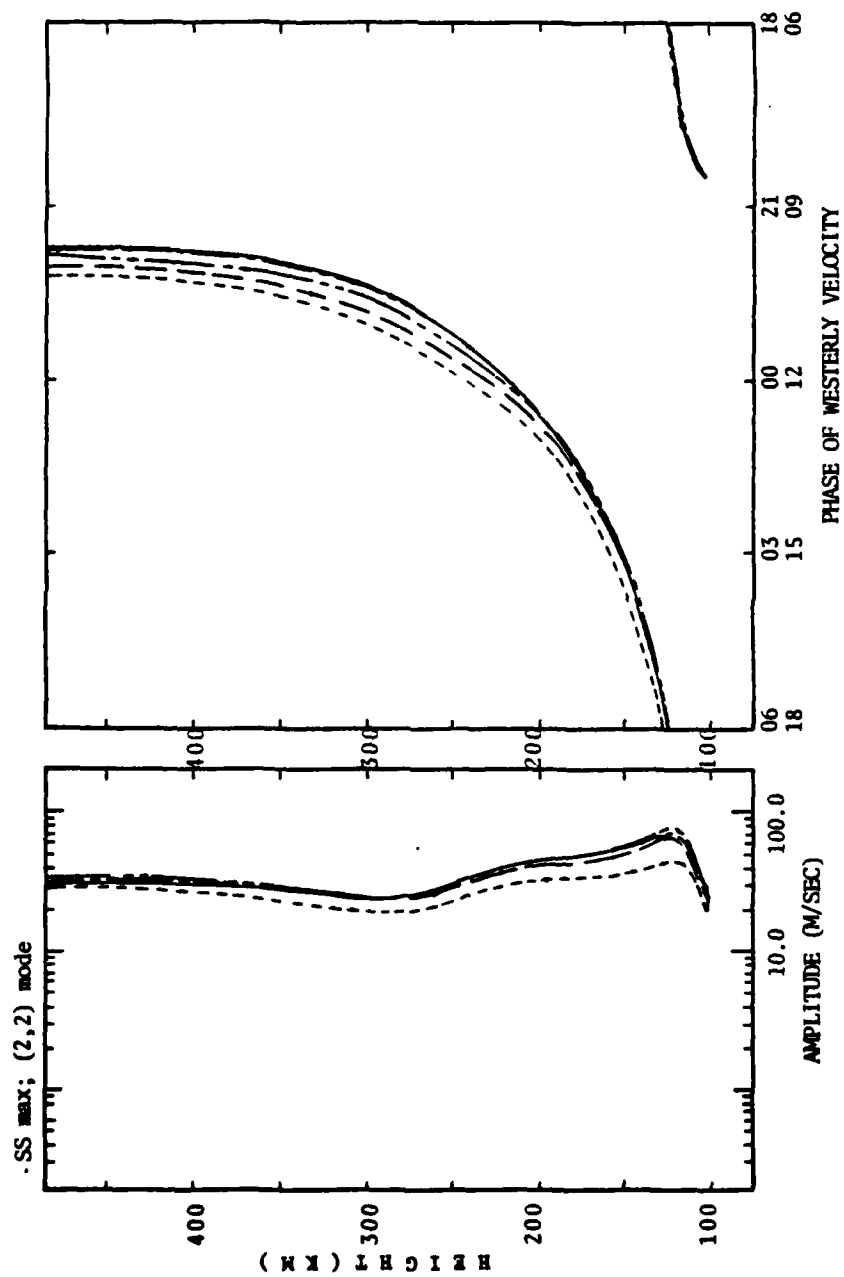


Fig. 6 — Same as Fig. 2 but for maximum sunspot conditions

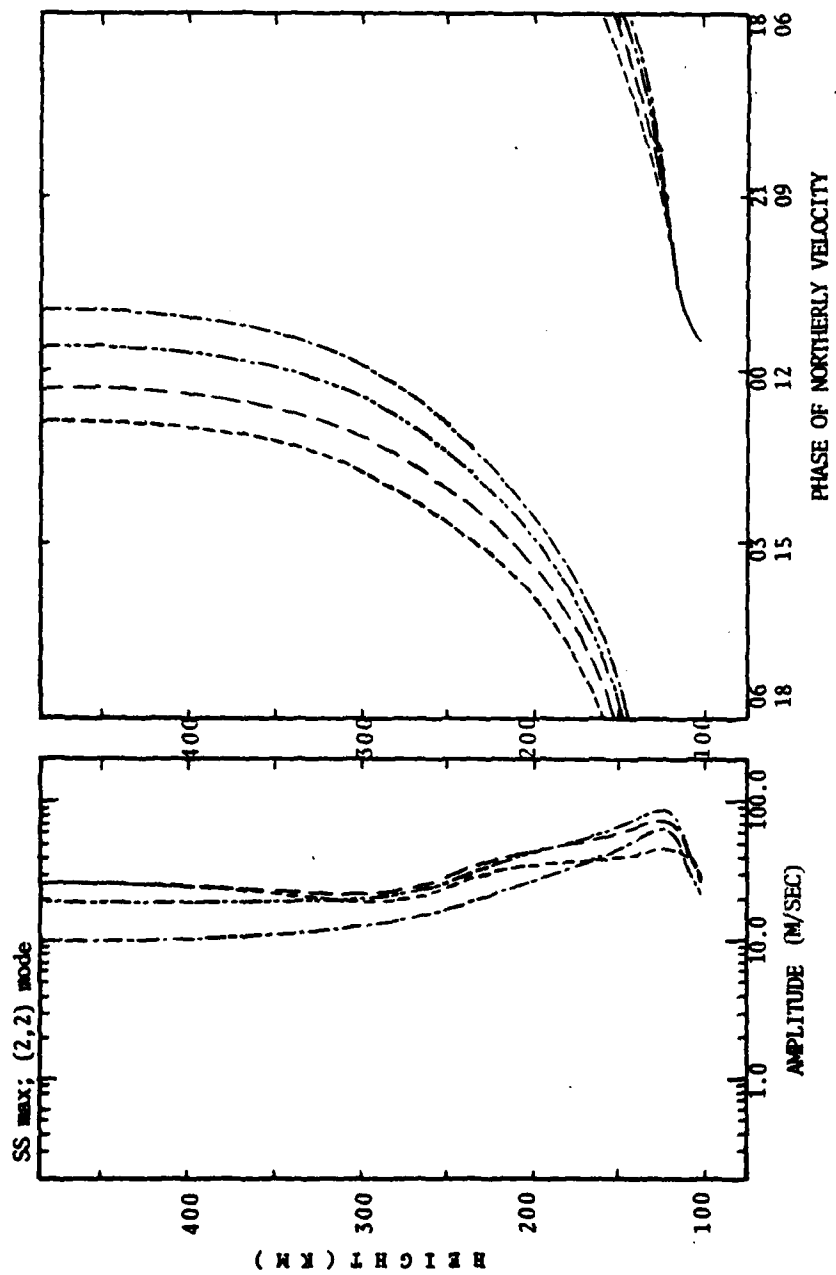


Fig. 7 — Same as Fig. 3 but for maximum sunspot conditions

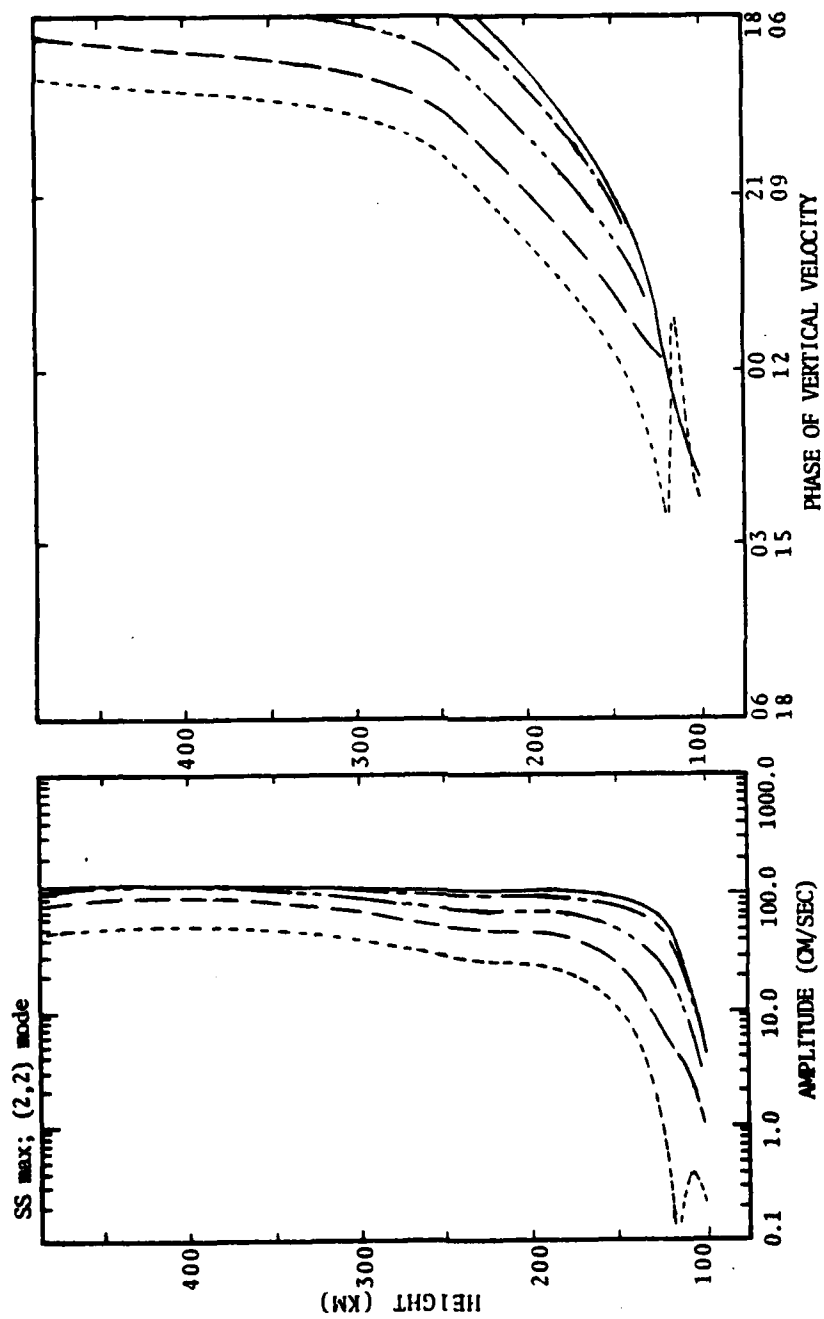


Fig. 8 — Same as Fig. 4 but for maximum sunspot conditions

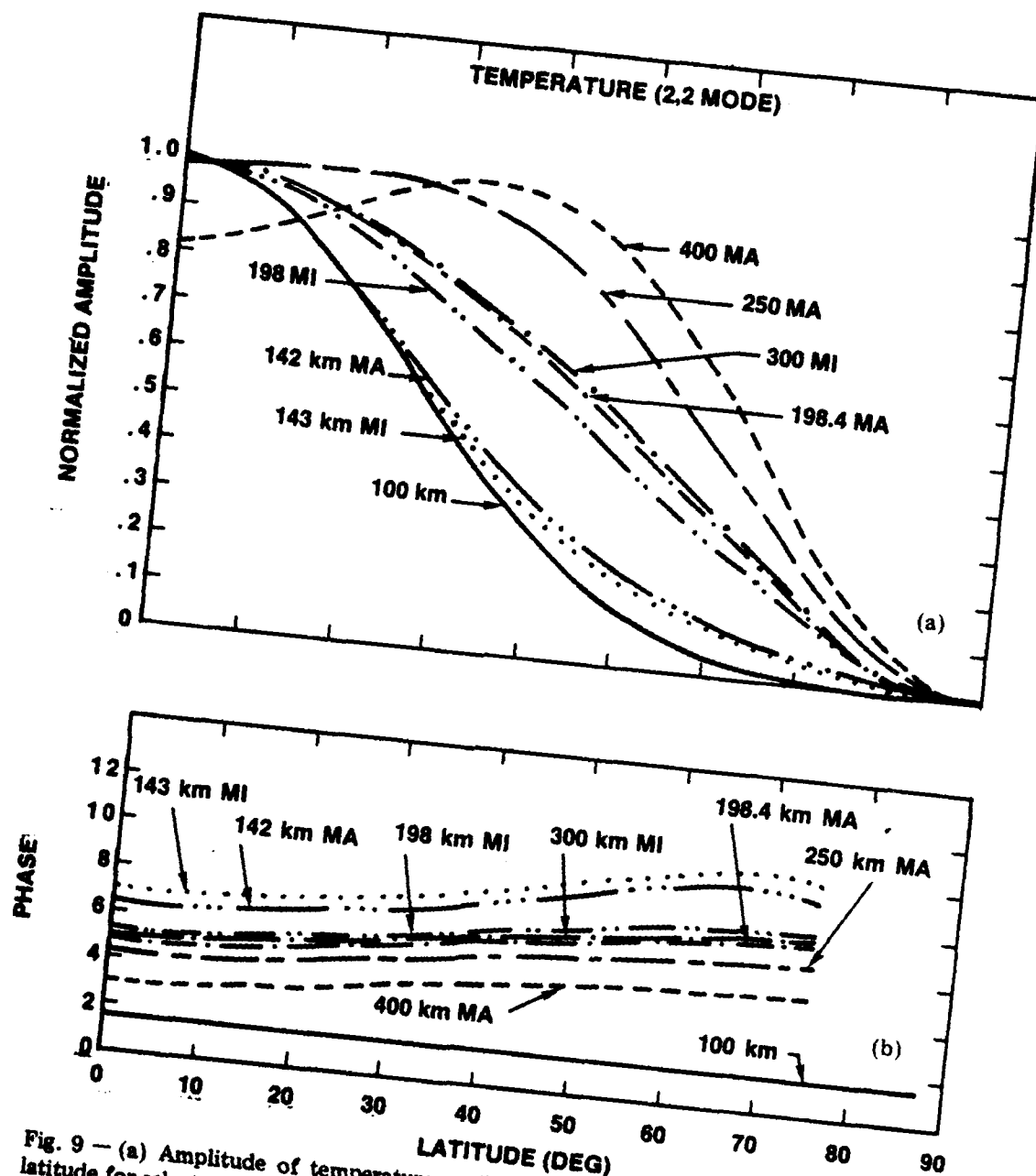


Fig. 9 — (a) Amplitude of temperature oscillation of the 2,2 HME as a function of latitude for selected altitudes and sunspot conditions (values normalized by maximum value at each altitude). MI refers to sunspot minimum; MA refers to sunspot maximum. Values at 100 km are essentially independent of sunspot conditions. (b) Phase of temperature oscillation (time of maximum, local time) of the 2,2 HME as a function of latitude for selected altitudes and sunspot conditions.

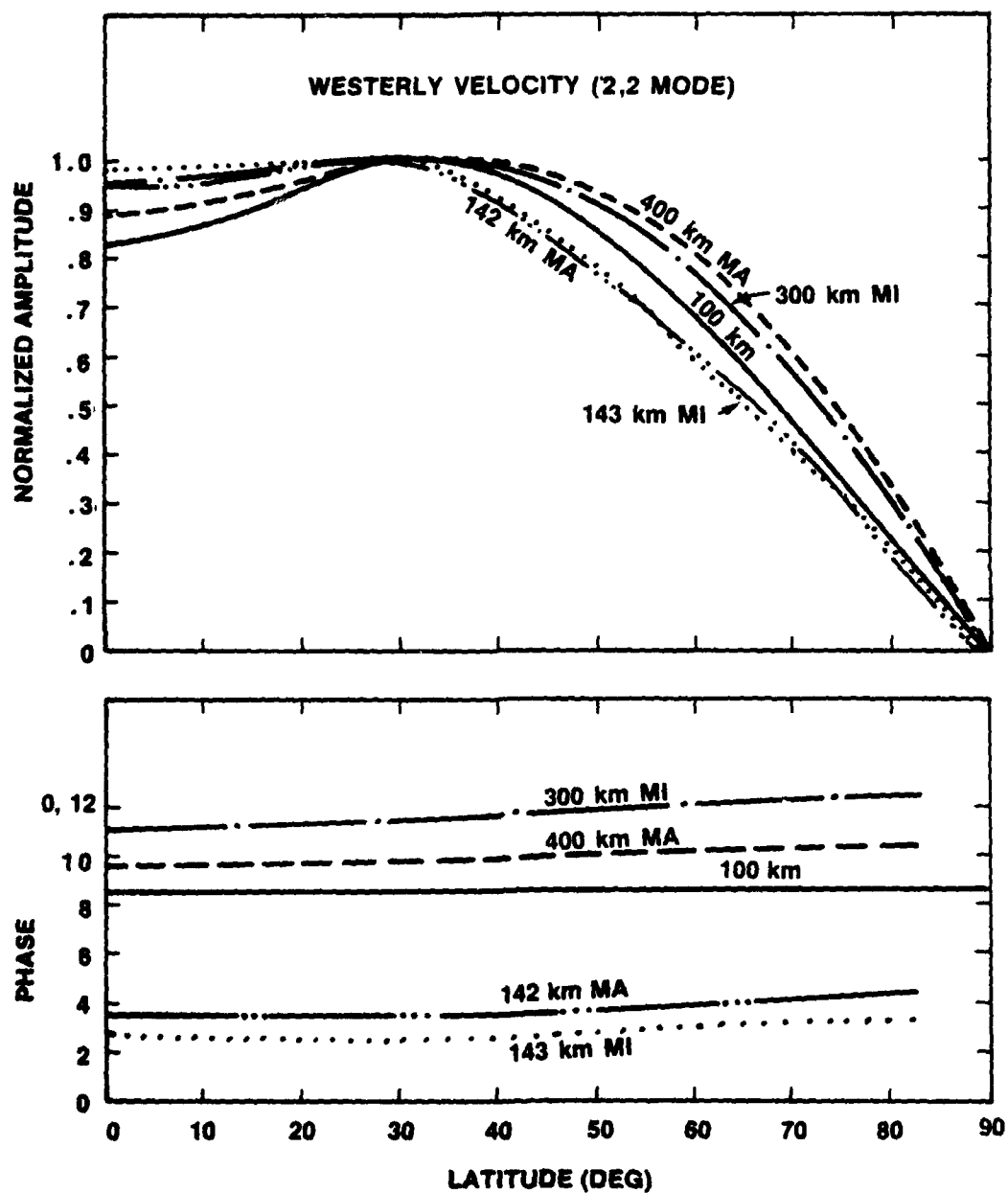


Fig. 10 — Same as 9, but for the westerly velocity oscillation of the 2,2 HME

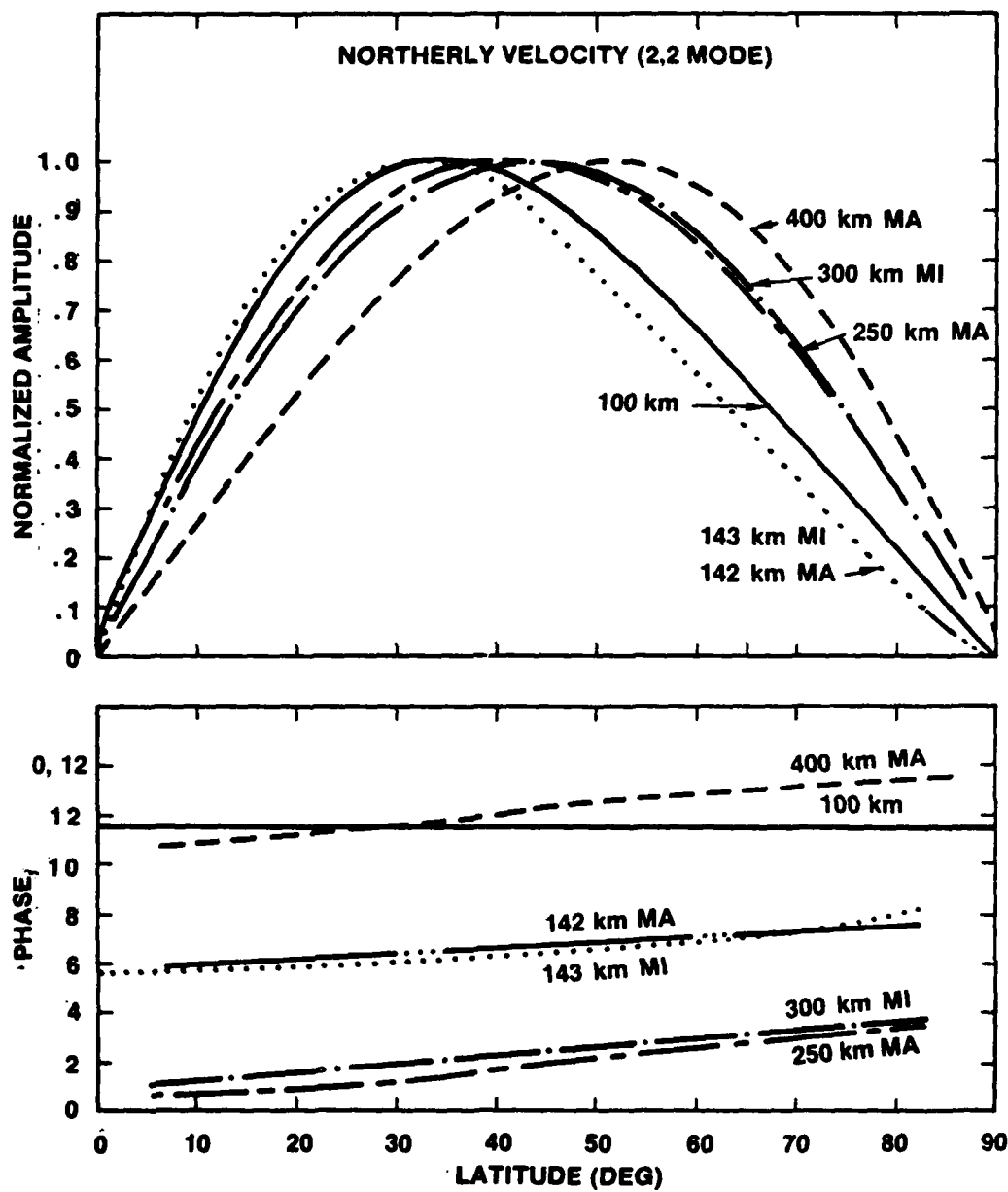


Fig. 11 — Same as 9 but for the northerly velocity oscillation of the 2,2 HME



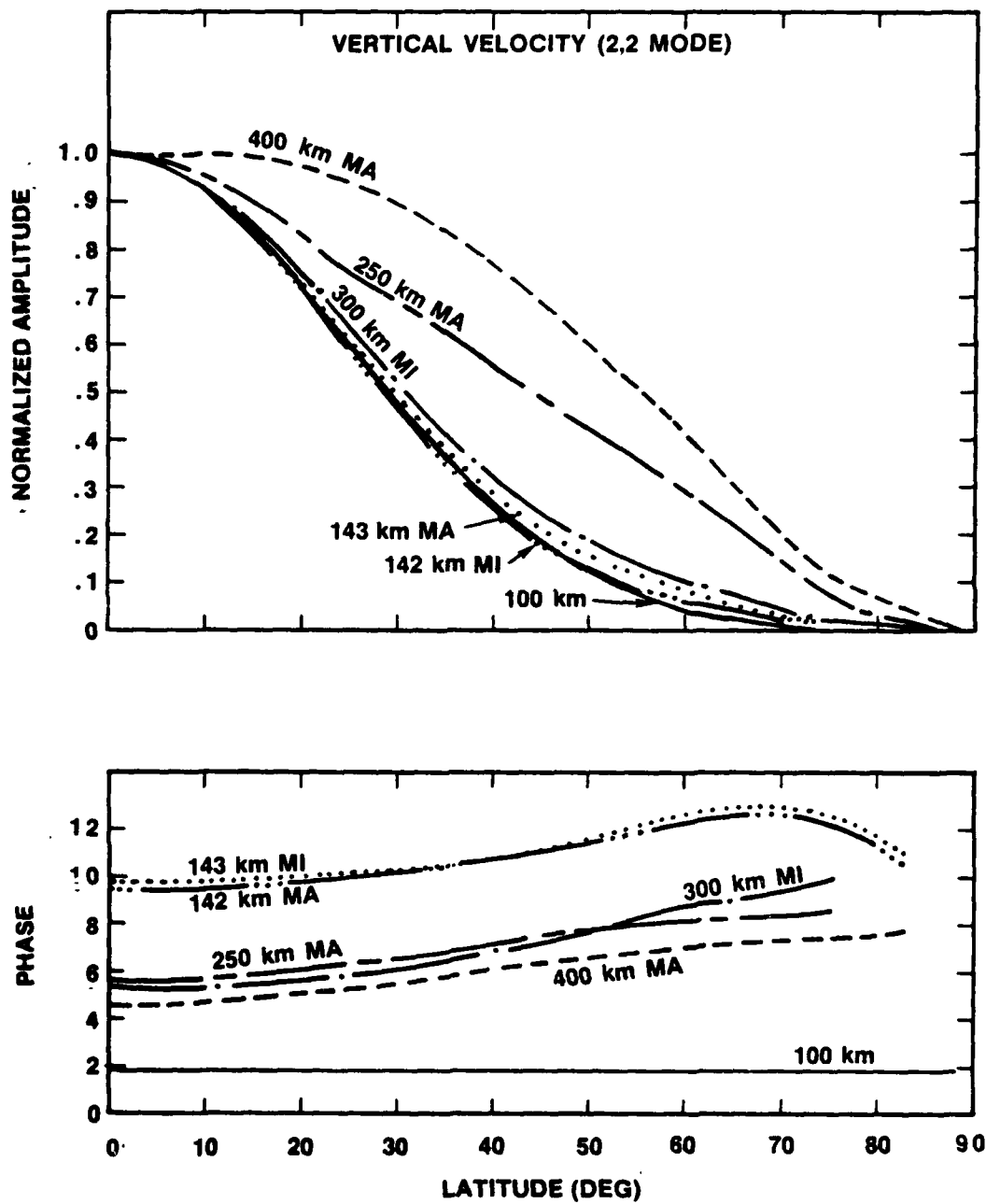


Fig. 12 — Same as 9 but for the vertical velocity oscillation of the 2,2 HME

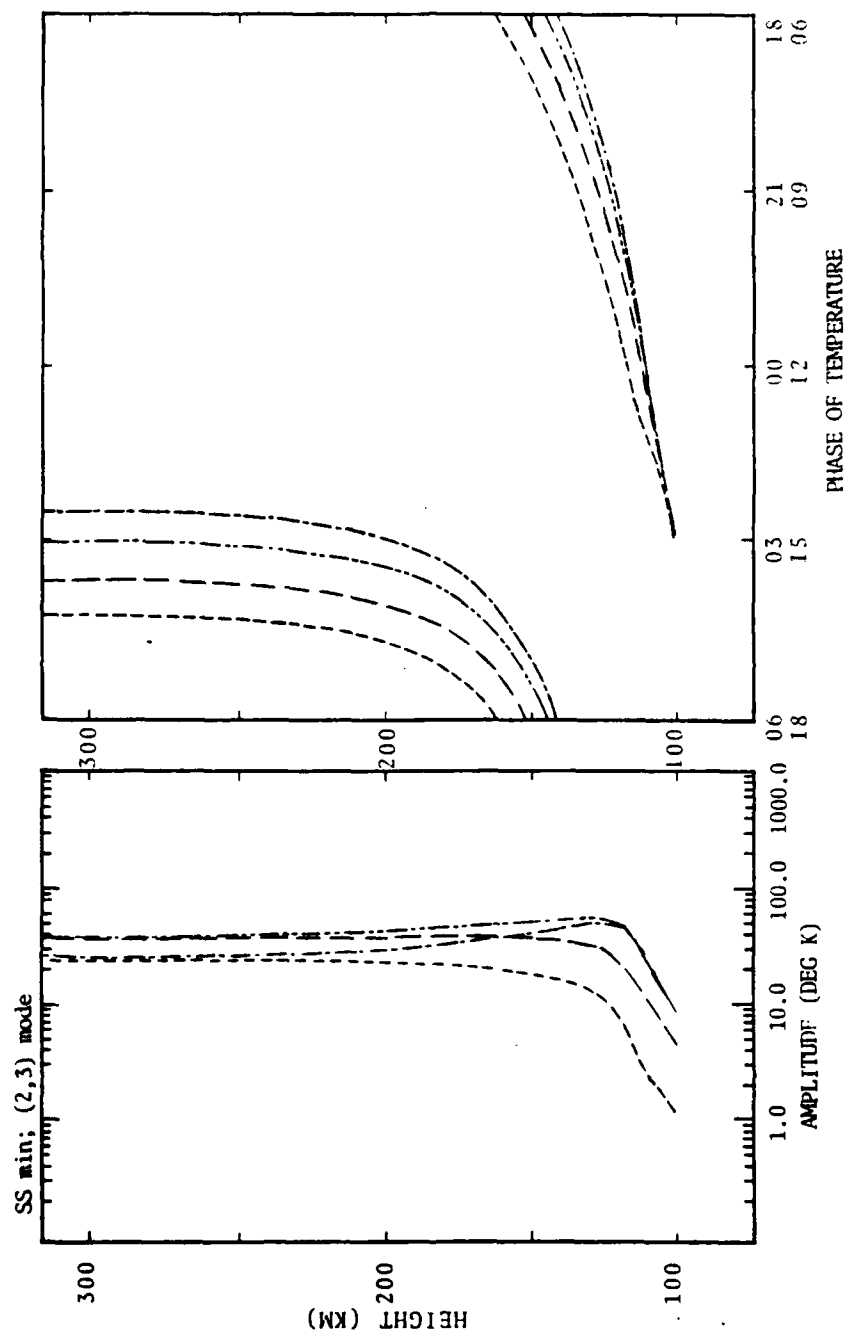


Fig. 13 -- Same as 1 but for the 2,3 HME

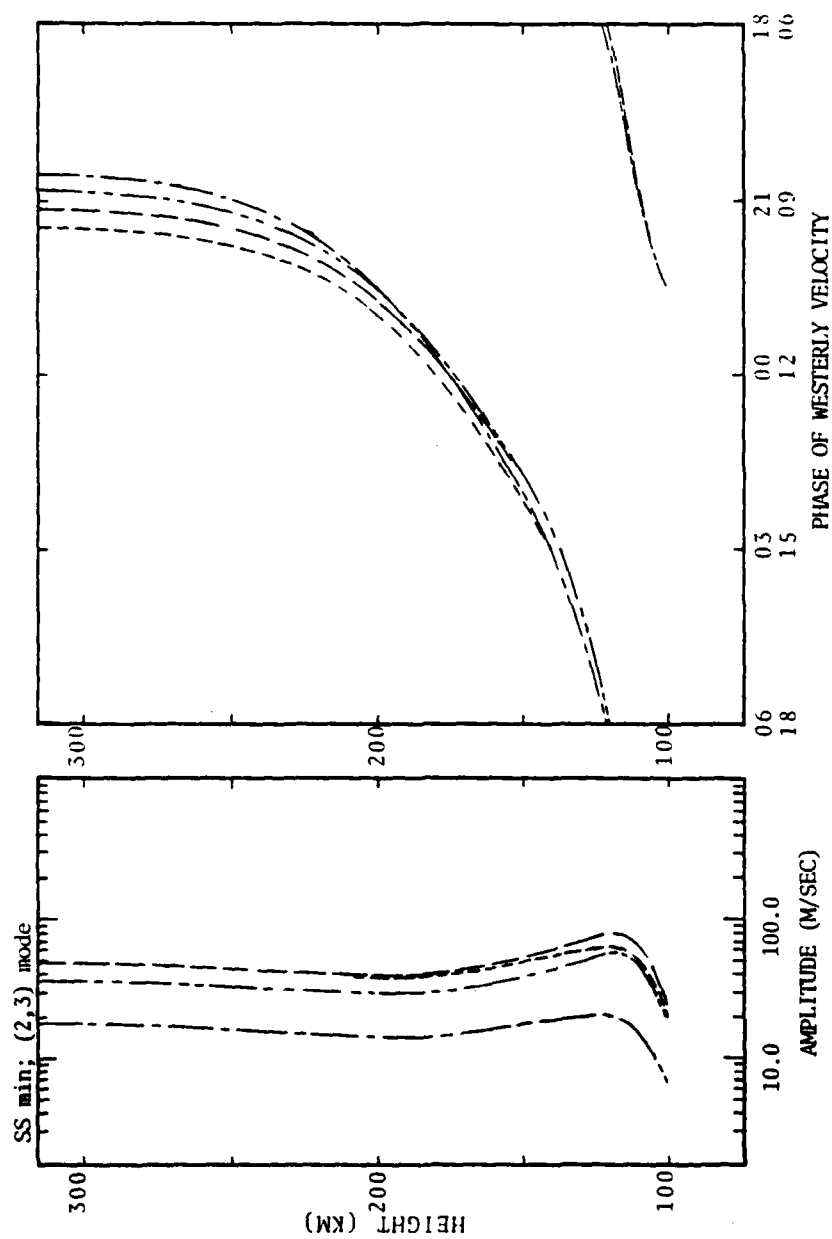


Fig. 14 -- Same as 2 but for the 2,3 HME

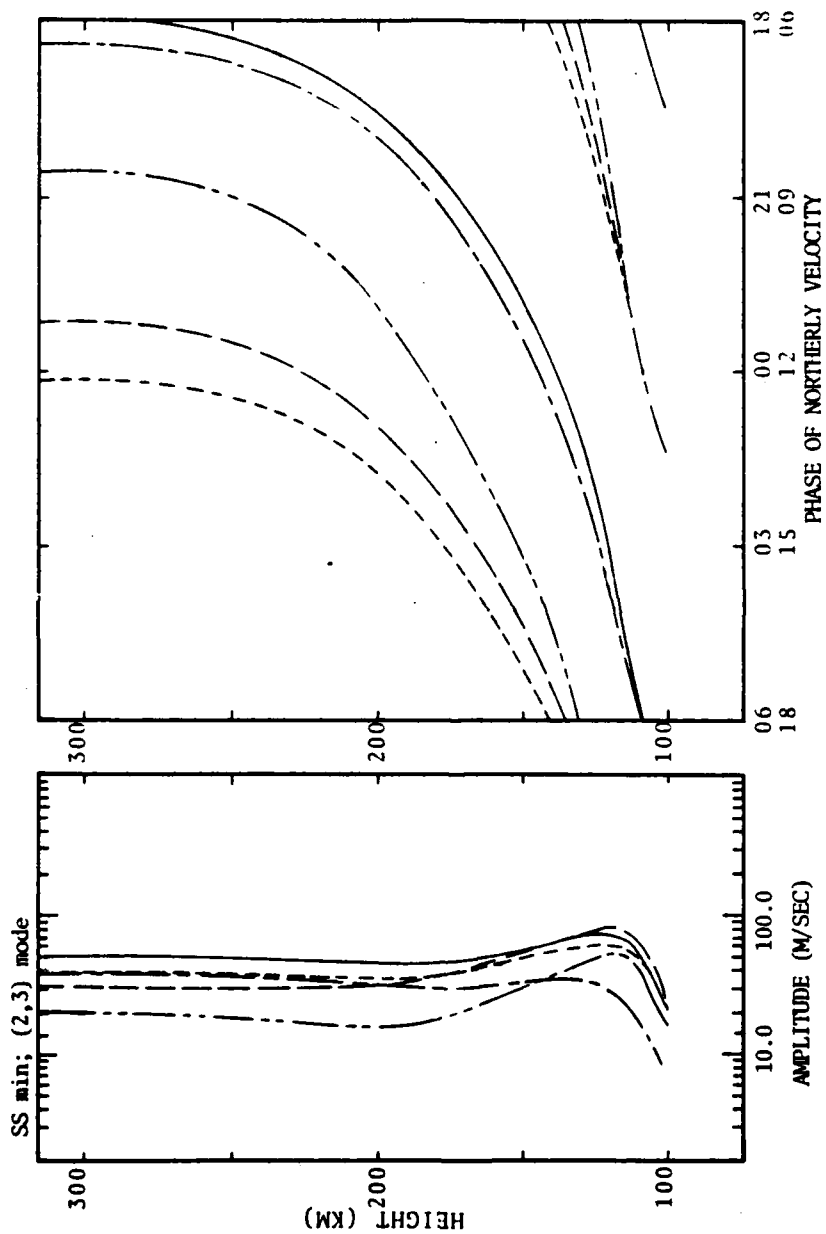


Fig. 15 -- Same as 3 but for the 2,3 HME

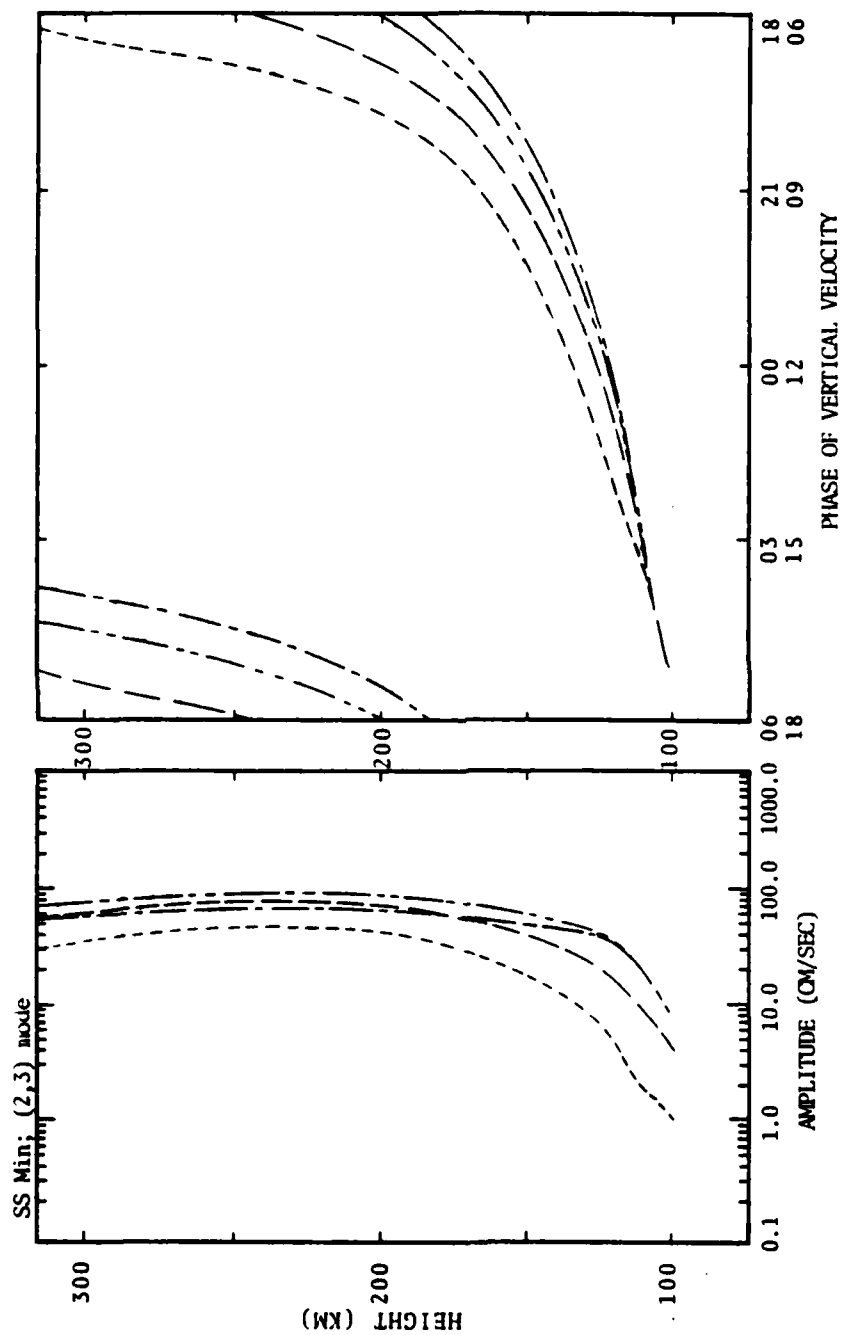


Fig. 16 — Same as 4 but for the 2,3 HME

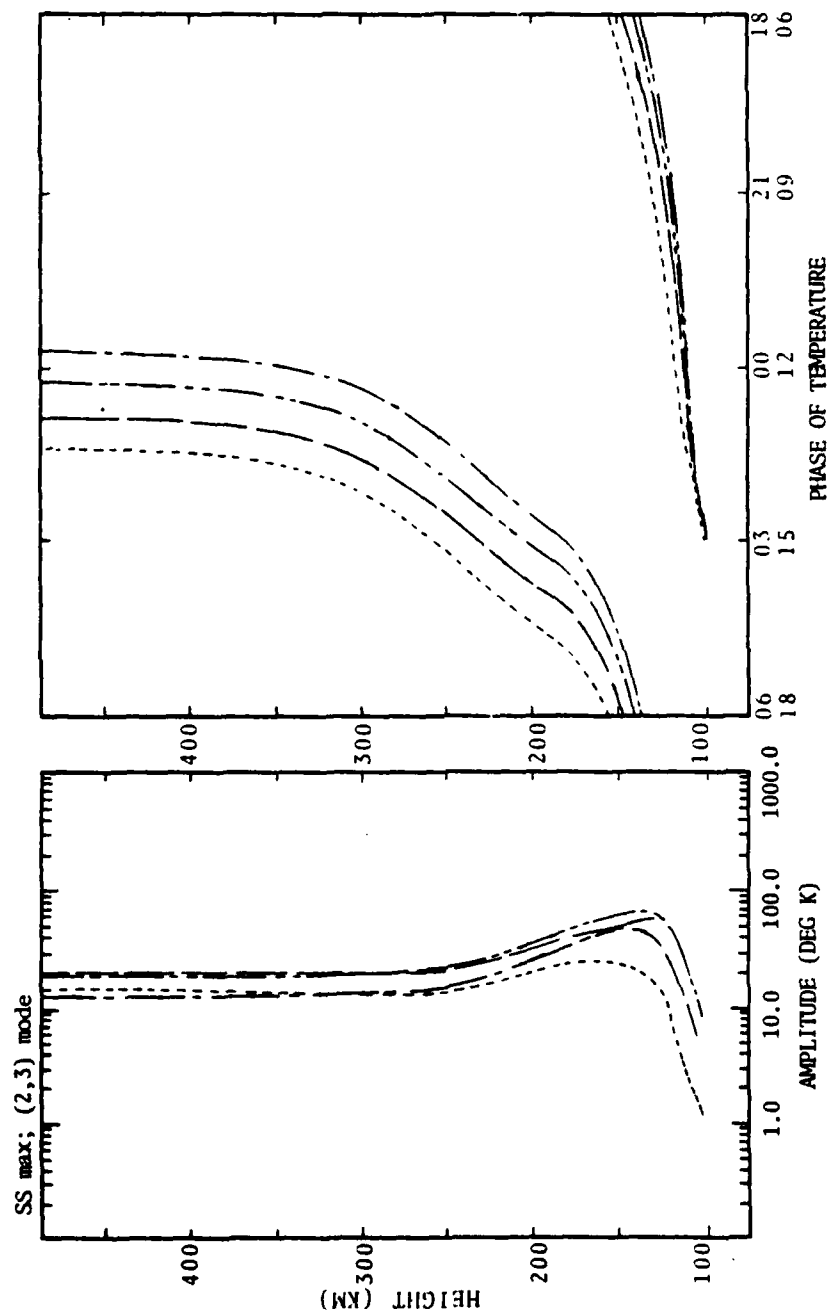


Fig. 17 -- Same as 5 but for the 2,3 HME

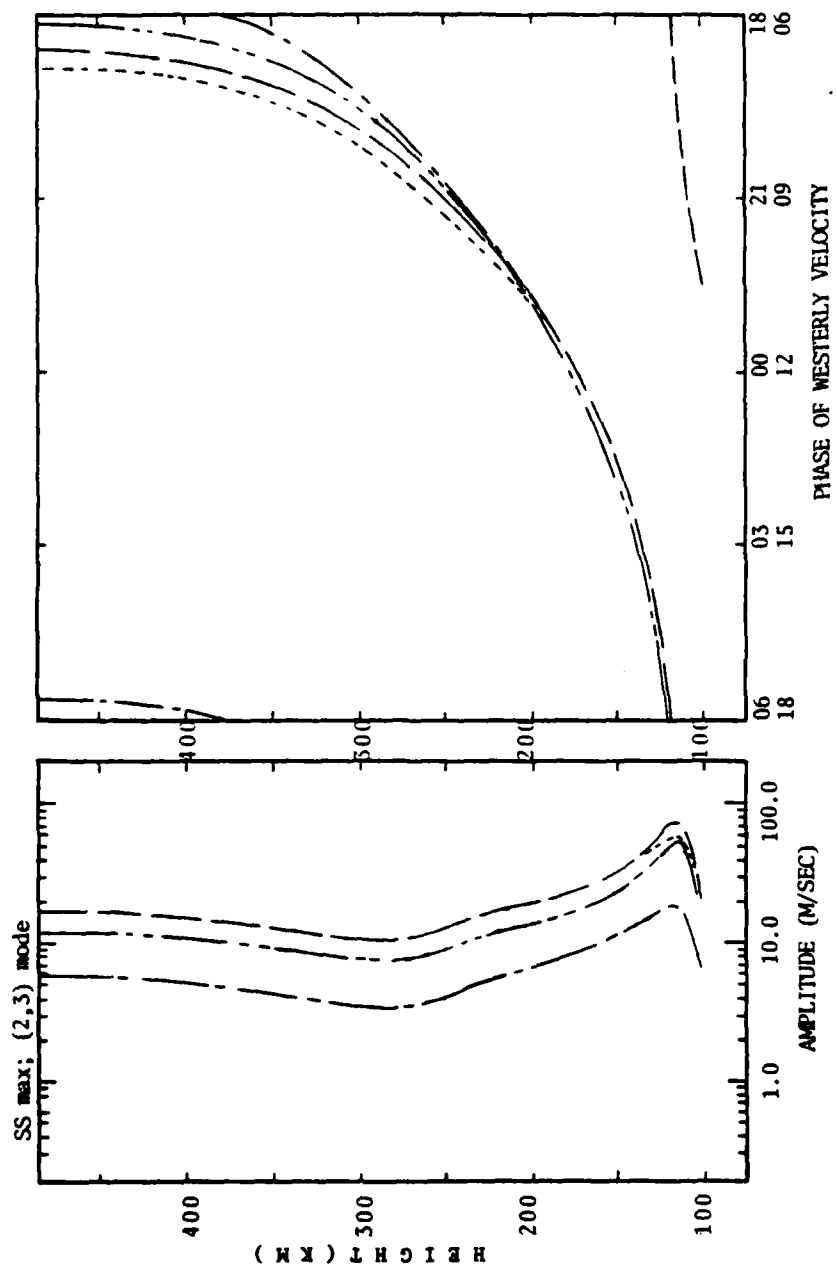


Fig. 18 — Same as 6 but for the 2,3 HME

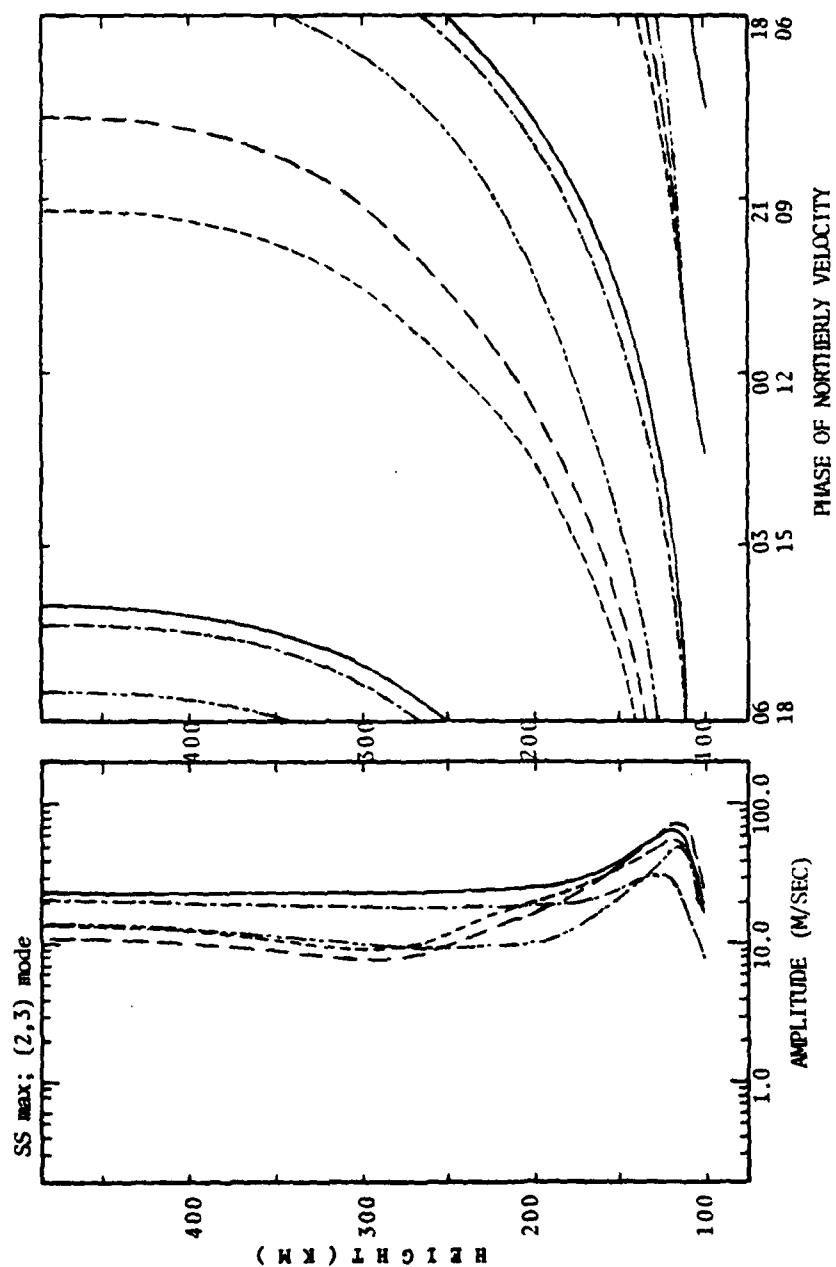


Fig. 19 -- Same as 7 but for the 2,3 HME



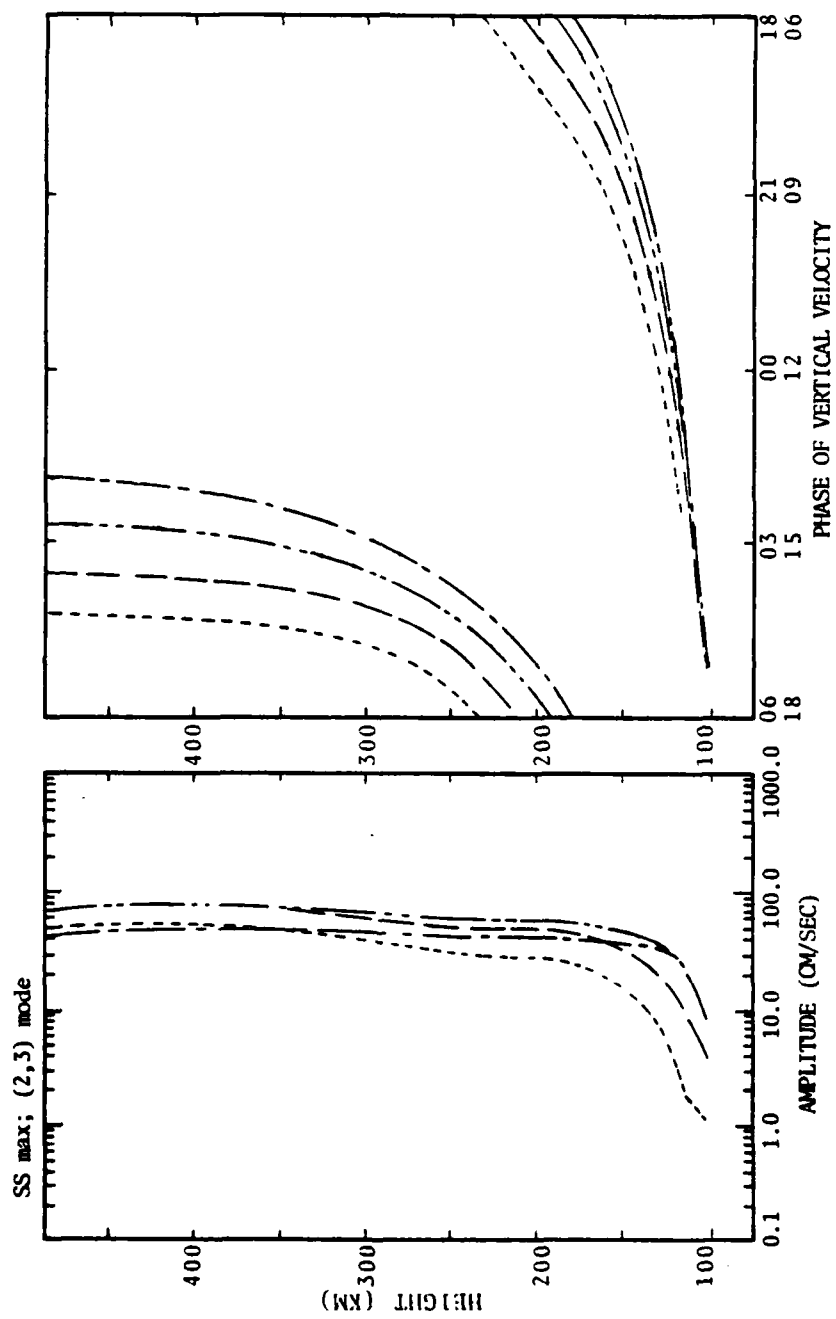


Fig. 20 — Same as 8 but for the 2,3 HME.

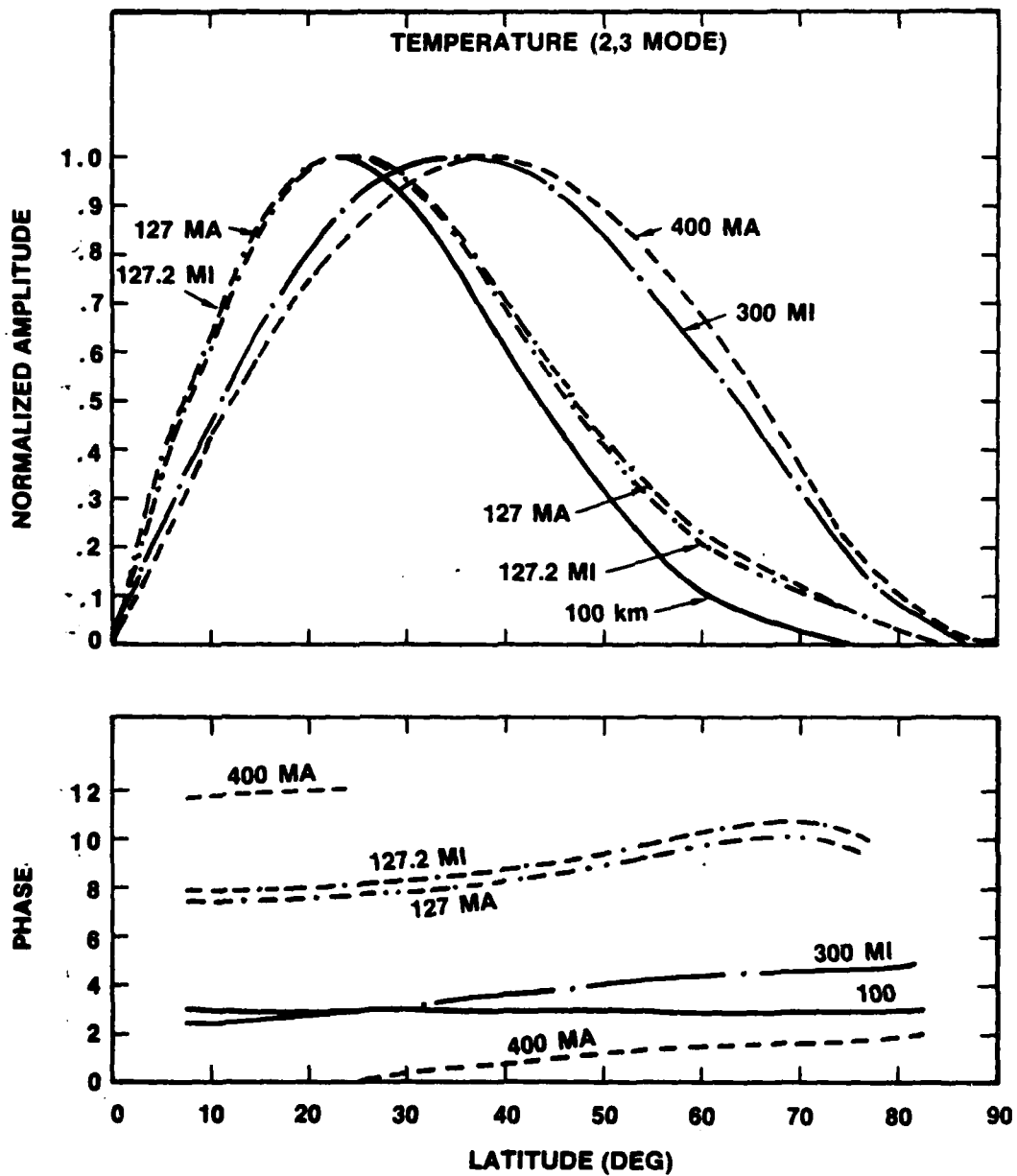


Fig. 21 — Same as 9 but for the 2,3 HME

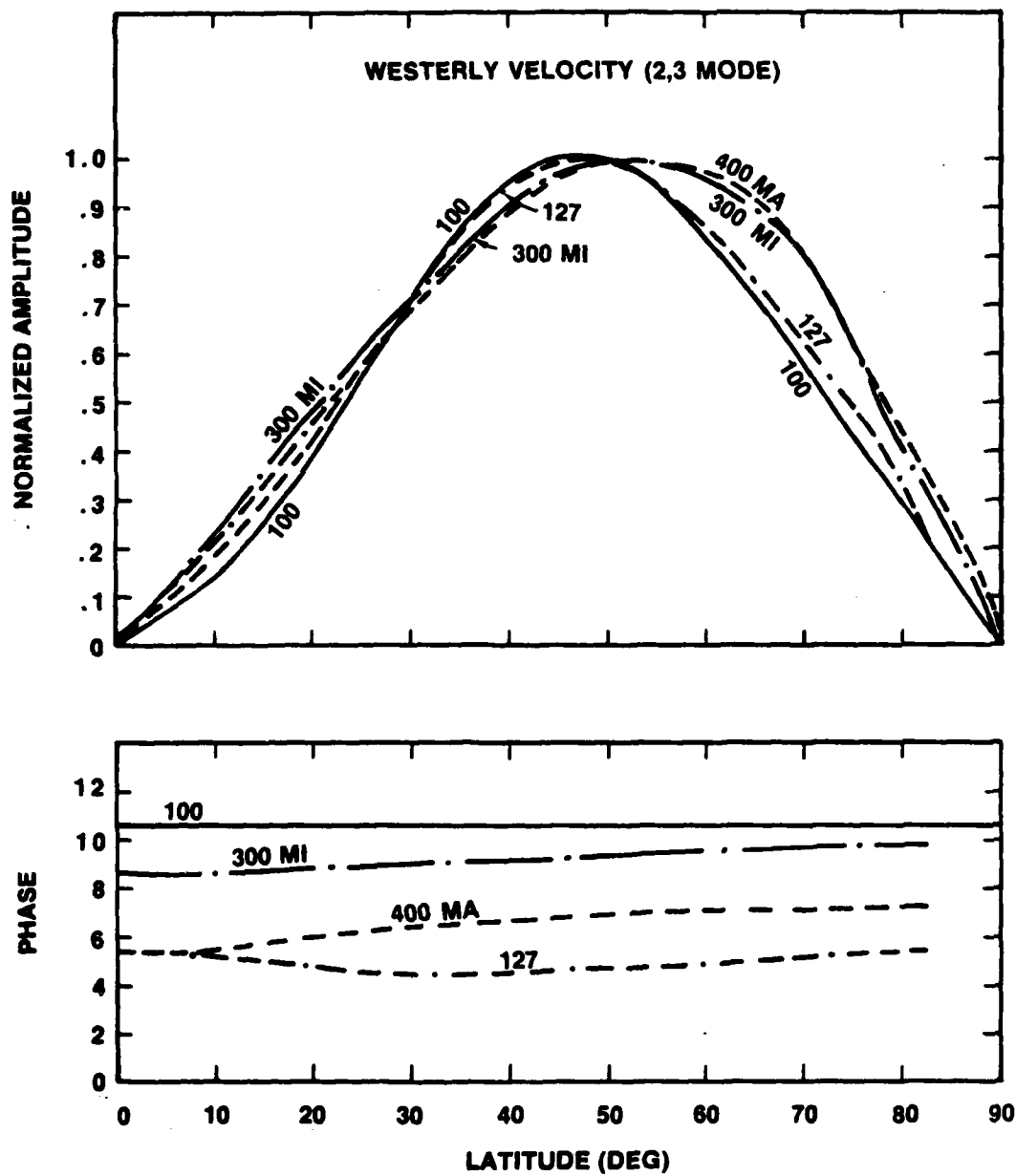


Fig. 22 — Same as 10 but for the 2,3 HME

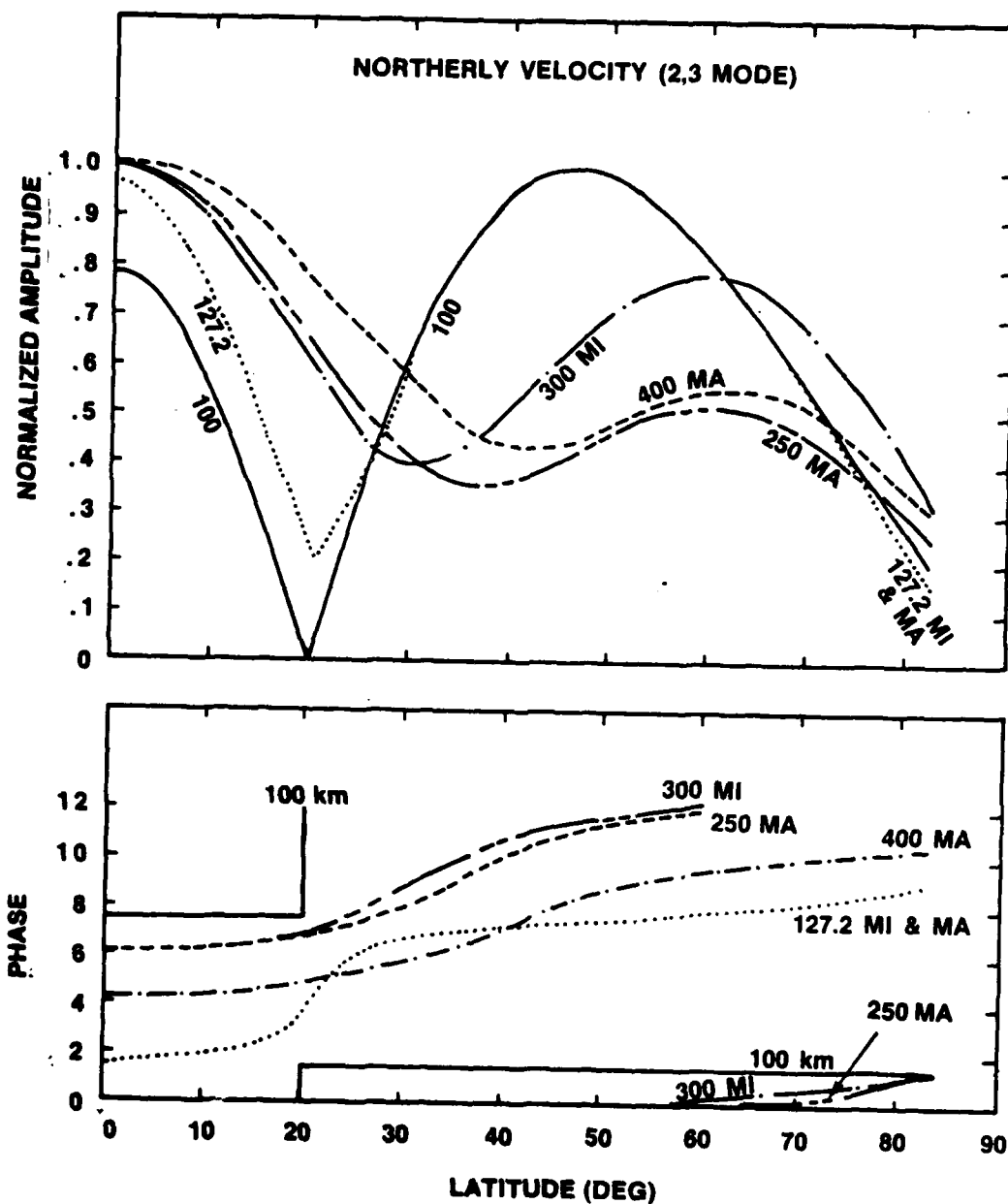


Fig. 23 — Same as 11 but for the 2,3 HME

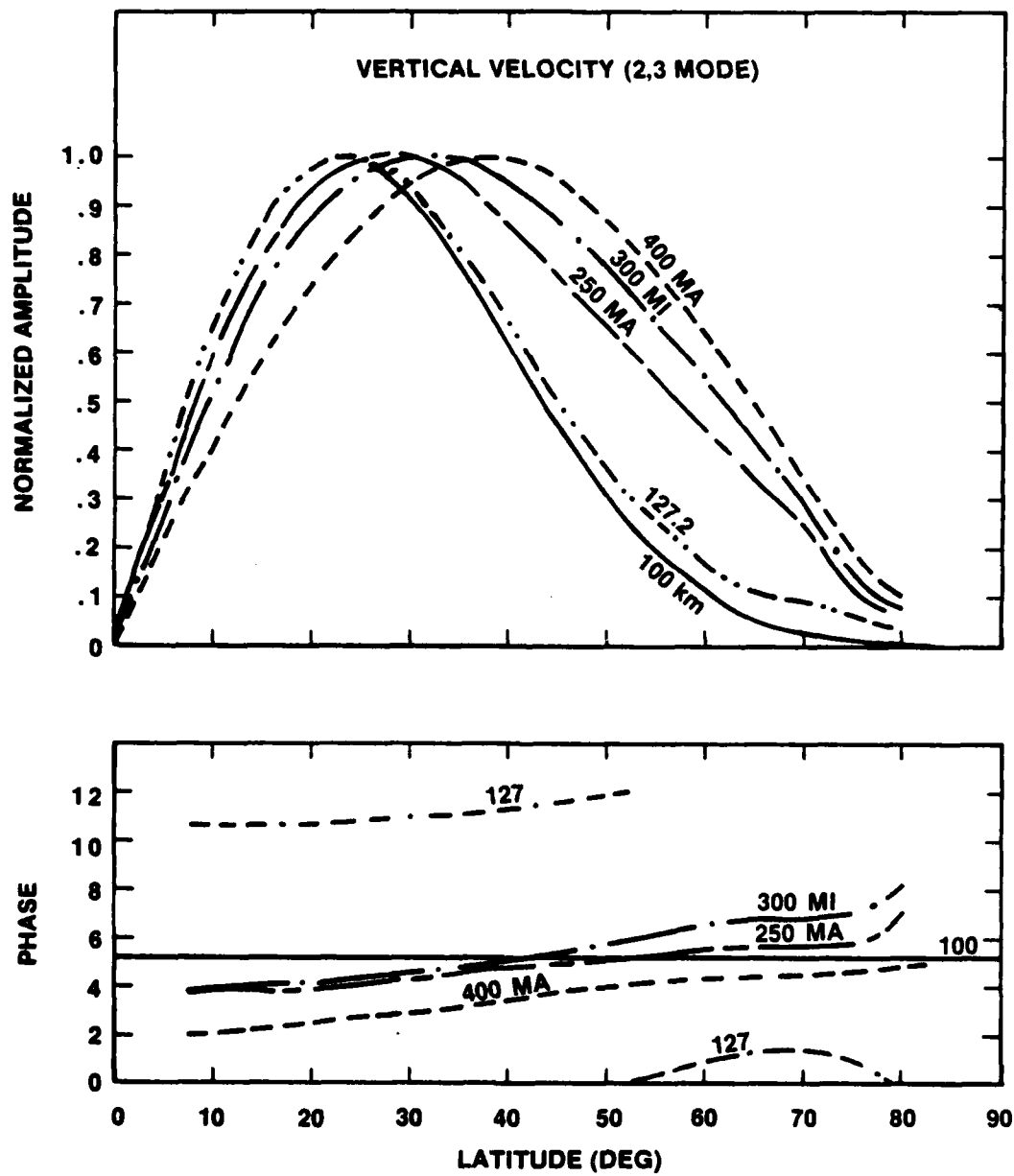


Fig. 24 — Same as 12 but for the 2,3 HME

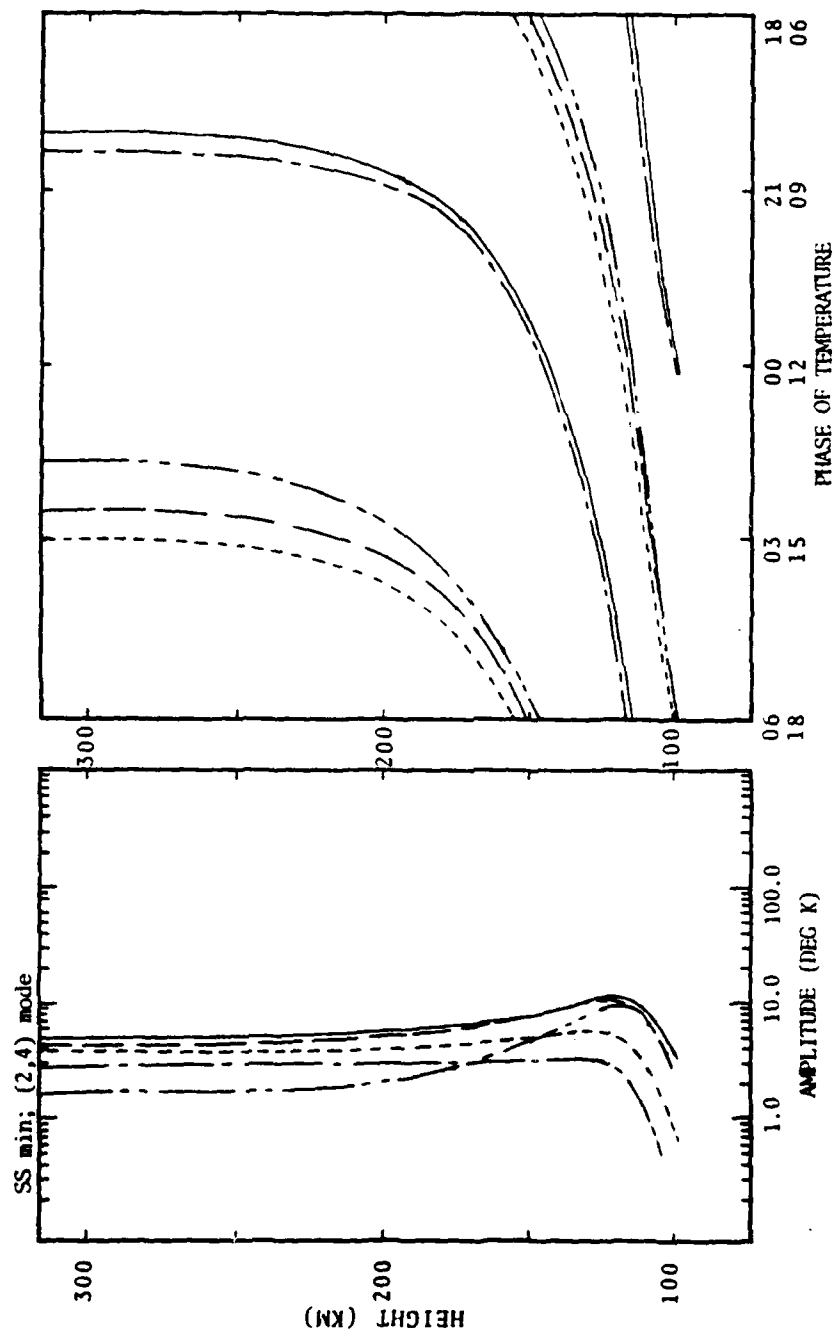


Fig. 25 — Same as 1 but for the 2,4 HME

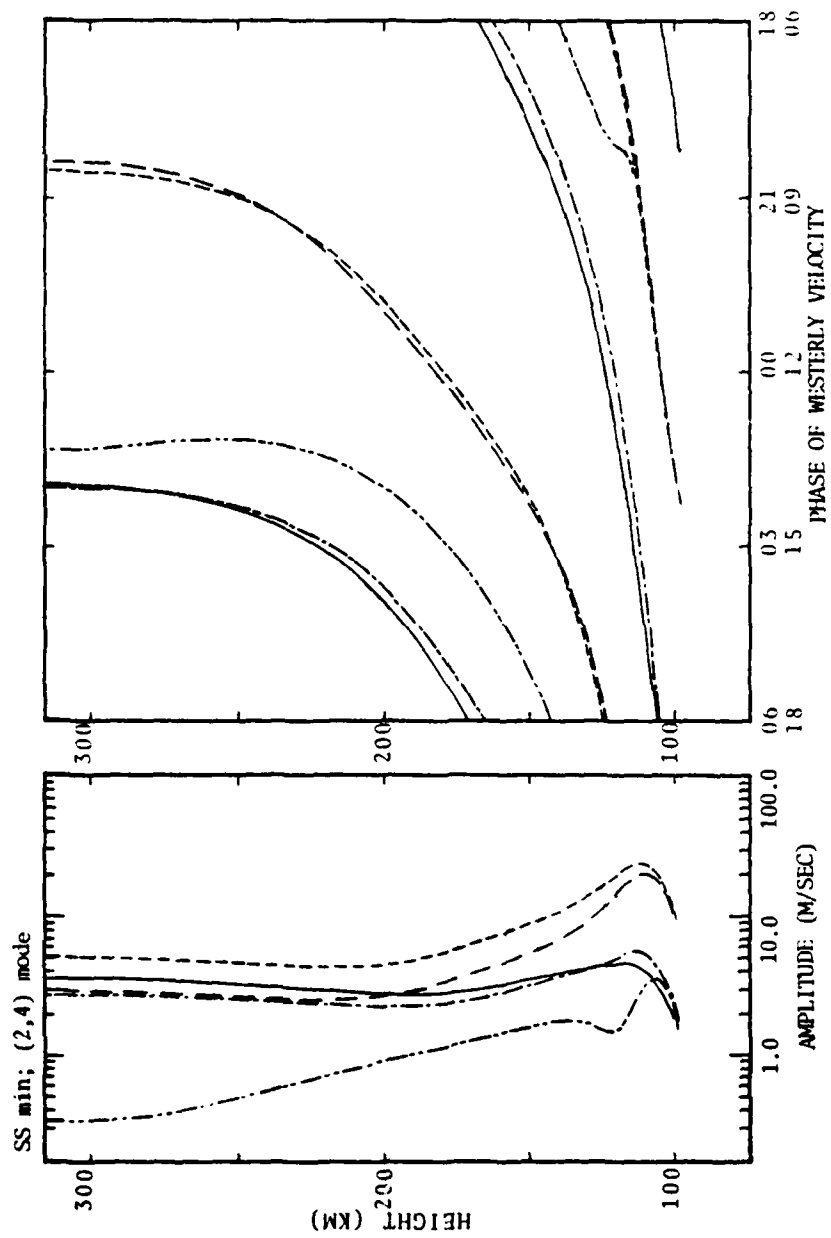


Fig. 26 — Same as 2 but for the 2,4 HME

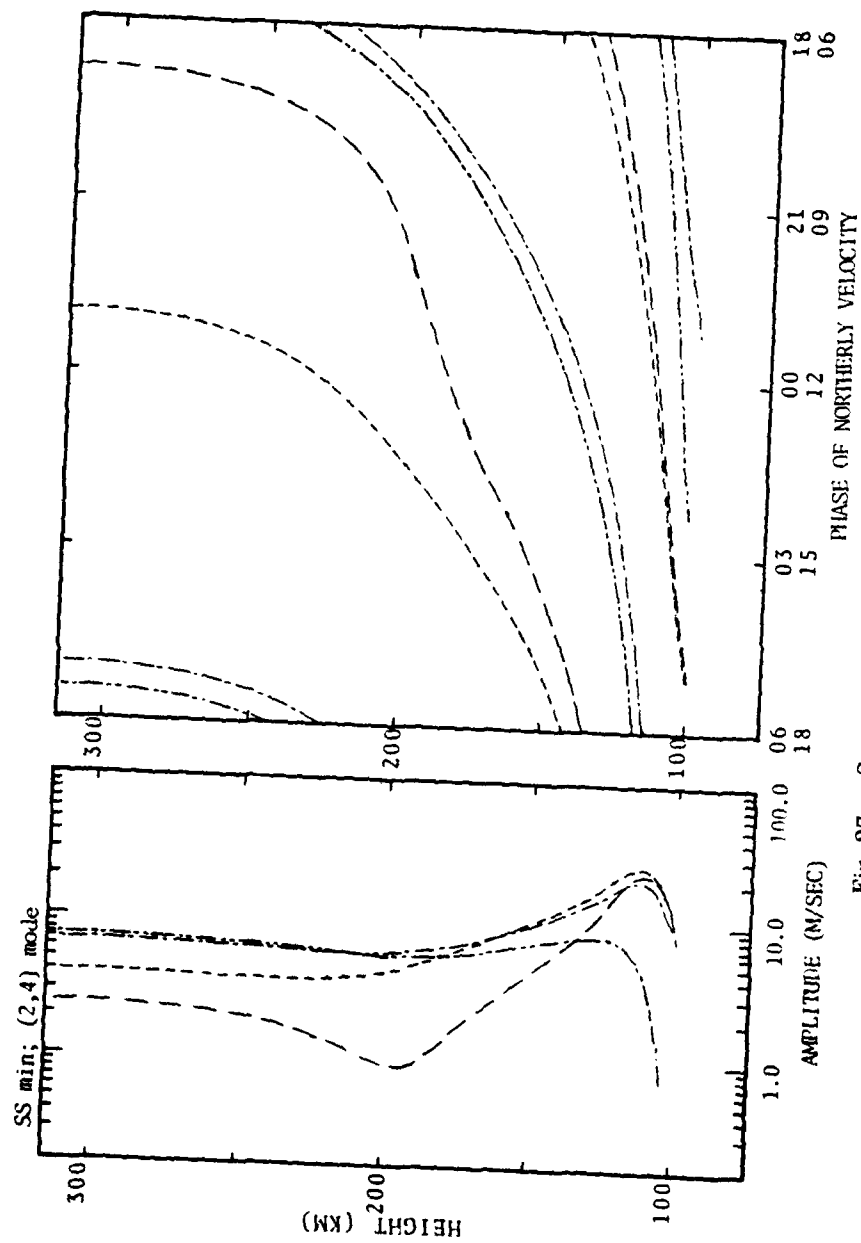


Fig. 27 — Same as 3 but for the 2,4 HME



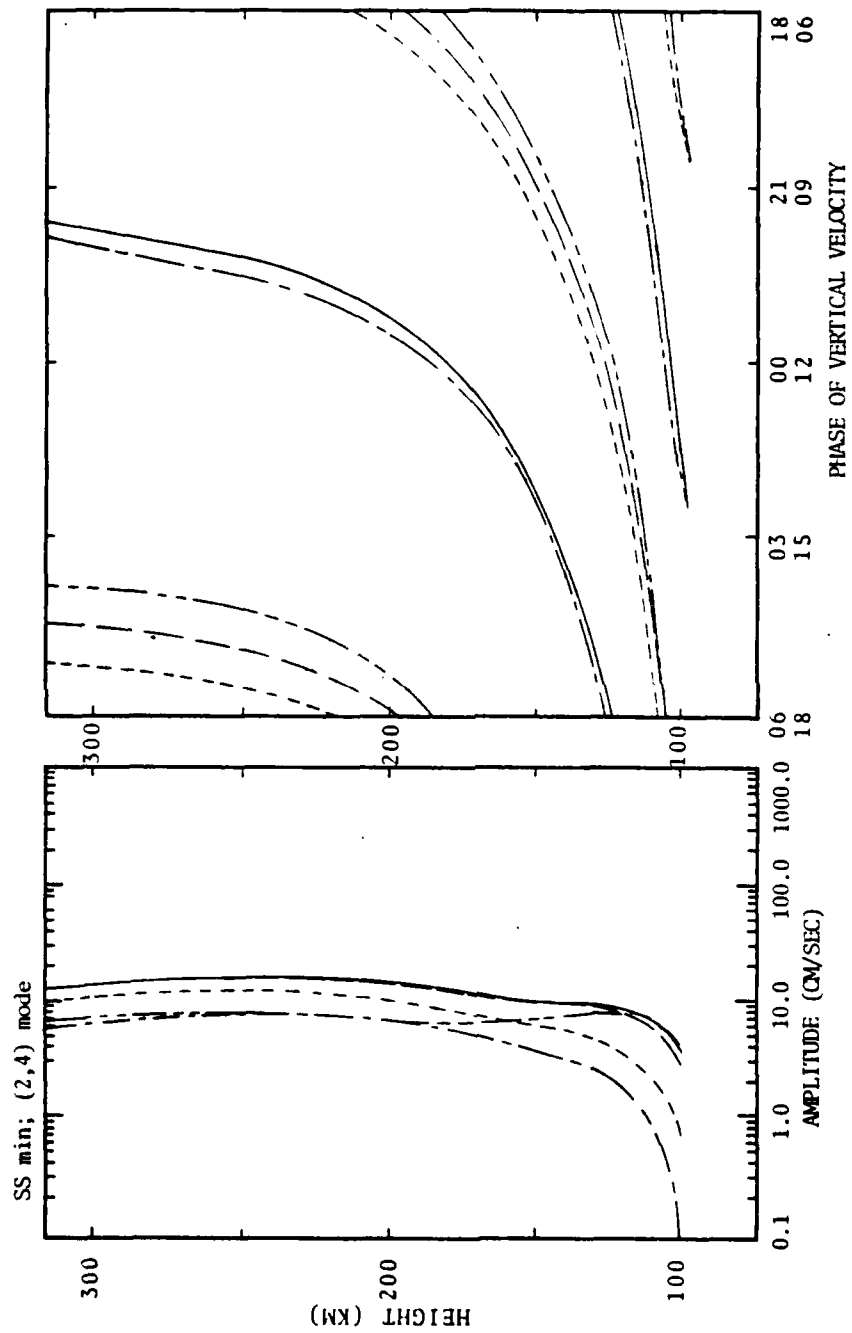


Fig. 28 — Same as 4 but for the 2,4 HIME

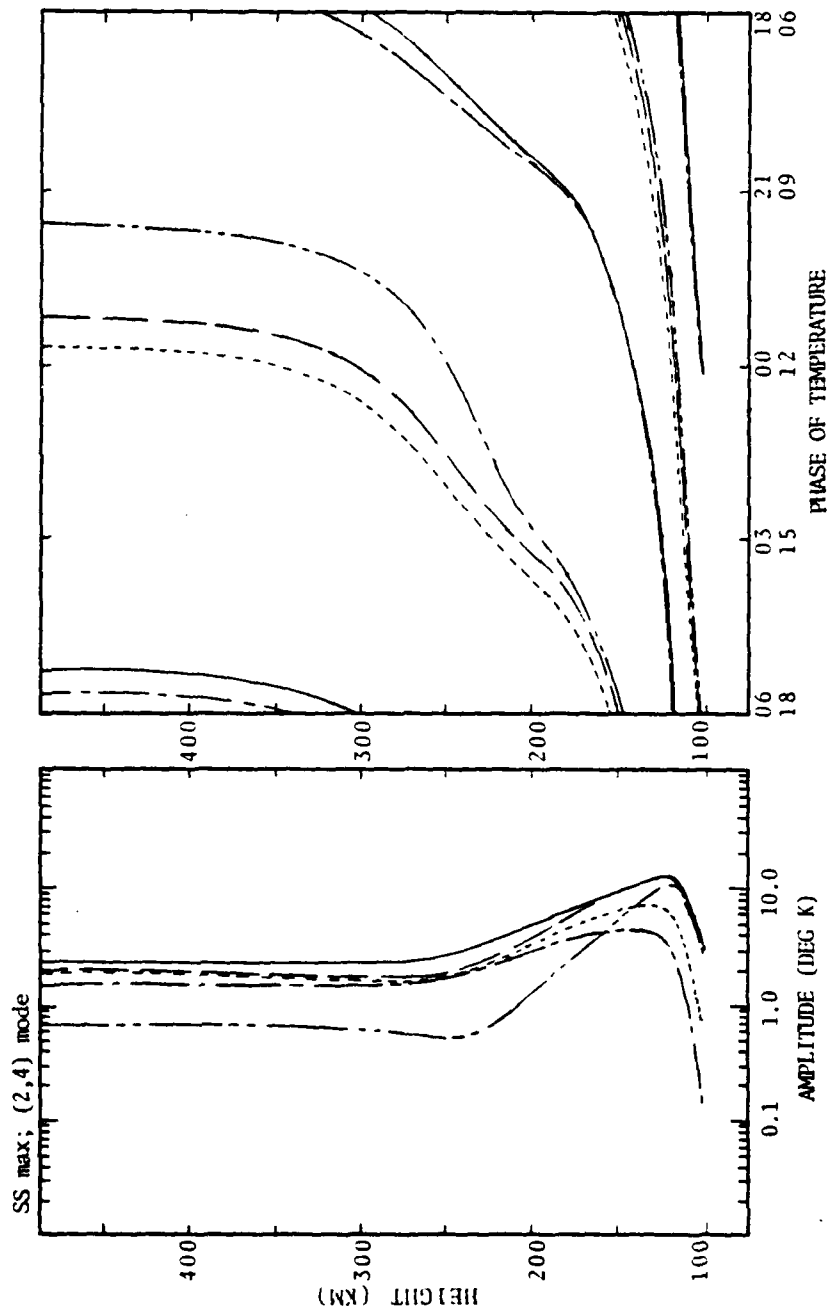


Fig. 29 — Same as 5 but for the 2,4 HME

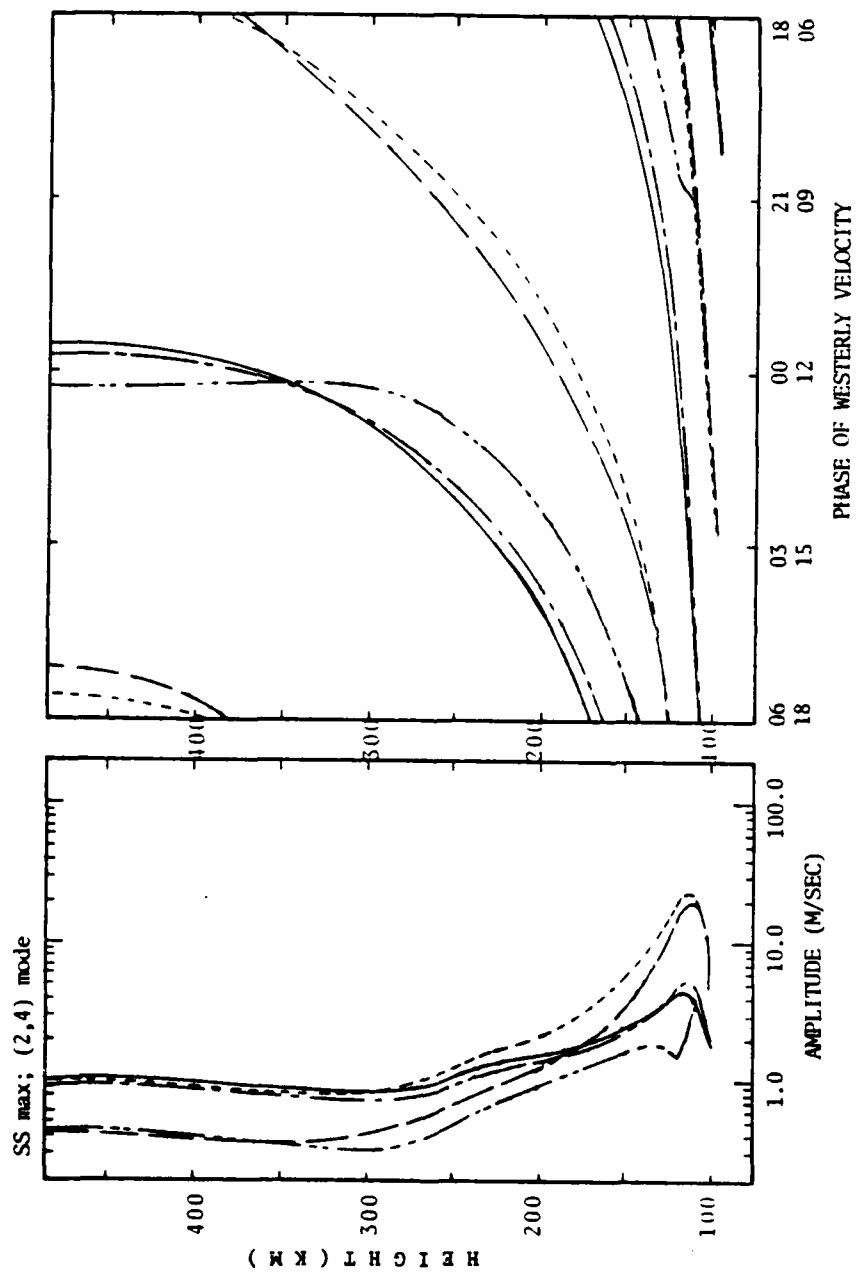


Fig. 30 — Same as 6 but for the 2,4 HME

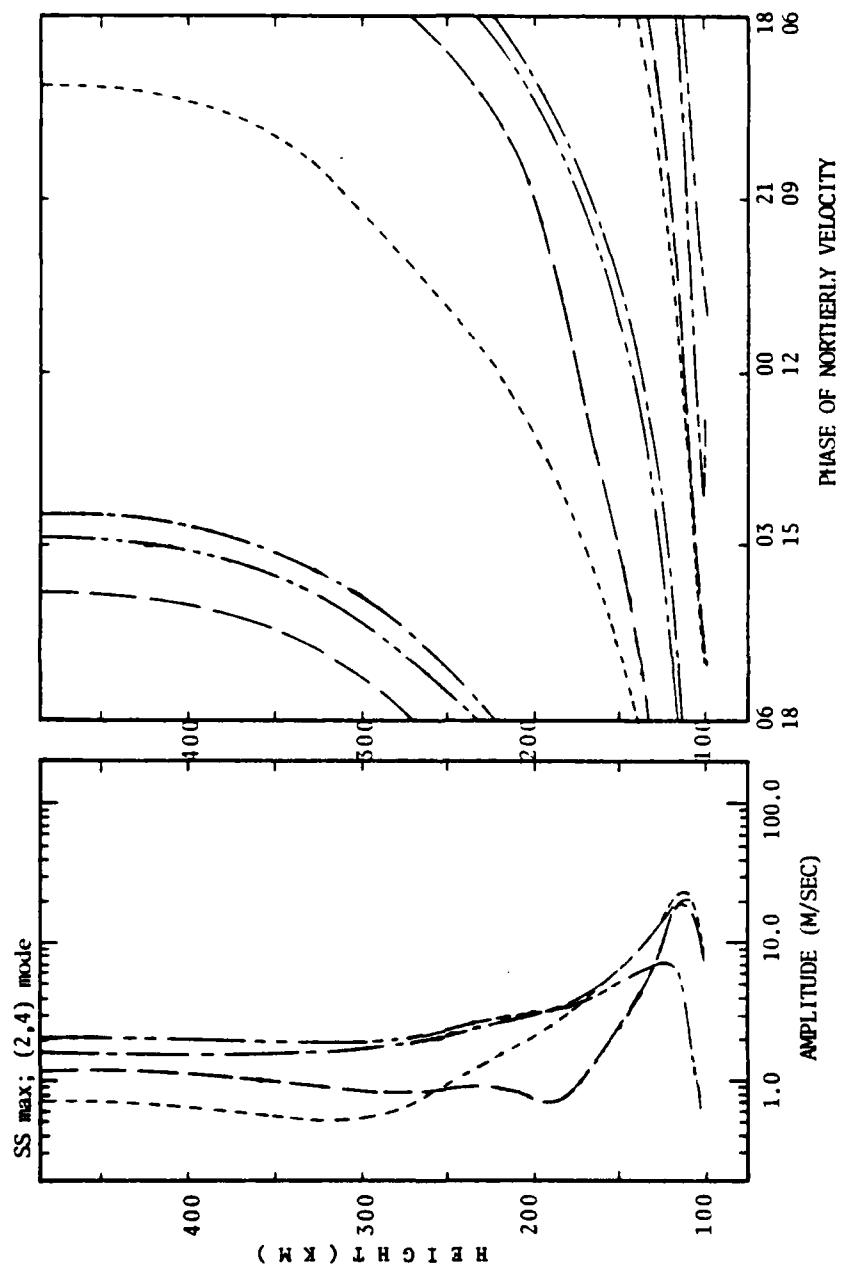


Fig. 31 — Same as 7 but for the 2,4 HME

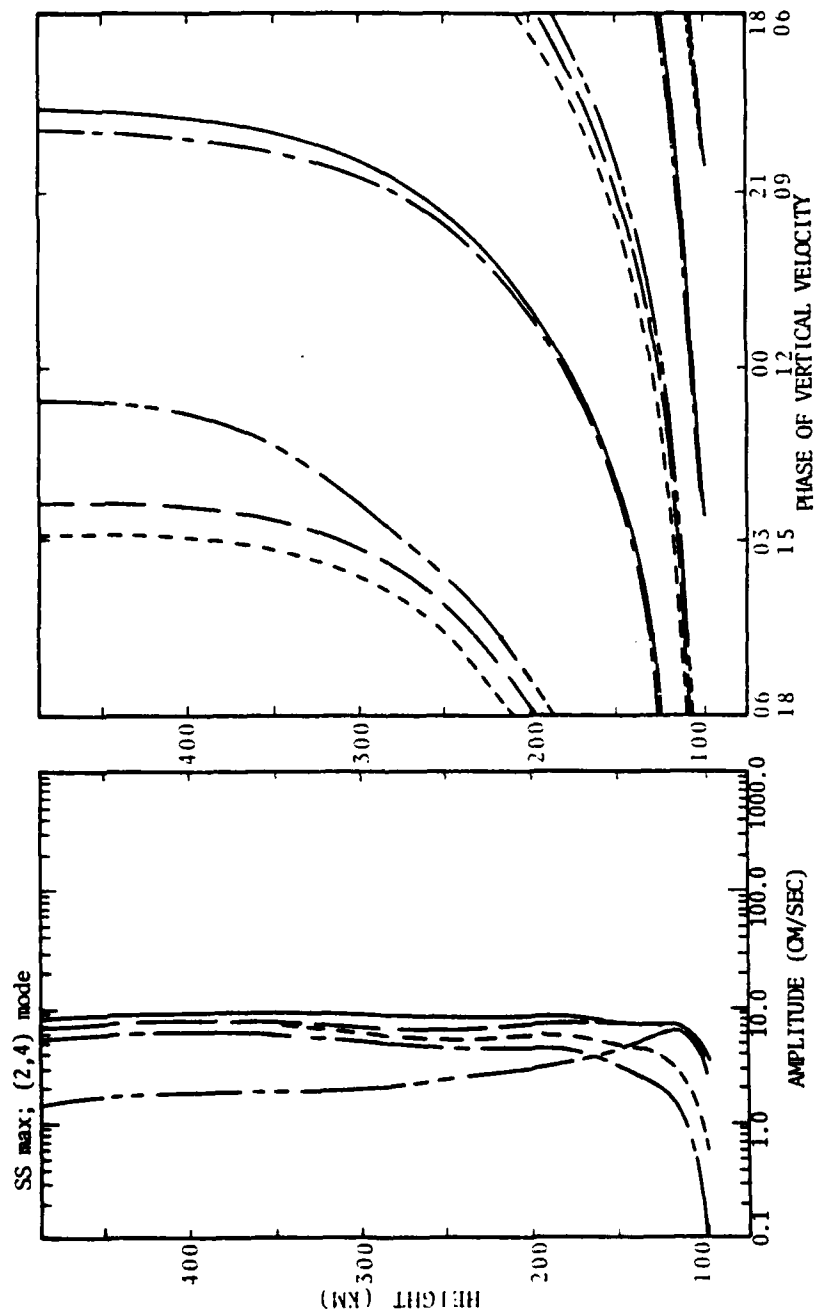


Fig. 32 — Same as 8 but for the 2,4 HME

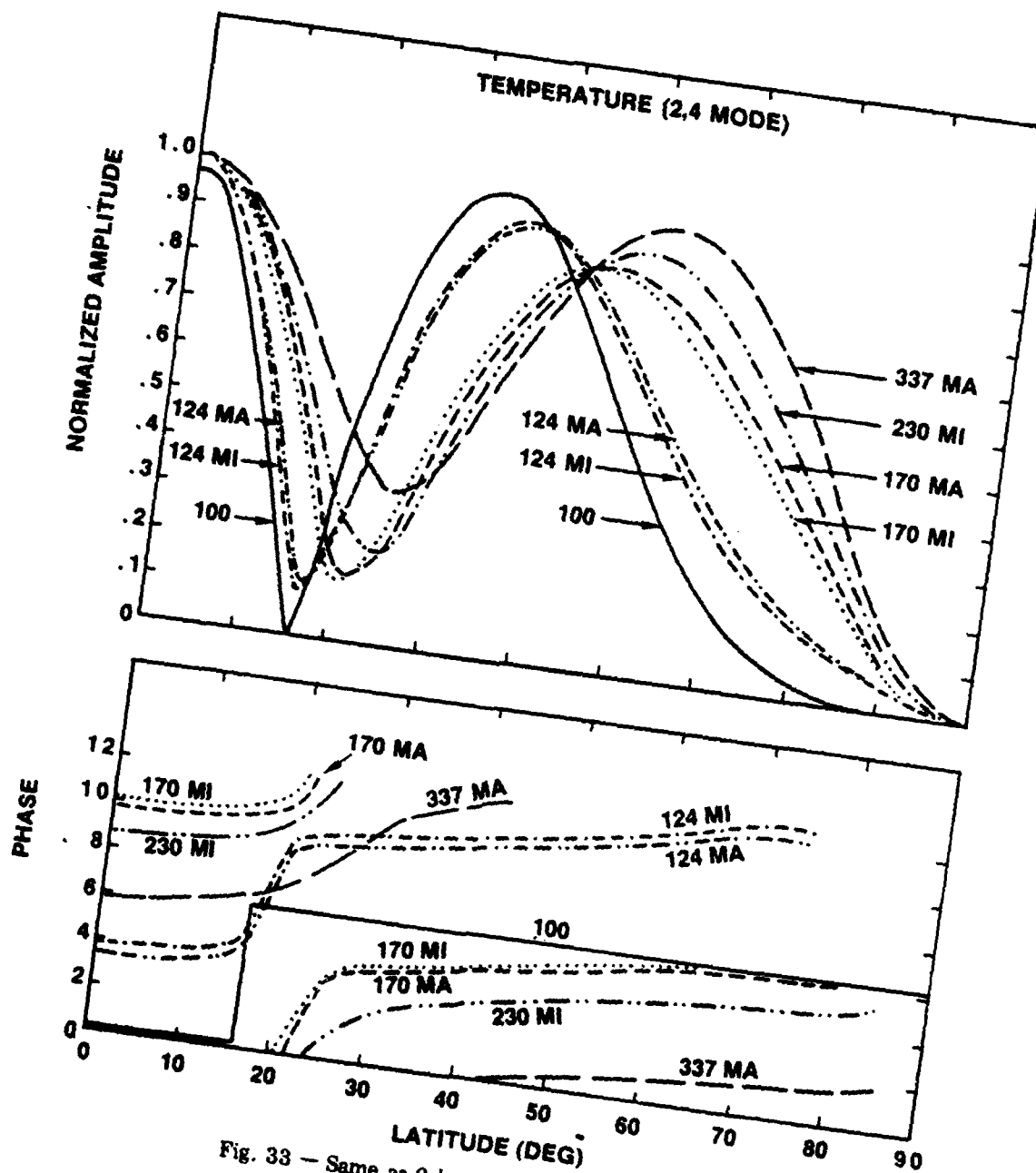


Fig. 33 - Same as 9 but for the 2,4 HME

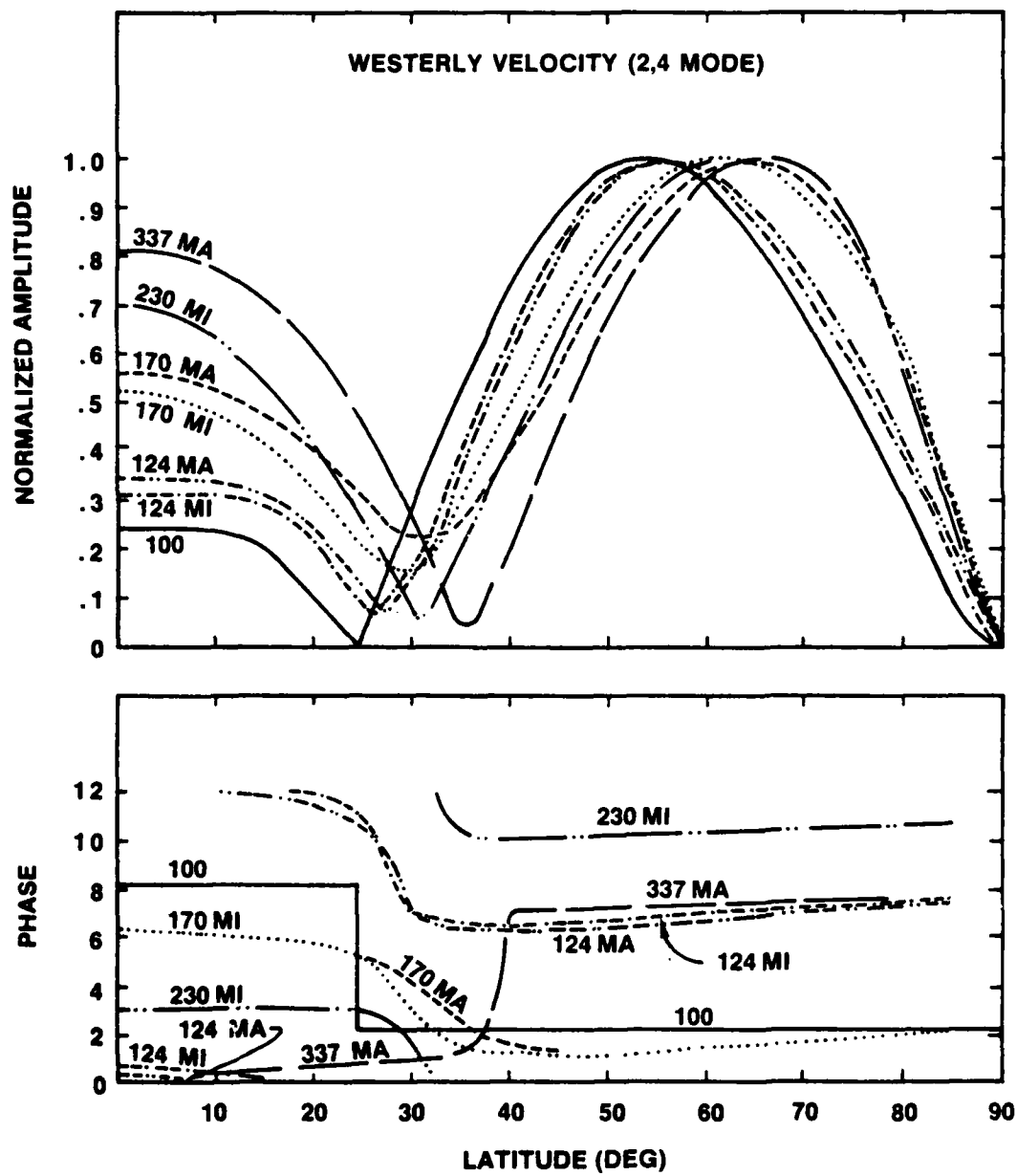


Fig. 34 — Same as 10 but for the 2,4 HME

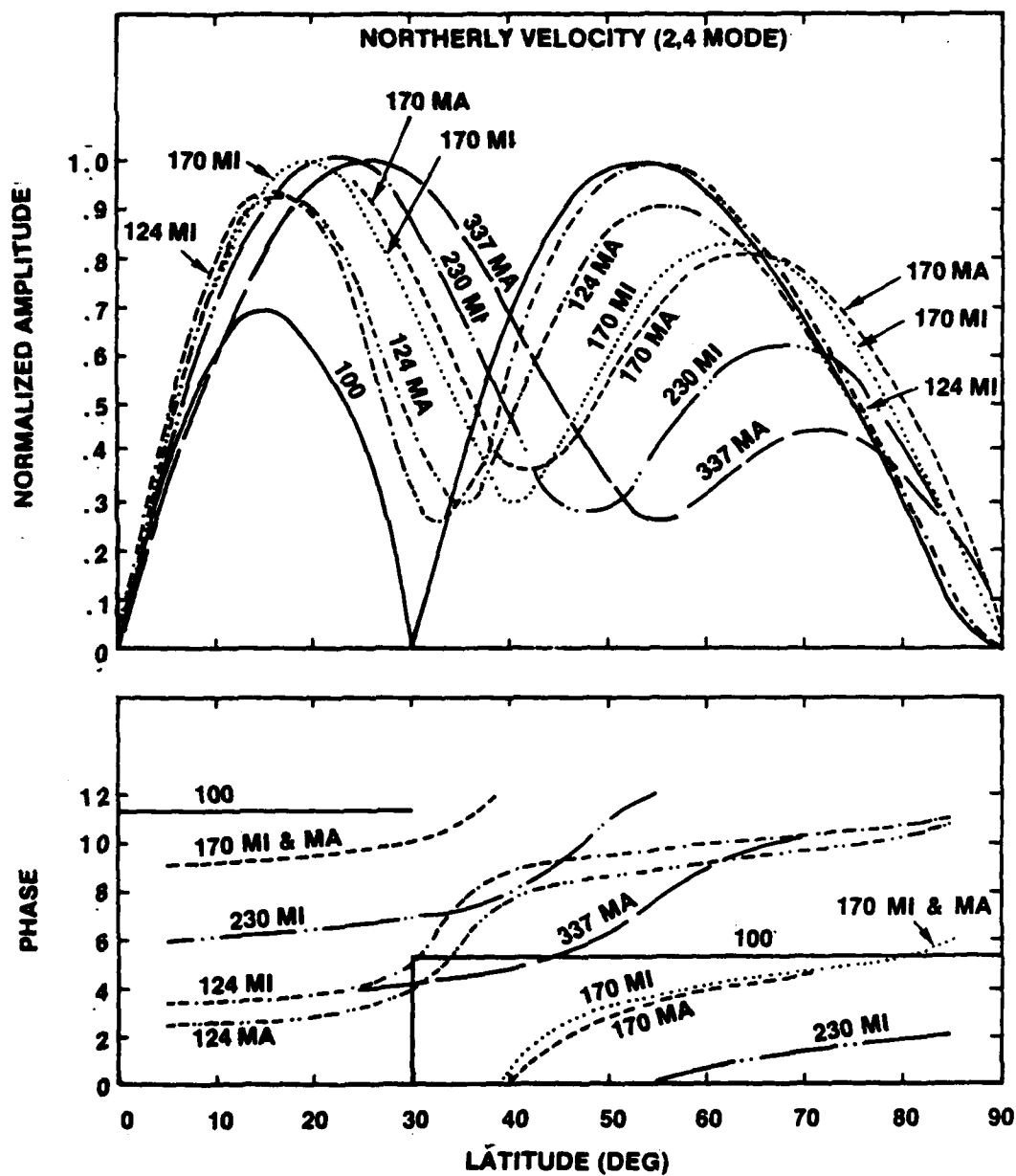


Fig. 35 — Same as 11 but for the 2,4 HME



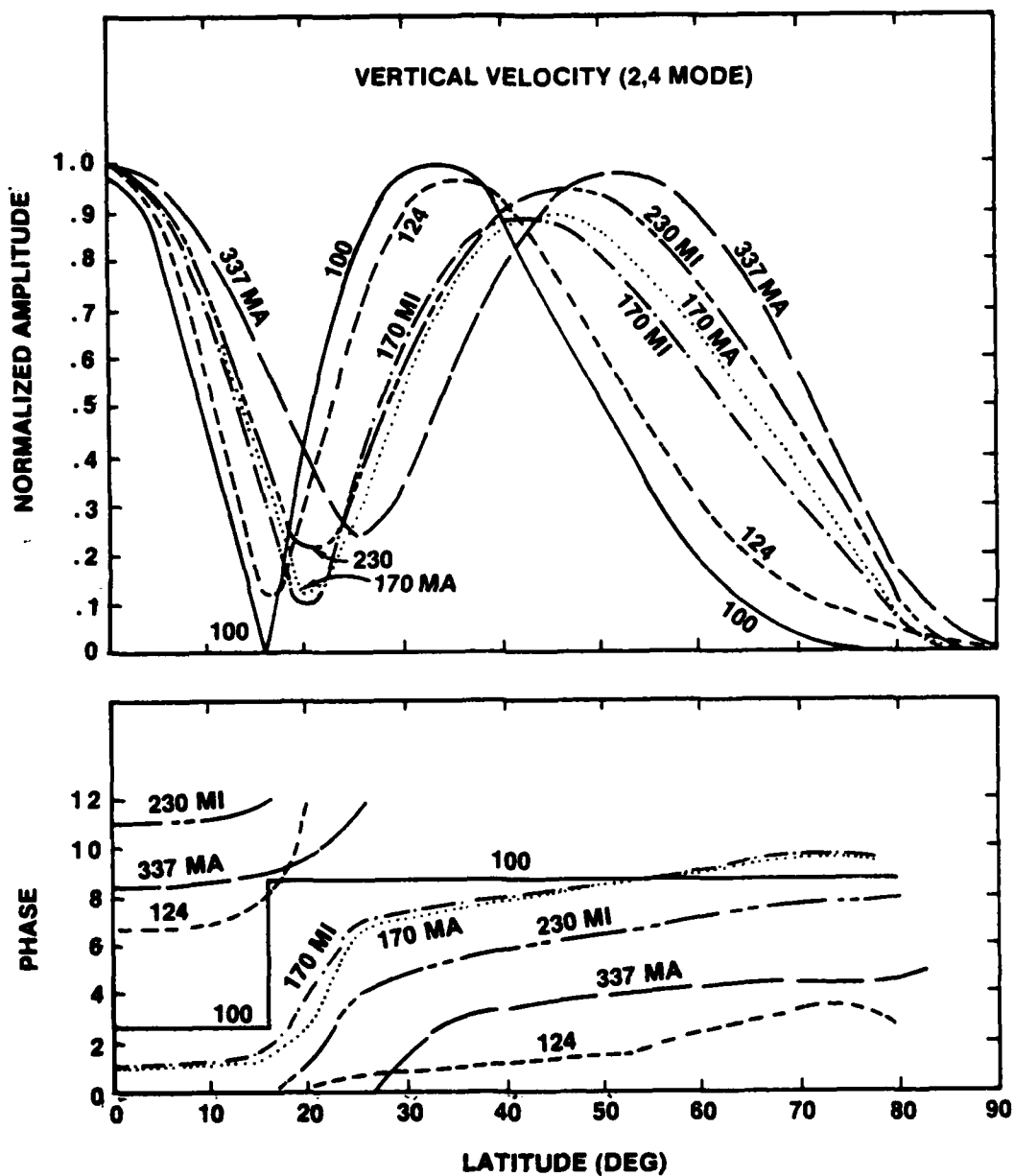


Fig. 36 — Same as 12 but for the 2,4 HME

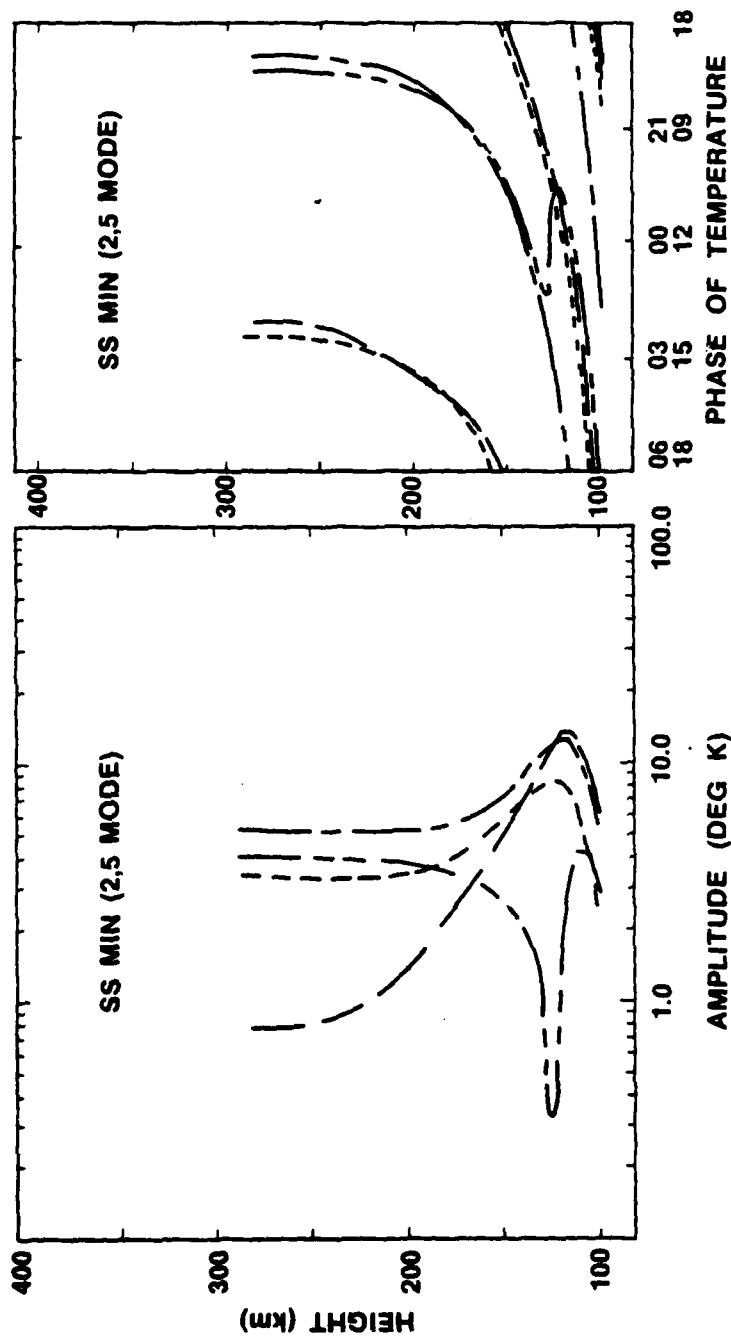


Fig. 37 — Same as 1 but for the 2,5 HME

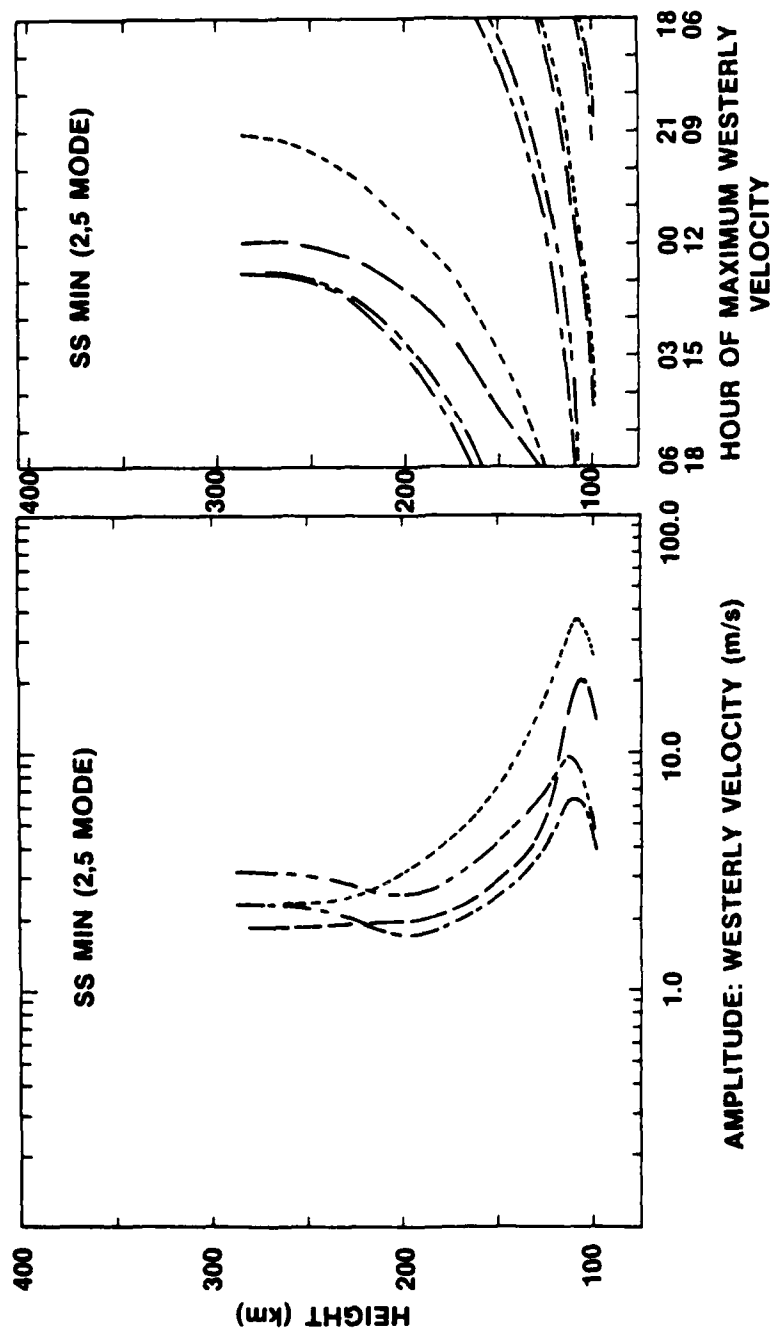


Fig. 38 — Same as 2 but for the 2,5 HME

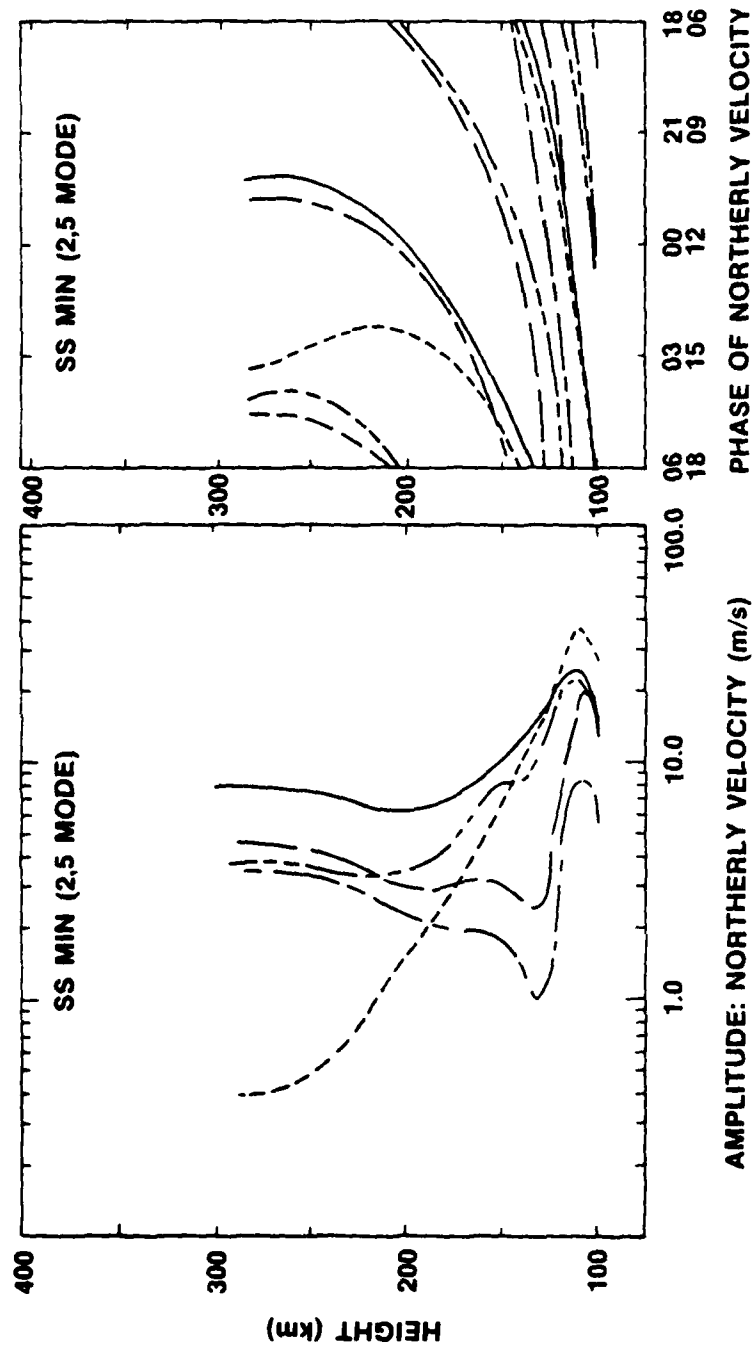


Fig. 39 — Same as 3 but for the 2,5 HME

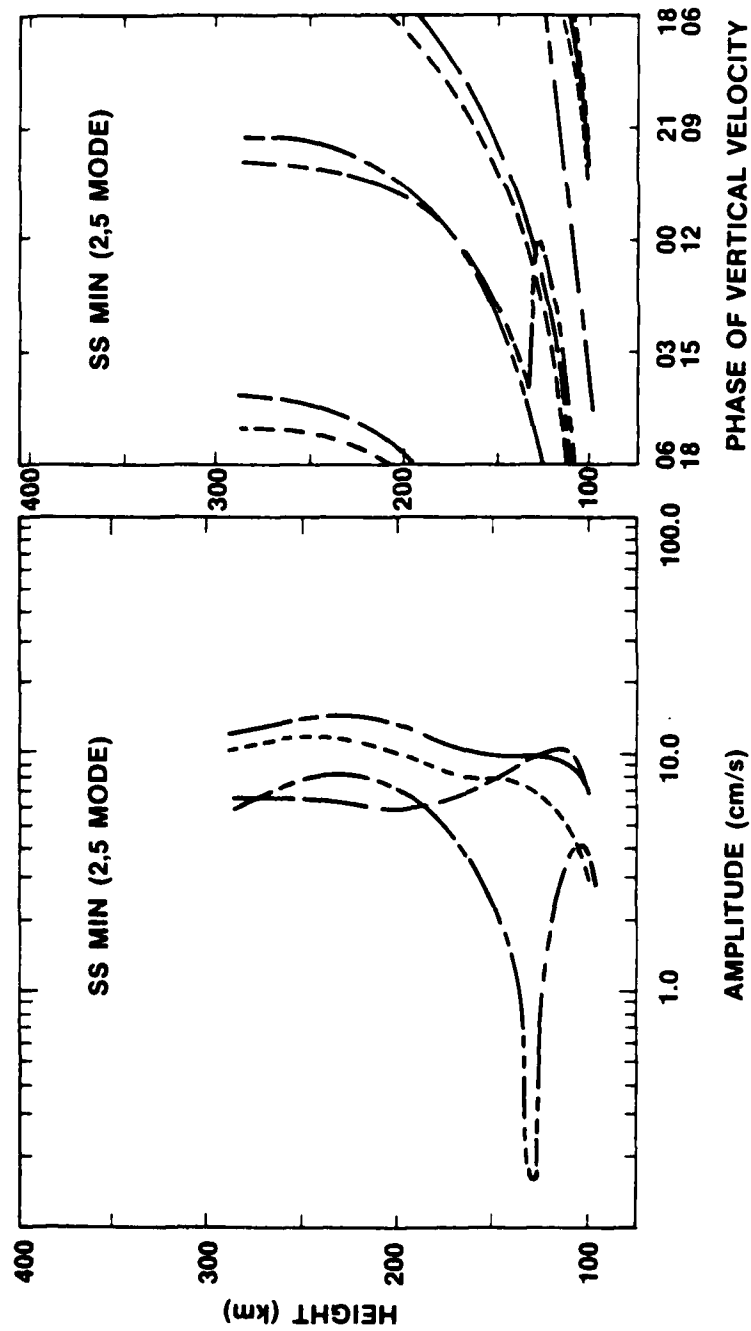


Fig. 40 — Same as 4 but for the 2,5 HME

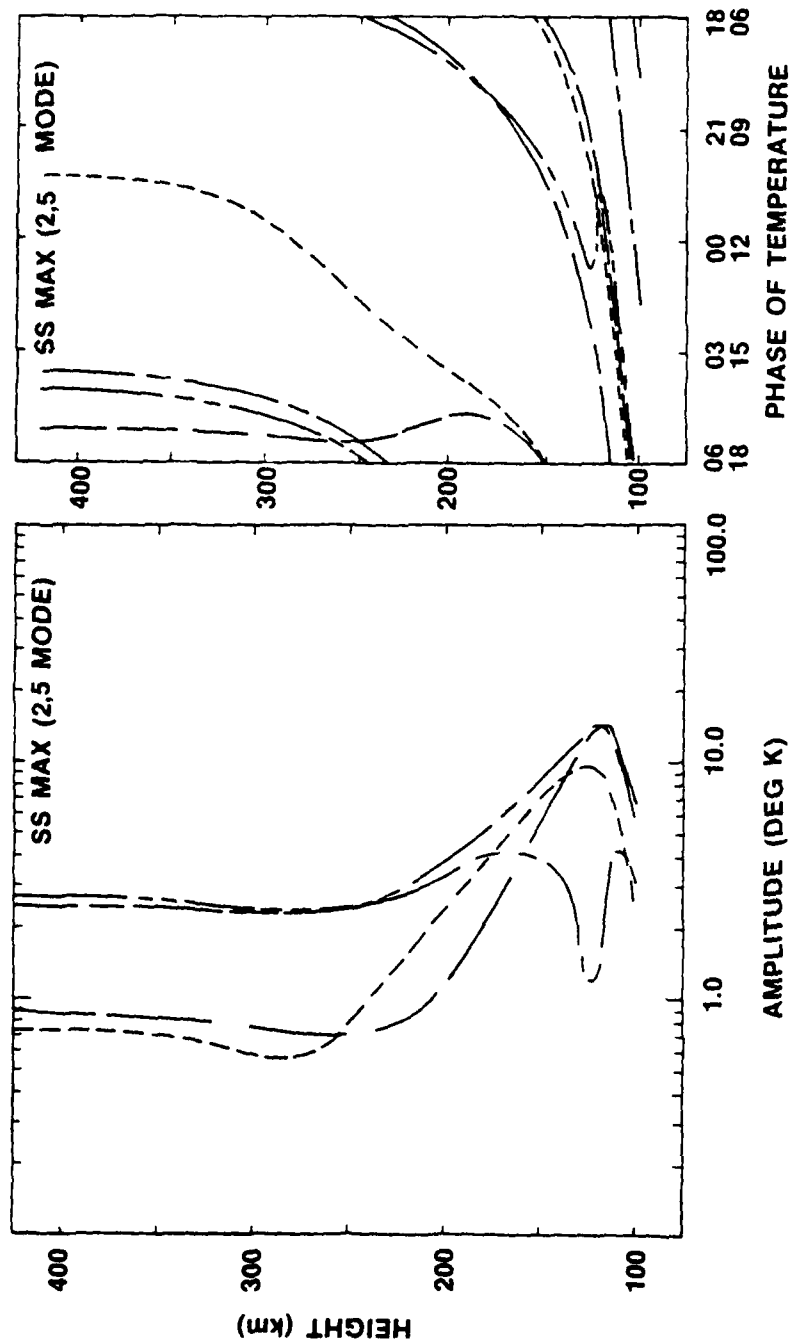


Fig. 41 — Same as 5 but for the 2,5 HME

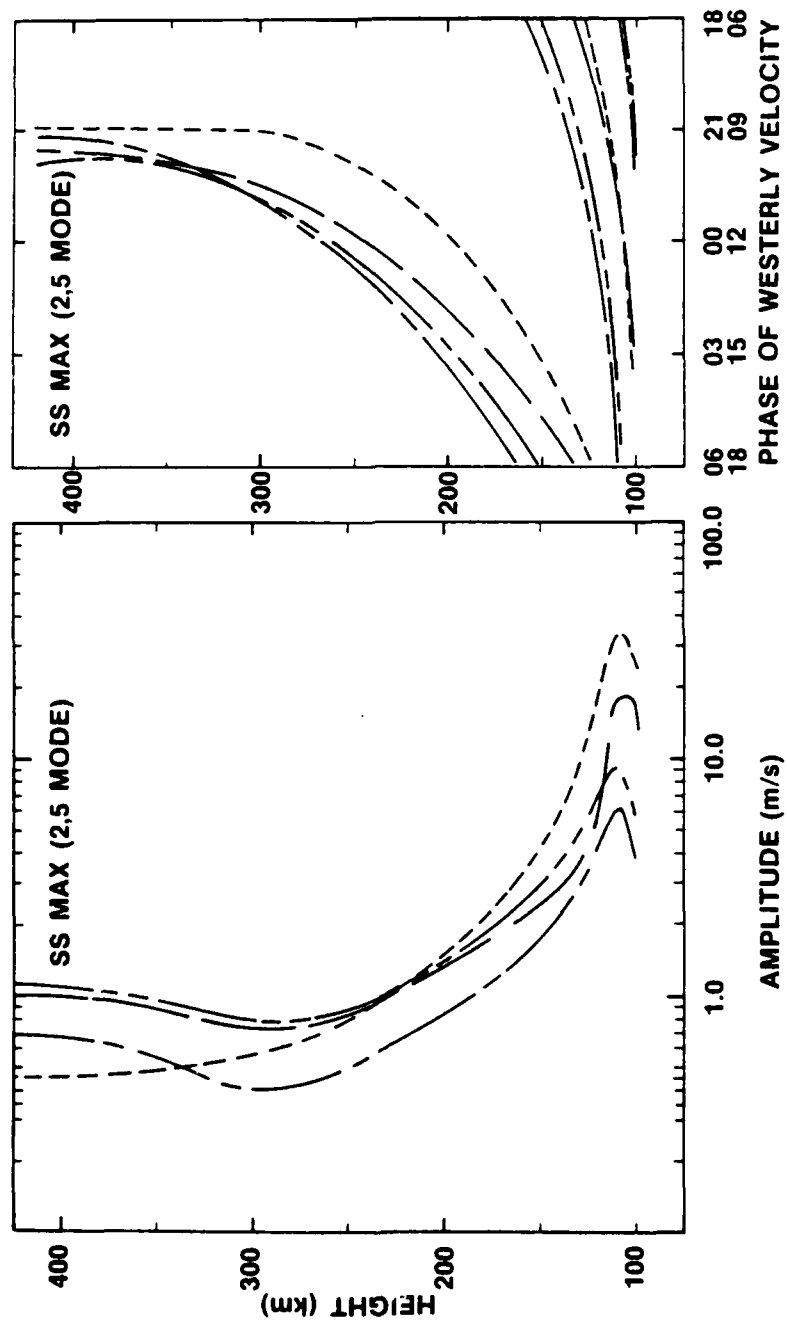


Fig. 42 — Same as 6 but for the 2,5 IIME





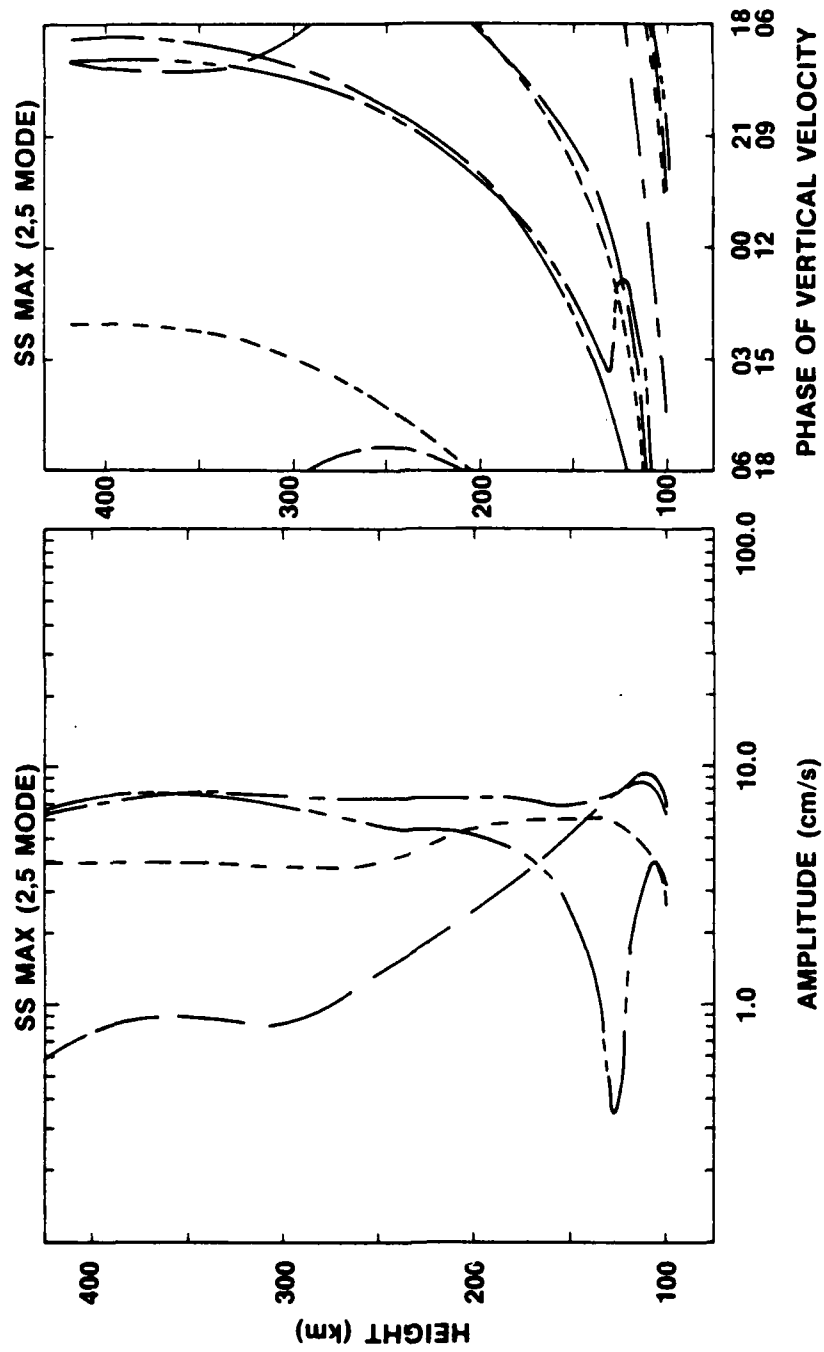


Fig. 44 — Same as 8 but for the 2,5 HME

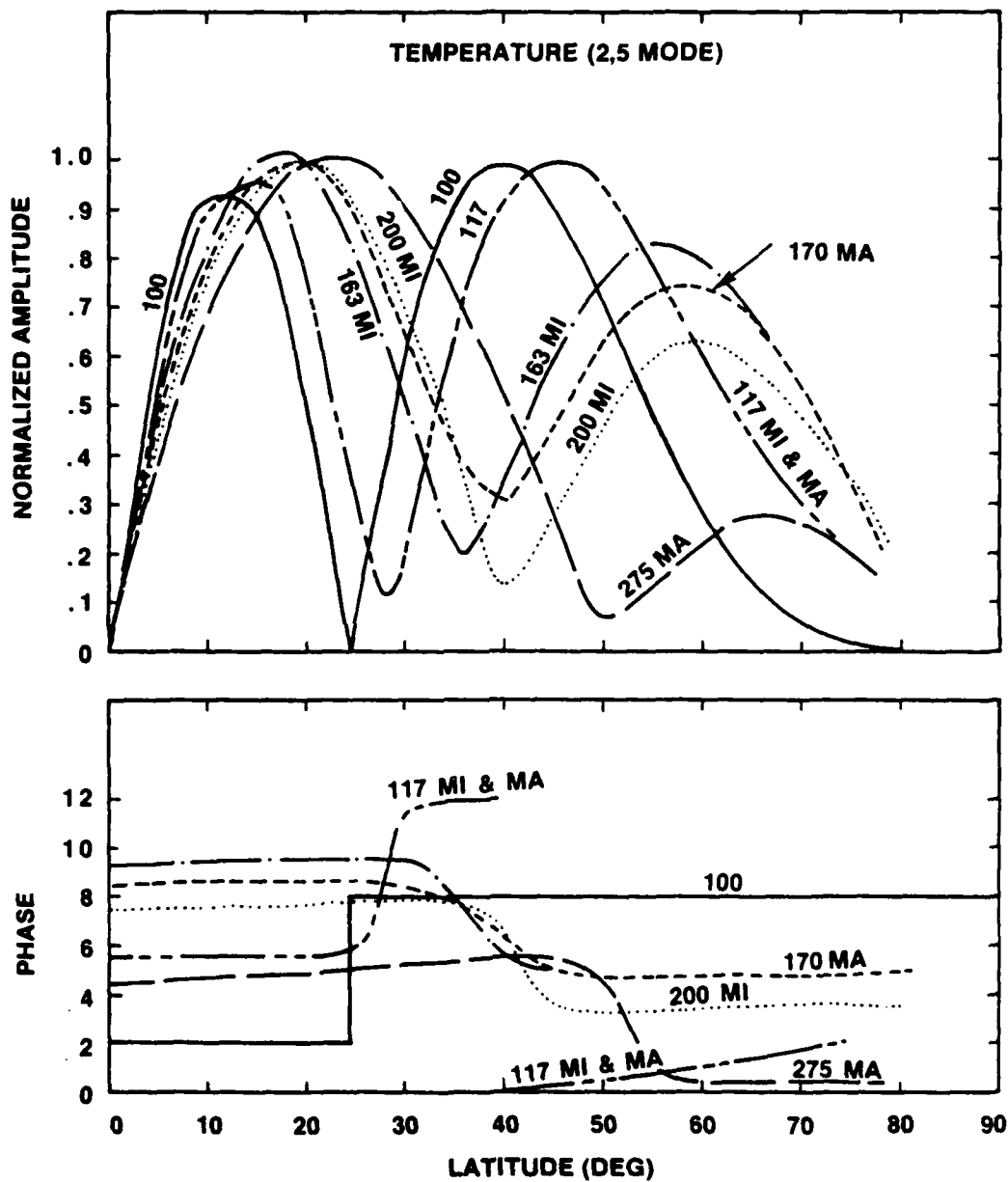


Fig. 45 — Same as 9 but for the 2,5 HME

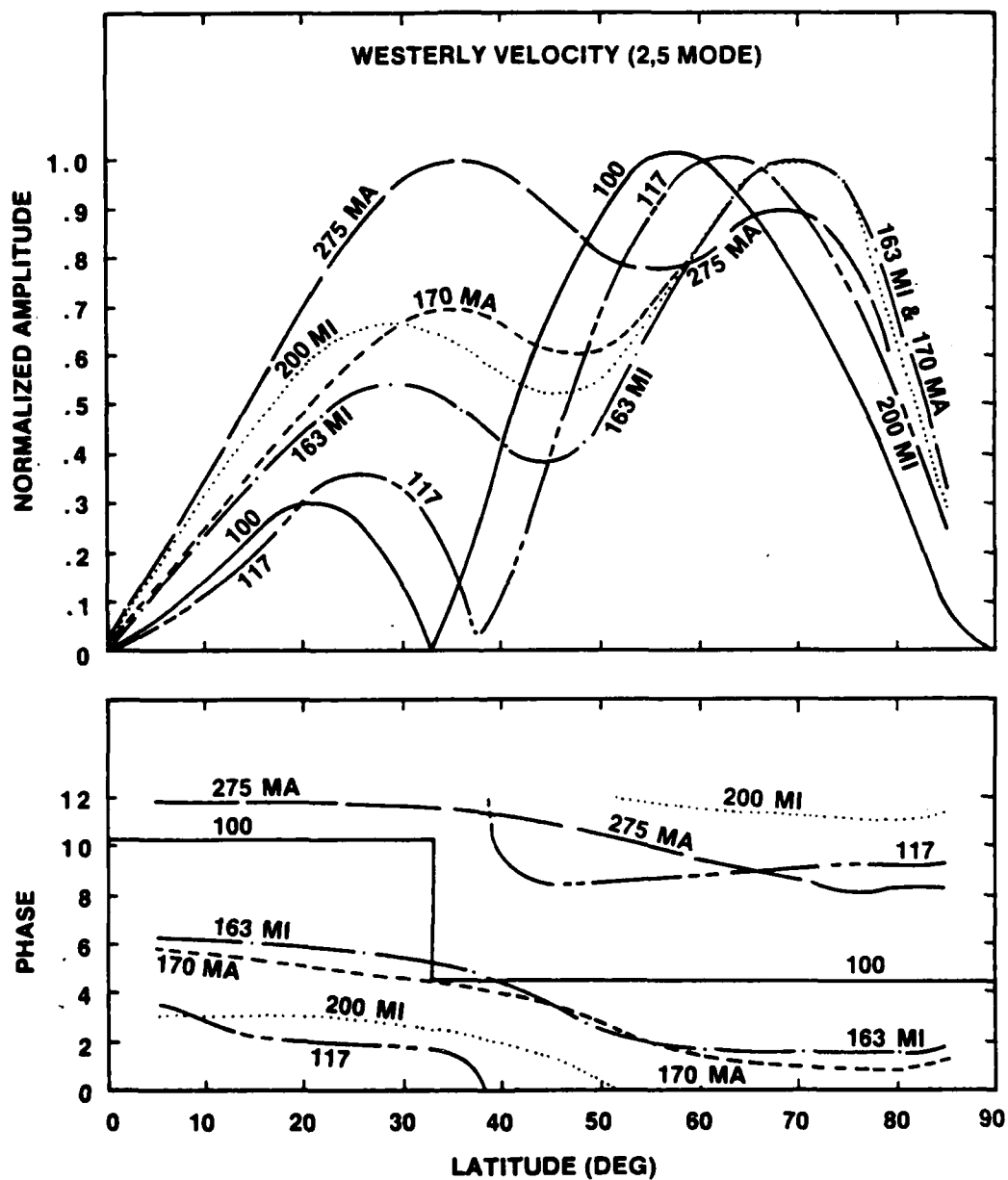


Fig. 46 — Same as 10 but for the 2,5 HME

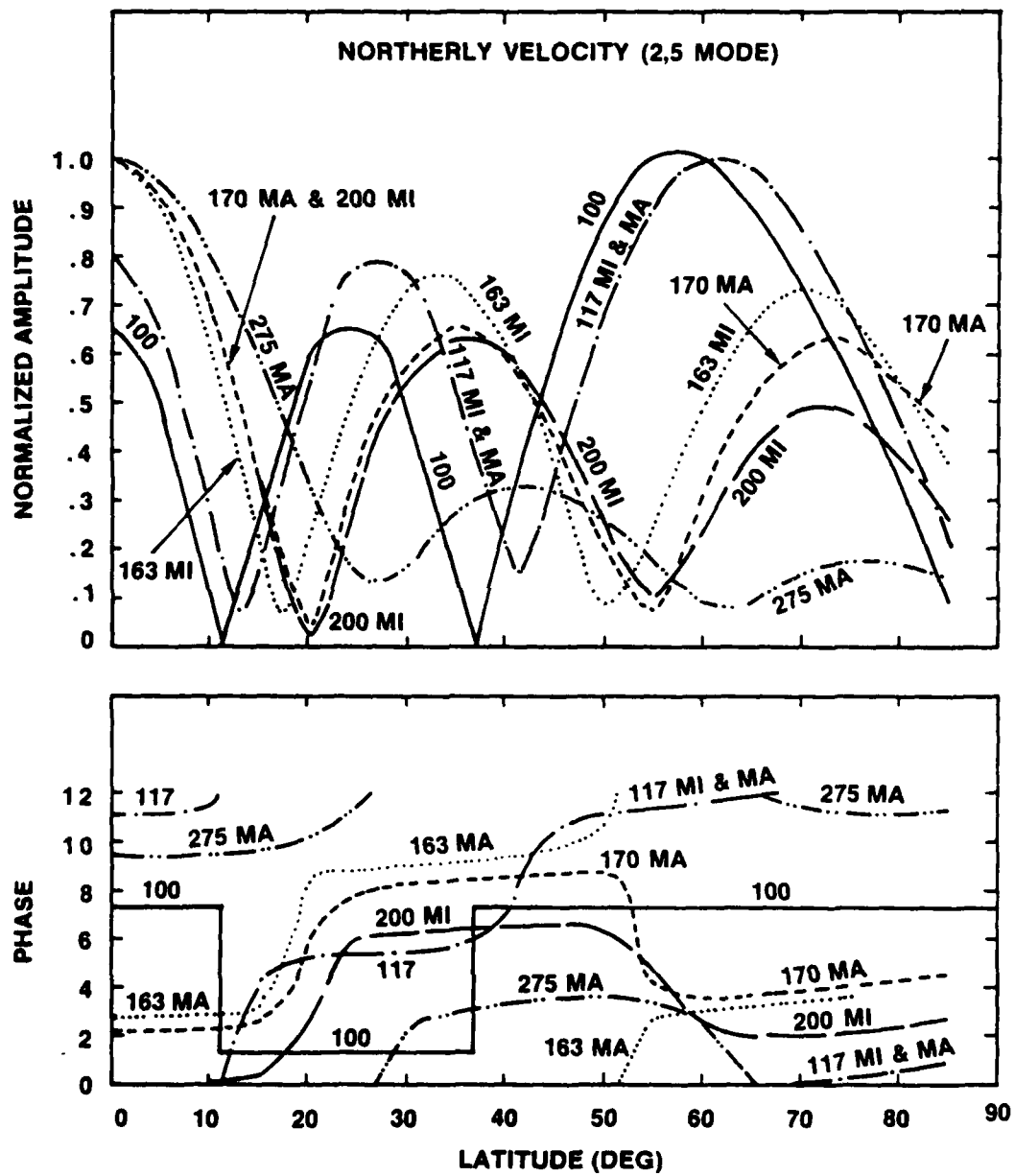


Fig. 47 — Same as 11 but for the 2,5 HME

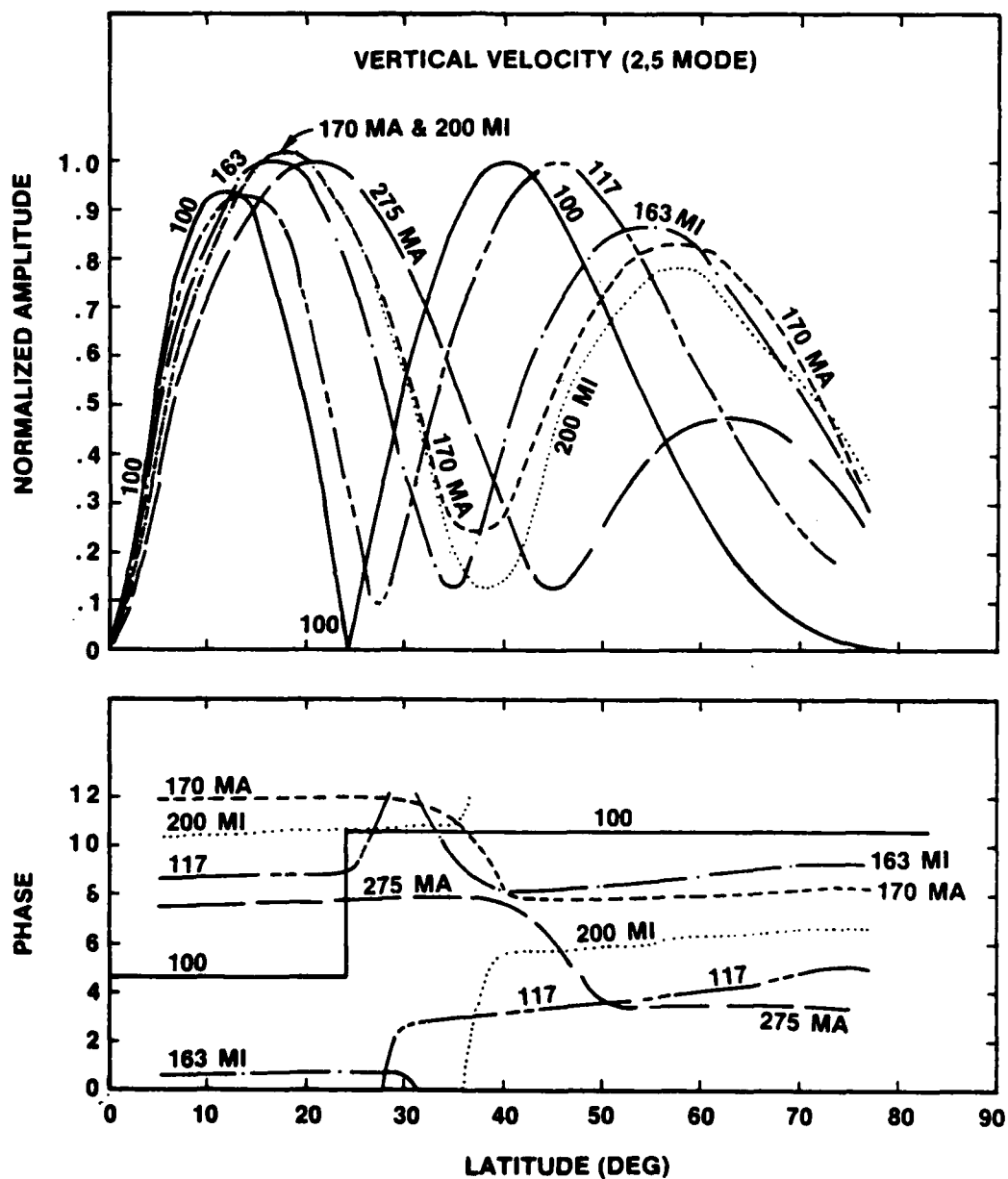


Fig. 48 — Same as 12 but for the 2,5 HME

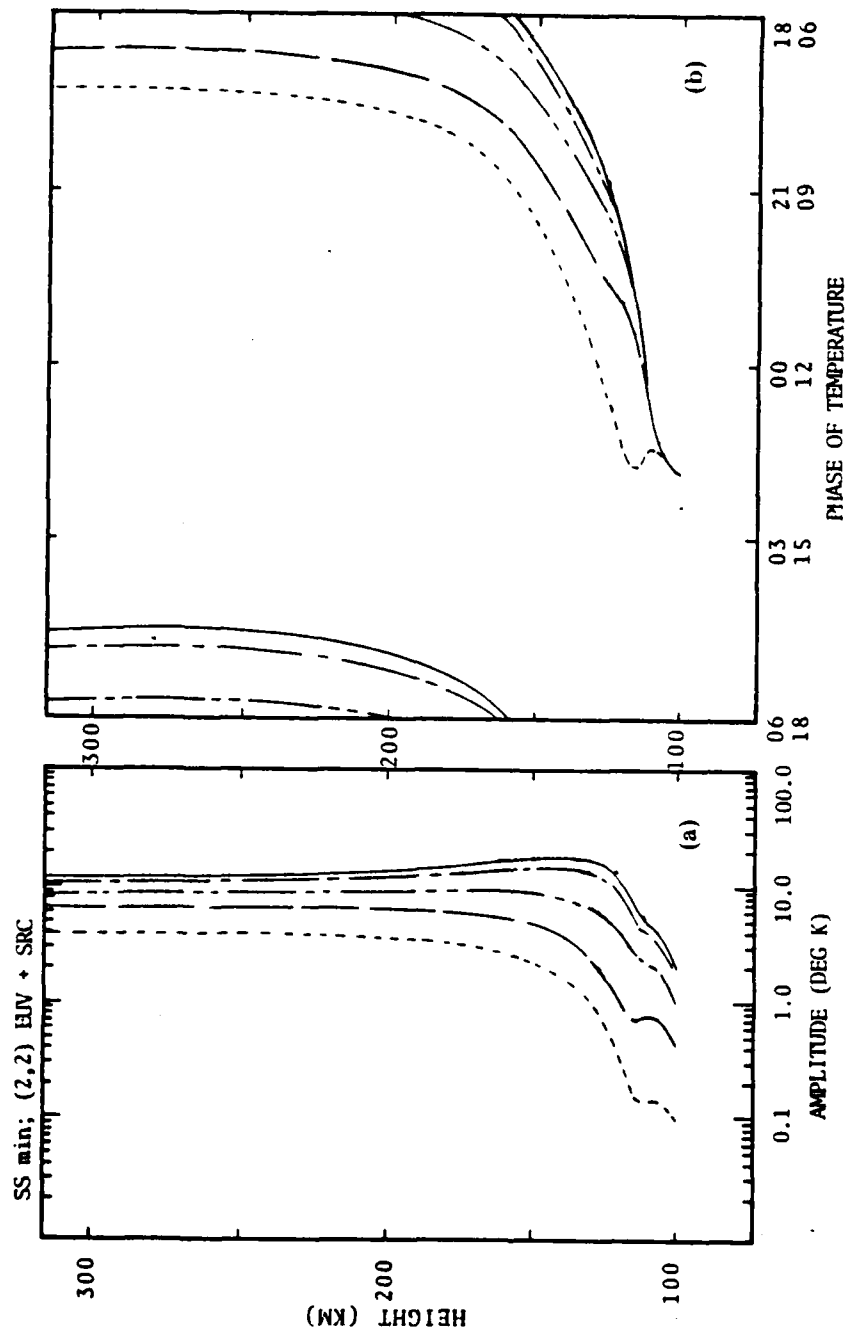


Fig. 49 — (a) Amplitude of the semidiurnal temperature oscillation forced by absorption in the EUV and Schumann-Runge continuum as a function of altitude at selected latitudes for sunspot minimum conditions. See Fig. 1 for line conventions. See text for further details. (b) Phase (hour of maximum, local time) of the semidiurnal temperature oscillation described in 49(a).

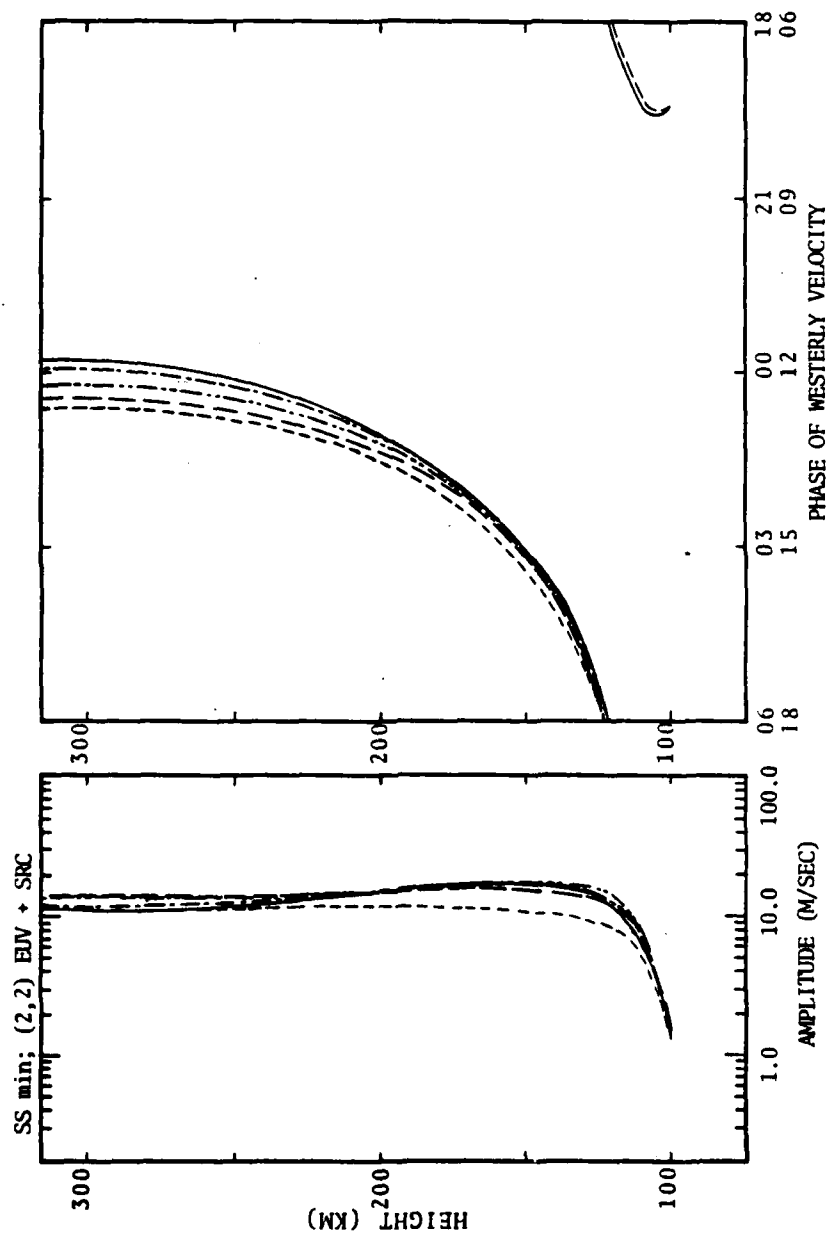


Fig. 50 — Same as 49 but for the westerly velocity oscillation

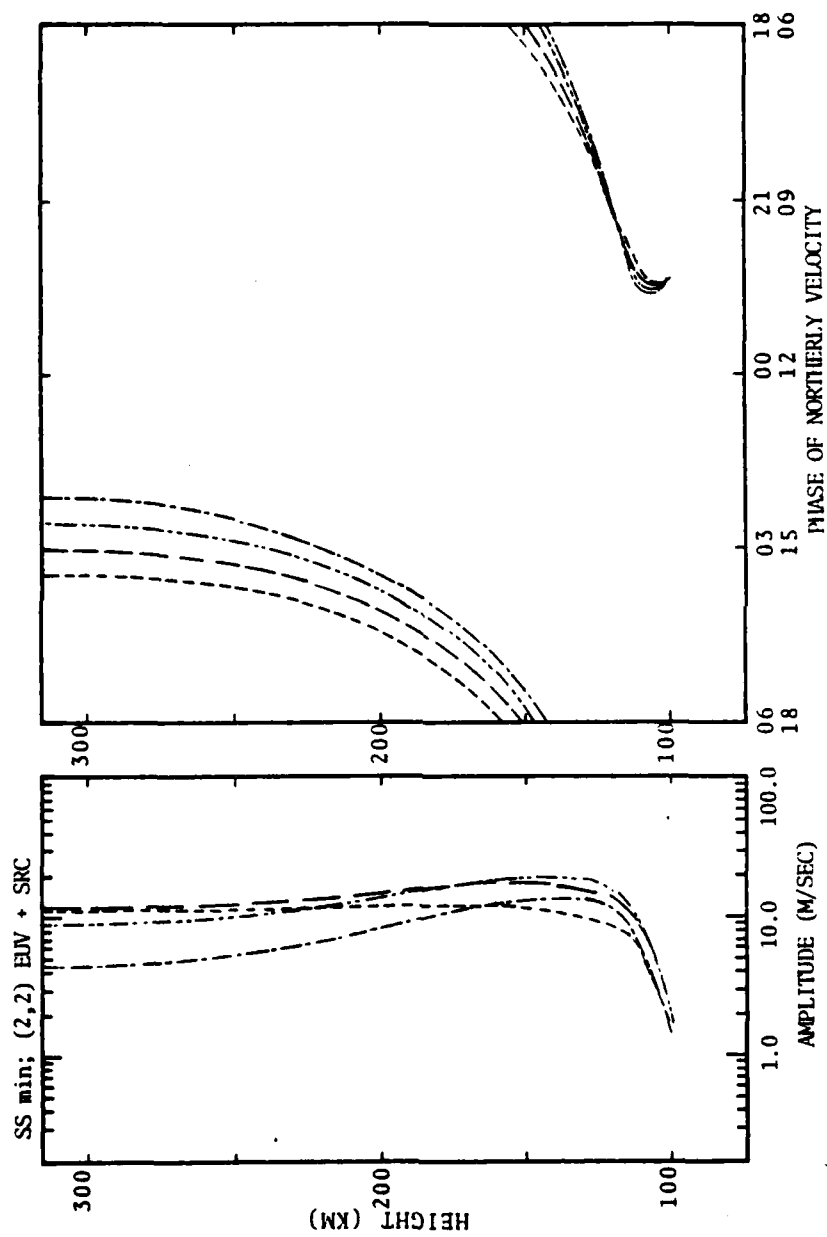


Fig. 51 — Same as 49 but for the northerly velocity oscillation



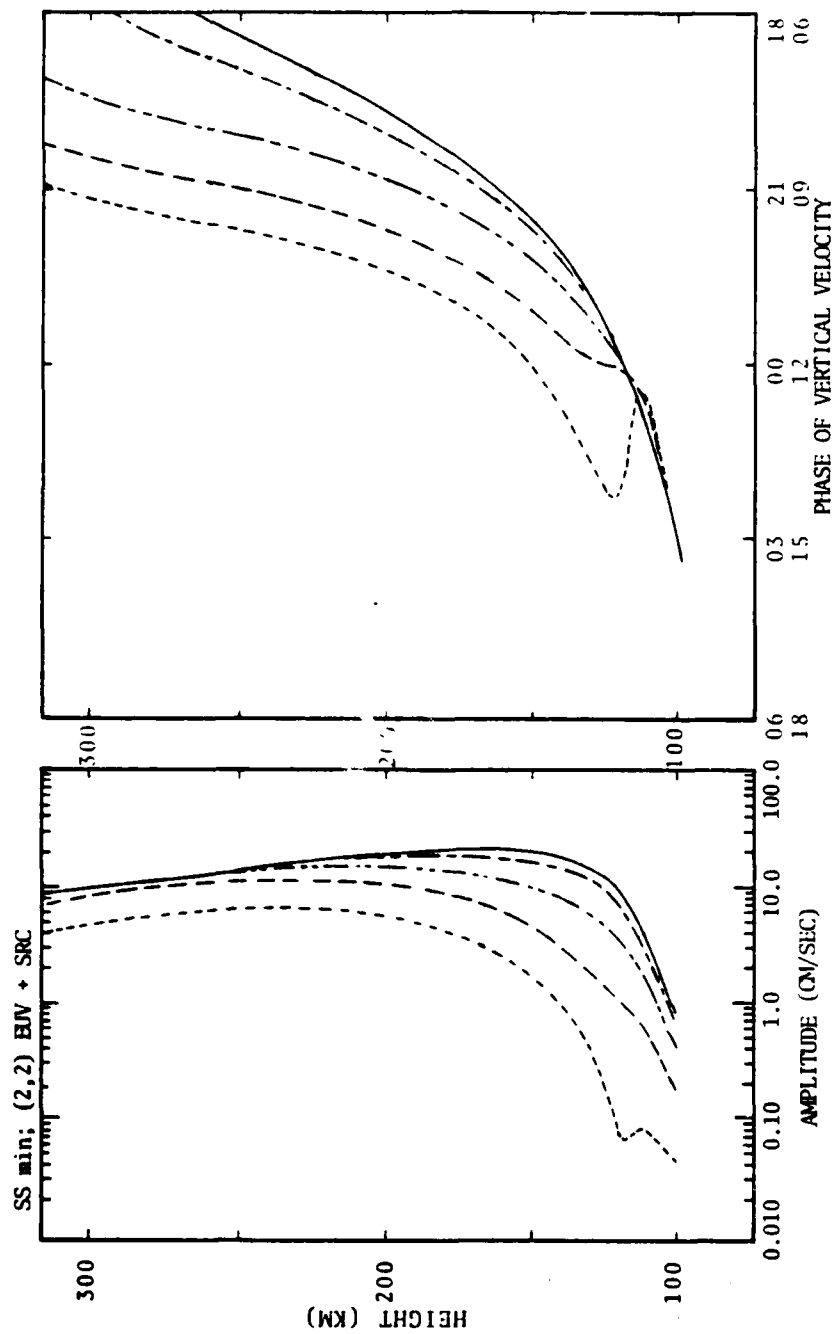


Fig. 52 — Same as 49 but for the vertical velocity oscillation

SS max : (2,2) EUV + SRC

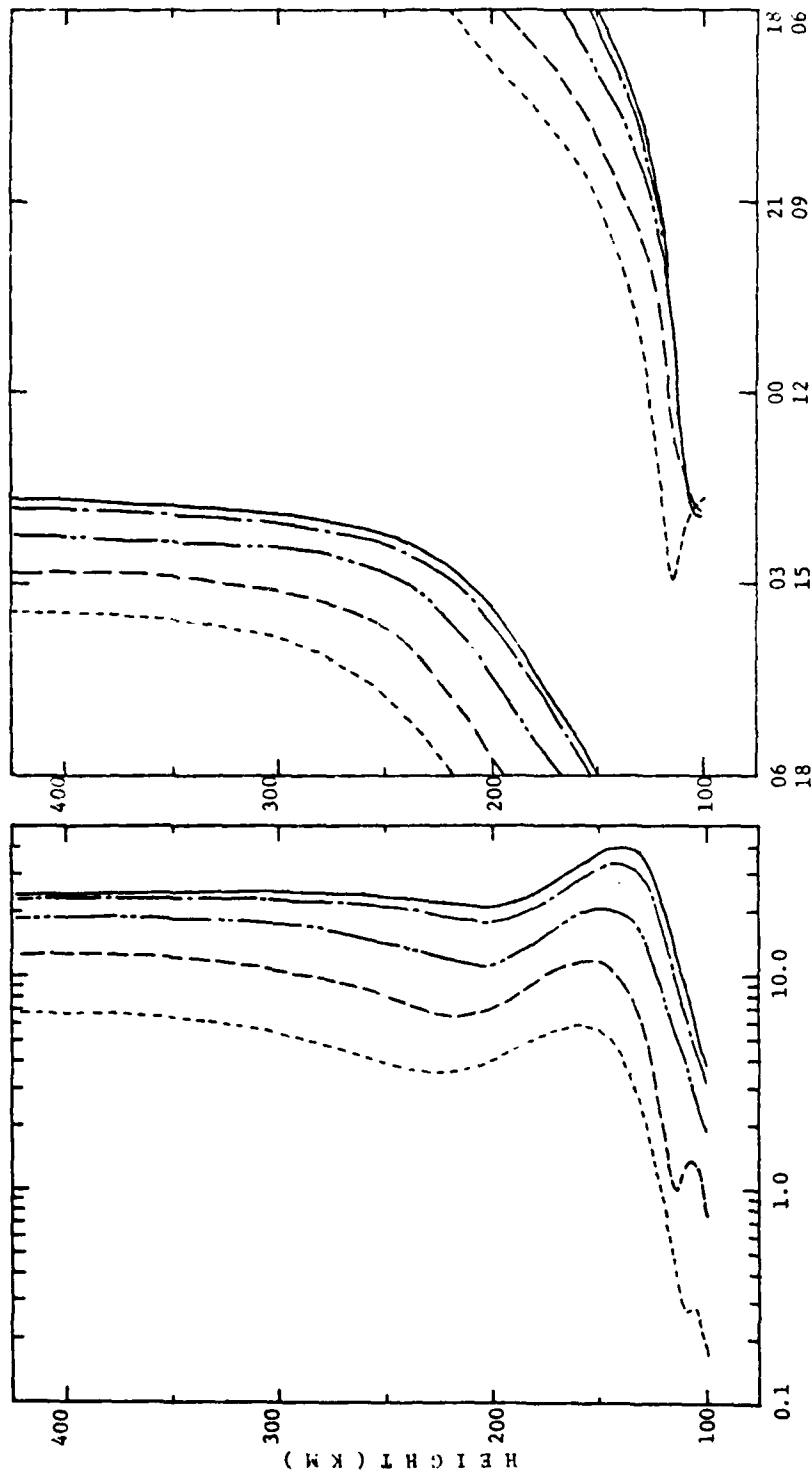


Fig. 53 — Same as 49 but for sunspot maximum conditions

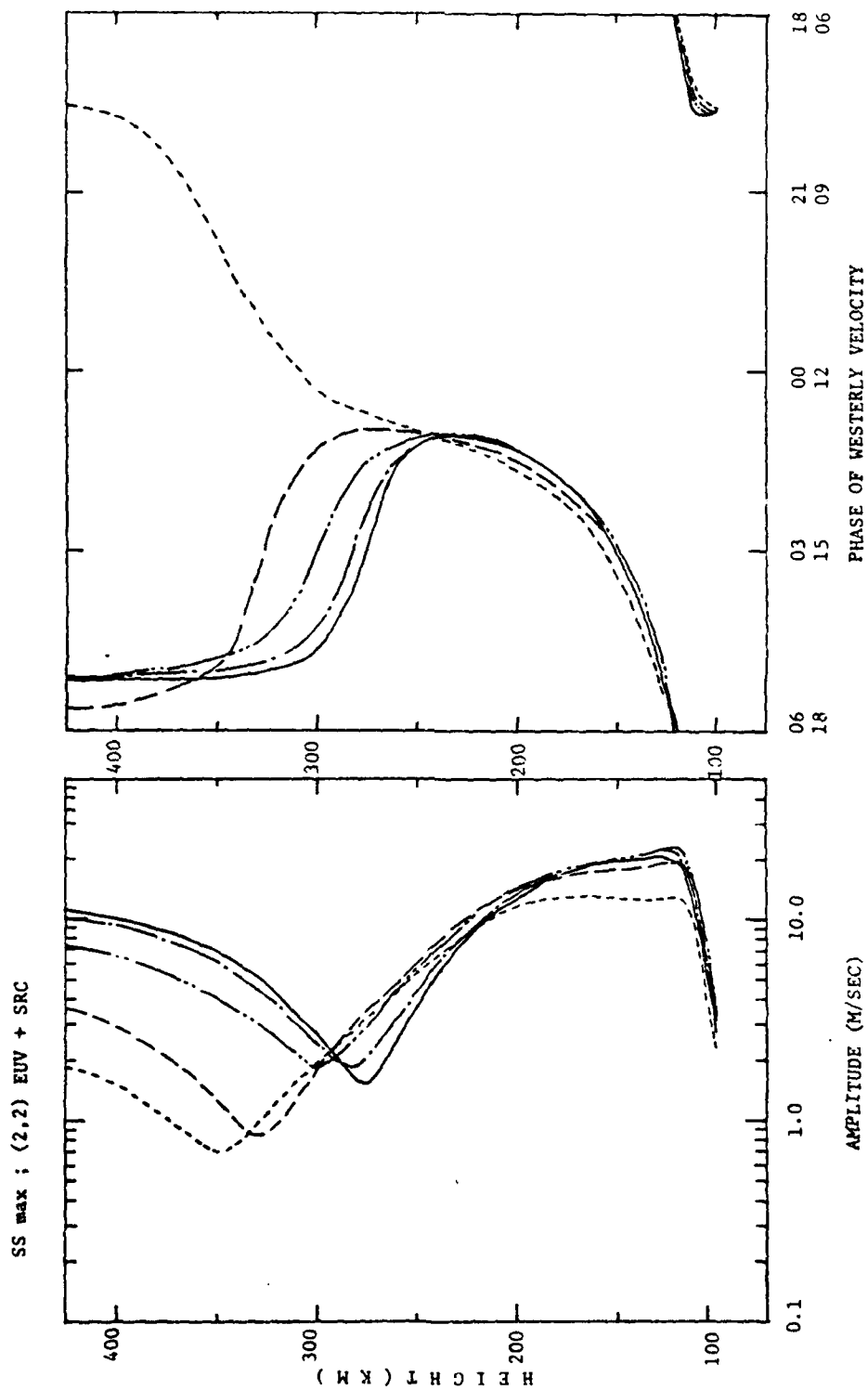


Fig. 54 - Same as 50 but for sunspot maximum conditions

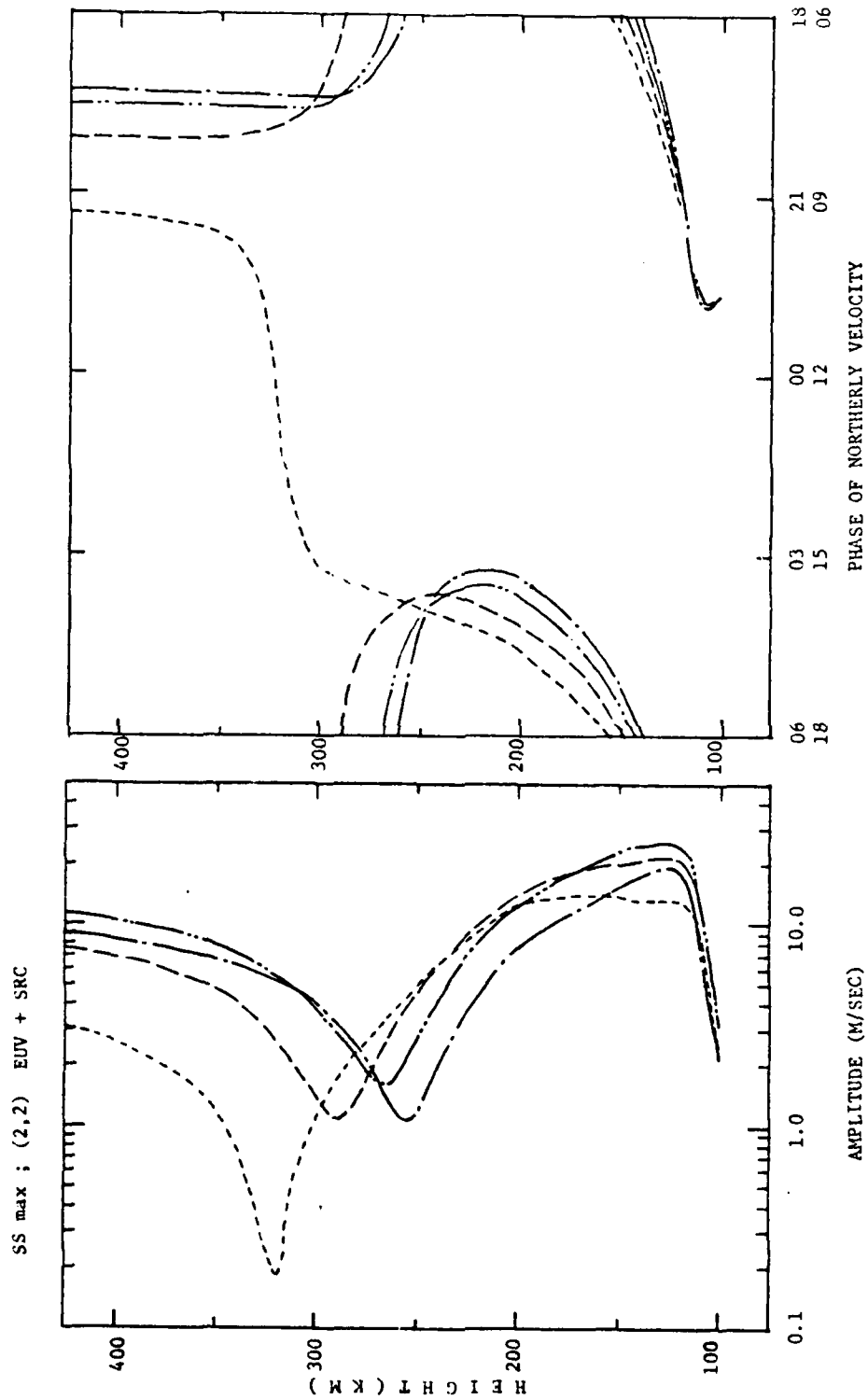


Fig. 55 — Same as 51 but for sunspot maximum conditions

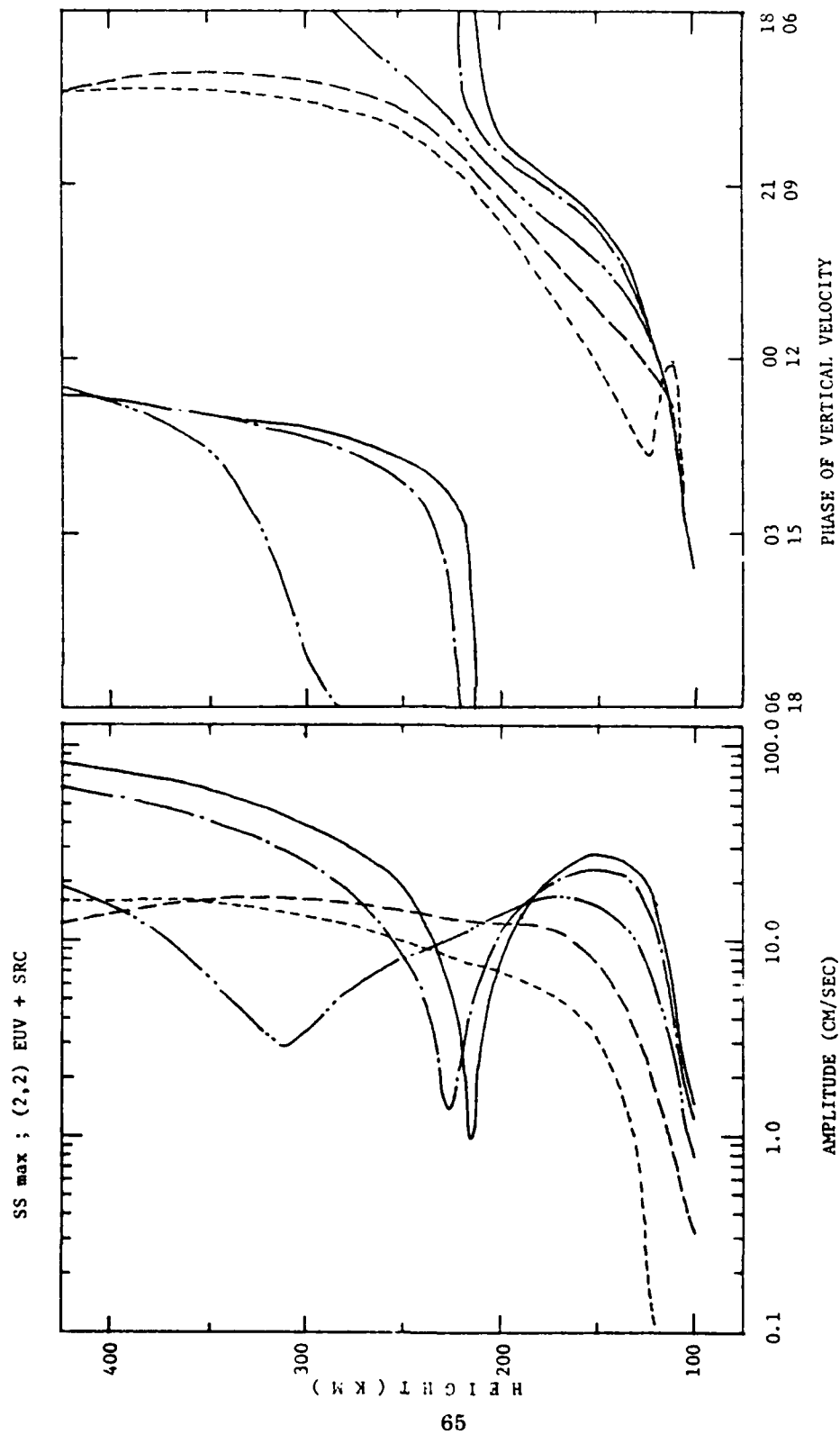


Fig. 56 — Same as 52 but for sunspot maximum conditions

DISTRIBUTION LIST

DIRECTOR

Defense Advanced Rsch Proj Agency  
Architect Building  
1400 Wilson Blvd.  
Arlington, VA 22209  
ATTN: Strategic Tech Office

Defense Communication Engineer Center  
1860 Wiehle Avenue  
Reston, VA 22090  
ATTN: .CODE R820 R. L. Crawford  
ATTN: CODE \$410 W. D. Dehart

DIRECTOR

Defense Communications Agency  
Washington, D. C. 20305  
ATTN: CODE 960  
ATTN: CODE 480

Defense Documentation Center

Cameron Station  
Alexandria, VA 22341 12 copies  
ATTN: TC

DIRECTOR

Defense Intelligence Agency  
Washington, D. C. 20301  
ATTN: W. Wittig DC-7D  
ATTN: DT-1B

DIRECTOR

Defense Nuclear Agency  
Washington, D. C. 20305  
ATTN: STSI Archives  
ATTN: STVL  
ATTN: STTL Tech Library 2 copies  
ATTN: DDST  
ATTN: RAAE

DIR OF DEFENSE RSCH & ENGINEERING

Washington, D. C. 20301  
ATTN: DD/S&SS John B. Walsh  
ATTN: OAD/EPS LTS. W. A. Whitaker

COMMANDER  
Field Command  
Defense Nuclear Agency  
Kirtland AFB, NM 87115  
ATTN: FCPR

Interservice Nuclear Weapons School  
Kirtland AFB, NM 87115  
ATTN: Document Control

DIRECTOR  
Joint Strat TGT Planning Staff Jcs  
Offutt AFB  
Omaha, NB 68113  
ATTN: JLTW-2  
ATTN: JPST G. D. Burton  
ATTN: JPST MAJ. J. S. Green

CHIEF  
Livermore Division Fld Command DNA  
Lawrence Livermore Laboratory  
P. O. Box 808  
Livermore, CA 94550  
ATTN: FCPRL

COMMANDER  
National Military Comd Sys Support Ctr  
Pentagon  
Washington, D. C. 20301  
ATTN: B211  
ATTN: DP Director for CSPO

DIRECTOR  
National Security Agency  
Ft. George G. Meade, Md. 20755  
ATTN: W14 Pat Clark  
ATTN: Frank Leonard

OJCS/J-3  
The Pentagon  
Washington, D. C. 20301  
ATTN: J-3 OPS ANAL BR. COL. Underhill

OJCS/J-6  
The Pentagon  
Washington, D. C. 20301  
ATTN: J-6

DIRECTOR  
Telecommunications & Comd & Con Sys  
Washington, D. C. 20301  
ATTN: ASST DIR Info & Space Sys  
ATTN: DEP ASST. SEC Sys

Weapons Ststems Evaluation Group  
400 Army Navy Drive  
Arlington, VA 22202  
ATTN: DOCUMENT CONTROL

COMMANDER  
Harry Diamond Laboratories  
2800 Powder Mill Road  
Adelphi, MD 20783  
ATTN: AMXDO-NP

COMMANDER  
TRASANA  
White Sands Missile Range, NM 88002  
ATTN: EAB

DIRECTOR  
U. S. Army Ballistic Research Labs  
Aberdeen Proving Ground, MD 21003  
ATTN: AM-CA Franklin E. Niles

U. S. Army Communications CMD  
C-E Services Division  
Pentagon Rm. 2D513  
Washington, D. C. 20310  
ATTN: CEAD

COMMANDER  
U. S. Army Electronics Command  
Fort Monmouth, N.J. 07703  
ATTN: AMSEL-TL-ENS Hans A. Bomke

COMMANDER  
U. S. Army Material Command  
5001 Eisenhower Avenue  
Alexandria, VA 22333  
ATTN: AMCRD-WN-RE John F. Corrigan

COMMANDER  
U. S. Army Material Command  
Foreign and Scientific Tech Center  
220 7th St. N. E.  
Charlottesville, VA 22901  
ATTN: P. A. Crowley  
ATTN: R. Jones



COMMANDER  
U. S. Army Missile Command  
Redstone Arsenal  
Huntsville, AL 35809  
ATTN: AMSMI-YTT W. G. Preussel, Jr.

COMMANDER  
U. S. Army Nuclear Agency  
Fort Bliss, TX 79916  
ATTN: USANUA-W. J. Berbert

CHIEF of Naval Research  
Department of the Navy  
Arlington, VA 22217  
ATTN: CODE 464 Jacob L. Warner  
ATTN: CODE 464 Thomas P. Quinn

COMMANDER  
Naval Air Systems Command  
Headquarters  
Washington, D. C. 21260  
ATTN: AIR 5381

COMMANDER  
Naval Electronics Systems Command  
Naval Electronic Systems CMD HQS  
Washington, D. C. 20360  
ATTN: NAVALEX 034 T. Barry Hughes  
ATTN: PME 106-1 Satellite Comm Project Off  
ATTN: John E. Doncarlos  
ATTN: PME 117

COMMANDER  
Naval Electronics Laboratory Center  
San Diego, CA 92152  
ATTN: William F. Moler  
ATTN: CODE 22001 Verne E. Hildebrand  
ATTN: R. Eastman

COMMANDING OFFICER  
Naval Intelligence Support CTR  
4301 Suitland Road, Bldg. 5  
Washington, D. C. 20390  
ATTN: Mr. Dubbin Stic 12

DIRECTOR  
Naval Research Laboratory  
Washington, D. C. 20375  
ATTN: HDQ COMM DIR Bruce Wald  
ATTN: CODE 5460 Radio Propagation BR  
ATTN: CODE 7701 J. D. Brown

ATTN: CODE 7700, T. P. Coffey 25 Copies

ATTN: CODE 7750, Branch Head 150 Copies

COMMANDER  
Naval Space Surveillance System  
Dahlgren, VA 22448  
ATTN: CAPT. J. H. Burton

COMMANDER  
Naval Surface Weapons Center  
White Oak, Silver Spring, MD. 20910  
ATTN: CODE 1224 Navy Nuc Prgms Off

DIRECTOR  
Strategic Systems Project Office  
Navy Department  
Washington, D. C. 20376  
ATTN: NSP-2141

COMMANDER  
ADC/AD  
ENT AFB CO 80912  
ATTN: ADDA

AF Cambridge Rsch Labs, AFSC  
L. G. Hanscom Field  
Bedford, MA 01730  
ATTN: LKB Kenneth S. W. Champion  
ATTN: OPR James C. Ulwick

AF Weapons Laboratory, AFSC  
Kirtland AFB, NM 87117  
ATTN: John M. Kamm SAS  
ATTN: SUL

AFTAC  
Patrick AFB, FL 32925  
ATTN: TF MAJ. E. Hines  
ATTN: TF/CAPT. Wiley  
ATTN: TN

Air Force Avionics Laboratory, AFSC  
Wright-Patterson AFB, OH 45433  
ATTN: AFAL AVWE Wade T. Hunt

Assistant Chief of Staff  
Studies and Analysis  
Headquarters, U. S. Air Force  
Washington, D. C. 20330  
ATTN: LTC. A.D. Dayton

Headquarters  
Electronic Systems Division, (AFSC)  
L. G. Hanscom Field  
Bedford, MA 01730  
ATTN: XRE LT. Michaels  
ATTN: LTC J. Morin CDEF XRC  
ATTN: YSEV LTC. David C. Sparks

COMMANDER  
Foreign Technology Division, AFSC  
Wright-Patterson AFB, OH 45433  
ATTN: TD-BTA LIBRARY

HQ USAF/RD  
Washington, D. C. 20330  
ATTN: RDQ

COMMANDER  
Rome Air Development Center, AFSC  
Griffiss AFB, N.Y. 13440  
ATTN: EMTLD Doc Library

COMMANDER IN CHIEF  
Strategic Air Command  
Offutt AFB, NM 68113  
ATTN: XPFS MAJ. Brian G. Stephan

544IES  
Offutt AFB, NB 68113  
ATTN: RDPO LT. Alan B. Merrill

Los Alamos Scientific Laboratory  
P. O. Box 1663  
Los Alamos, NM 87544  
ATTN: DOC CON for R. F. Taschek

Sandia Laboratories  
P. O. Box 5800  
Albuquerque, NM 87115  
ATTN: DOC CON for A. Dean Thornbrough  
ATTN: DOC CON for W. D. Brown  
ATTN: DOC CON for D. A. Dahlgren, ORG 1722  
ATTN: DOC CON for J. P. Martin, ORG 1732

University of California  
Lawrence Livermore Laboratory  
P. O. Box 808  
Livermore, CA 94550  
ATTN: Tech Info Dept L-3

Department of Commerce  
National Oceanic & Atmospheric Admin.  
Environmental Research Laboratories  
Boulder, CO 80302  
ATTN: Joseph H. Pope  
ATTN: C. L. Rufenach

Department of Commerce  
Office of Telecommunications  
Institute for Telecom Science  
Boulder, CO 80302  
ATTN: Glenn Falcon  
ATTN: William F. Utlaut  
ATTN: G. Reed  
ATTN: L. A. Berry

Department of Transportation  
Transportation Rsch. System Center  
Kendall Square  
Cambridge, MA 02142  
ATTN: TER G. Harowles

NASA  
Goddard Space Flight Center  
Greenbelt, MD 20771  
ATTN: CODE 750 T. Golden

NASA  
600 Independence Ave., S.W.  
Washington, D. C. 20546  
ATTN: M. Dubin

Aerospace Corporation  
P. O. Box 92957  
Los Angeles, CA 90009  
ATTN: T. M. Salmi  
ATTN: S. P. Bower  
ATTN: V. Josephson  
ATTN: SMFA for PW

Analytical Systems Corporation  
25 Ray Avenue  
Burlington, MA 01803  
ATTN: Radio Sciences

Avco-Everett Research Laboratory, Inc.  
2385 Revere Beach Parkway  
Everett, MA 02149  
ATTN: Richard M. Patrick

Boeing Company, The  
P. O. Box 3707  
Seattle, WA 98124  
ATTN: D. Murray  
ATTN: Glen Keister

Brown Engineering Company, Inc.  
Cummings Research Park  
Huntsville, AL 35807  
ATTN: David Lambert MS 18

California at San Diego, Univ. of  
Building 500 Mathews Campus  
3172 Miramar Road  
La Jolla, CA 92037  
ATTN: Henry G. Booker

Calspan Corporation  
P. O. Box 235  
Buffalo, N.Y. 14221  
ATTN: Romeo A. Deliberis

Computer Sciences Corporation  
P. O. Box 530  
6565 Arlington, VA 22046  
ATTN: H. Blank  
ATTN: Barbara F. Adams

Comsat Laboratories  
P. O. Box 115  
Clarksburg, Md. 20734  
ATTN: R. R. Taur

Cornell University  
Department of Electrical Engineering  
Ithaca, N. Y. 14850  
ATTN: D. T. Farley, Jr.

ESL, Inc.  
495 Java Drive  
Sunnyvale, CA 93102  
ATTN: J. Roberts  
ATTN: V. L. Mower  
ATTN: James Marshall  
ATTN: R. K. Stevens

General Electric Company  
Tempo-Center for Advanced Studies  
816 State Street  
Santa Barbara, CA 93102  
ATTN: Don Chandler  
ATTN: DASIAC

General Electric Company  
P. O. Box 1122  
Syracuse, N.Y. 13201  
ATTN: F. A. Reibert

General Research Corporation  
P. O. Box 3587  
Santa Barbara, CA 93105  
ATTN: John Ise, Jr.

Geophysical Institute  
University of Alaska  
Fairbanks, AK 99701  
ATTN: Technical Library  
ATTN: Neil Brown  
ATTN: T. N. Davis

GTE Sylvania, Inc.  
189 B Street  
Needham Heights, MA 02194  
ATTN: Marshal Cross

HRB-Singer, Inc.  
Science Park, Science Park Road  
P. O. Box 60  
State College, PA 16801  
ATTN: Larry Feathers

Illinois, University of  
Department of Electrical Engineering  
Urbana, IL 61801  
ATTN: K. C. Yeh

Institute for Defense Analyses  
400 Army-Navy Drive  
Arlington, VA 22202  
ATTN: Ernest Bauer  
ATTN: Hans Wolfhard  
ATTN: J. M. Aein  
ATTN: Joel Bengston

Intl Tel & Telegraph Corporation  
500 Washington Avenue  
Nutley, N. J. 07110  
ATTN: Technical Library

Itt Electro-Physics Laboratories, Inc.  
9140 Old Annapolis Road  
Columbia, Md. 21043  
ATTN: John M. Kelso

John Hopkins University  
Applied Physics Laboratory  
8621 Georgia Avenue  
Silver Spring, MD 20910  
ATTN: Document Librarian

Lockheed Missiles & Space Co., Inc.  
P. O. Box 504  
Sunnyvale, CA 94088  
ATTN: Dept 60-12

Lockheed Missiles and Space Company  
3251 Hanover Street  
Palo Alto, CA 94304  
ATTN: Billy M. McCormac, Dept 52-14  
ATTN: Martin Walt, Dept 52-10  
ATTN: Richard G. Johnson, Dept 52-12

M.I.T. Lincoln Laboratory  
P. O. Box 73  
Lexington, MA 02173  
ATTN: Mr. Walden, X113  
ATTN: D. Clark  
ATTN: James H. Pannell L-246  
ATTN: Lib A-082 for David M. Towle

Martin Marietta Corporation  
Denver Distribution  
P. O. Box 179  
Denver, CO 80201  
ATTN: Special Projects Program 248

Maxwell Laboratories, Inc.  
9244 Balboa Avenue  
San Diego, CA 92123  
ATTN: A. J. Shannon  
ATTN: V. Fargo  
ATTN: A. N. Rostocker

McDonnell Douglas Corporation  
5301 Bolsa Avenue  
Huntington Beach, CA 92467  
ATTN: J. Moule  
ATTN: N. Harris

Mission Research Corporation  
735 State Street  
Santa Barbara, CA 93101  
ATTN: R. Hendrick  
ATTN: R. E. Rosenthal  
ATTN: R. Bogusch  
ATTN: David Sowle  
ATTN: M. Scheibe  
ATTN: P. Fischer

Mitre Corporation, The  
Route 62 and Middlesex Turnpike  
P. O. Box 208  
Bedford, MA 01730  
ATTN: S. A. Morin M/S  
ATTN: Chief Scientist W. Sen  
ATTN: G. Harding

Mitre Corporation, The  
Westgate Research Park  
1820 Dolley Madison Blvd.  
McLean, VA 22101  
ATTN: Allen Schneider

North Carolina State Univ at Raleigh  
North Carolina State Univ Campus  
Raleigh, N.C. 27507  
ATTN: SEC Officer for Walter A. Flood

Pacific-Sierra Research Corp.  
1456 Cloverfield Blvd.  
Santa Monica, CA 90404  
ATTN: E. C. Field, Jr.

Philco-Ford Corporation  
Western Development Laboratories Div  
3939 Fabian Way  
Palo Alto, CA 94303  
ATTN: J. T. Mattingley MS X22

Photometrics, Inc.  
442 Marrett Road  
Lexington, MA 02173  
ATTN: Irving L. Kofsky

R & D Associates  
P. O. Box 3580  
Santa Monica, CA 90403  
ATTN: Robert E. Lelevier  
ATTN: Forest Gilmore  
ATTN: Richard Latter  
ATTN: William B. Wright, Jr.



Rand Corporation, The  
1700 Main Street  
Santa Monica, CA 90406  
ATTN: Cullen Crain

Science Applications, Inc.  
P. O. Box 2351  
La Jolla, CA 92038  
ATTN: D. Sachs  
ATTN: E. A. Straker

Stanford Research Institute  
333 Ravenswood Avenue  
Menlo Park, CA 94025  
ATTN: L. L. Cobb  
ATTN: Walter G. Chestnut  
ATTN: Donald Neilson  
ATTN: David A. Johnson  
ATTN: Charles L. Rino  
ATTN: E. J. Fremouw

Stanford Research Institute  
306 Wynn Drive, N. W.  
Huntsville, AL 35805  
ATTN: Dale H. Davis

Tri-Com, Inc.  
12216 Parklawn Place  
Rockville, MD 20852  
ATTN: Darrel Murray

TRW Systems Group  
One Space Park  
Redondo Beach, CA 90278  
ATTN: P. H. Katsos  
ATTN: J. W. Lowry